

THE USE OF NATURAL ZEOLITE AS CATALYST
IN THE PRODUCTION OF ETHYLBENZENE

A Master's Thesis

35732

Presented by

Özlem Esen KARTAL

to

the Graduate School of Natural and Applied Sciences
of Middle East Technical University
in Partial Fulfillment for the Degree of

MASTER OF SCIENCE

in

CHEMICAL ENGINEERING

T.C. YÜKSEKÖĞRETİM BAKANLIĞI
DOKÜMAN FASİYOLU

MIDDLE EAST TECHNICAL UNIVERSITY

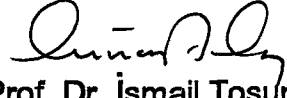
ANKARA

May , 1994


**I dedicate this thesis to
my grandmother and grandfather**




Approval of the Graduate School of Natural and Applied Sciences


for Prof. Dr. İsmail Tosun
Director

I certify that this thesis satisfies all the requirements as a thesis for the degree of Master of Science in Chemical Engineering.


Prof. Dr. Canan Özgen
Chairman of the Department

We certify that, we have read this thesis and that in our opinion it is fully adequate, in scope and quality, as a thesis for the degree of Master of Science in Chemical Engineering.


Prof. Dr. Işık Önal
Supervisor

Examining Committee in Charge

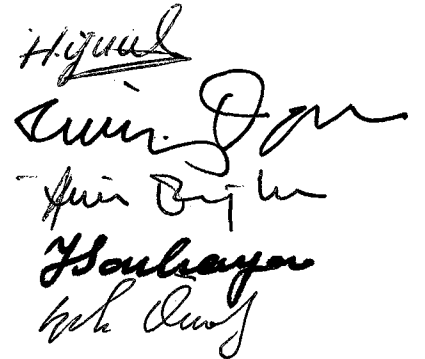
Prof. Dr. Hayrettin Yücel (Chairman)

Prof. Dr. Timur Doğu

Prof. Dr. İnci Eroğlu

Prof. Dr. Yüksel Sarıkaya

Prof. Dr. Işık Önal



ABSTRACT

THE USE OF NATURAL ZEOLITE AS CATALYST IN THE PRODUCTION OF ETHYLBENZENE

KARTAL, Özlem Esen

M.S. in Chemical Engineering

Supervisor : Prof.Dr. Işık ÖNAL

May, 1994, 126 pages

In this study, ZSM-5 zeolite catalysts were synthesized by using a natural zeolite, clinoptilolite, as a raw material. Clinoptilolite was treated with HCl acid in order to increase its $\text{SiO}_2 / \text{Al}_2\text{O}_3$ mol ratio. ZSM-5 samples were synthesized via hydrothermal crystallization by reacting HCl treated clinoptilolite, NaOH, TPABr and H_2O at 180°C for 110 hours. Characterization of hydrothermal reaction products by means of XRD and IR Spectrophotometer followed the transformation into H-form to make them acidic catalysts. Then, they were tested to investigate their catalytic performance in terms of benzene conversion, ethylbenzene yield and selectivity for vapor phase alkylation reaction in a catalyst test unit located at Research and Development Centre of Petkim in Yarımca.

Results of ZSM-5 synthesis showed that molar ratio of $\text{SiO}_2 / \text{Al}_2\text{O}_3$ in clinoptilolite is an important parameter to yield ZSM-5 as a single phase. In

addition, the optimum $\text{TPA}^+ / \text{TPA}^+ + \text{Na}^+$ ratio was found to be 0.5 for ZSM-5 crystallinity.

Catalytic test results indicated that catalytic performance of R 314 sample in the case of benzene conversion was close to that of reference sample and its performance on ethylbenzene yield and selectivity as observed at 400 °C could be improved in a considerable extent by increasing reaction temperature to 425 °C . However , TGA analysis showed that the amount of coke formed as reaction proceeds on catalyst was increased form 4.8 % at 400 °C to 12 % at 425 °C. The number of acid sites of R 314 and R 312 samples were found to be 3.7092×10^{13} and 3.073×10^{13} molecules / cm^2 respectively by ammonia desorption experiment by use of TGA.

Keywords : Clinoptilolite, ZSM-5, catalyst, alkylation, ethylbenzene

Science Code : 603. 02. 01

ÖZ

DOĞAL ZEOLİTELERİN ETİLBENZEN ÜRETİMİNDE KATALİZÖR OLARAK KULLANILABİLİRLİLİĞİNİN İNCELENMESİ

KARTAL, Özlem Esen

Yüksek Lisans Tezi, Kimya Mühendisliği Anabilim Dalı

Tez Yöneticisi : Prof.Dr. Işık Önal

Mayıs, 1994, 126 sayfa

Bu tezde, klinoptilolit doğal zeoliti kullanılarak ZSM-5 zeolit katalizörleri elde edilmiştir. Klinoptilolit HCl asit ile işlem görmesiyle $\text{SiO}_2 / \text{Al}_2\text{O}_3$ mol oranı yükseltilmiştir. ZSM-5 zeoliti, asitle işlem görmüş klinoptilolit, NaOH, TPABr ve H_2O kullanılarak $180\text{ }^\circ\text{C}$ ' de 110 saatte elde edilmiştir. Bu reaksiyon sonucu elde edilen ürünler, XRD ve IR Spektrofotometre ile karakterizasyon yapıldıktan sonra H-formuna dönüştürülerek asidik katalizörler haline getirilmiştir. Hazırlanan bu katalizörler, buhar fazı benzen alkilasyon reaksiyonunda benzen dönüşümü, etilbenzen verimi ve seçiciliği açısından Yarımca'da Petkim Araştırma ve Geliştirme Merkezi'nde kurulmuş olan katalizör test ünitesinde test edilmişlerdir.

Elde edilen sonuçlara göre klinoptilolitteki $\text{SiO}_2 / \text{Al}_2\text{O}_3$ mol oranının ZSM-5 eldesinde önemli bir parametre olduğu ortaya çıkmıştır. Ayrıca ZSM-5 kristalinitesi için optimum $\text{TPA}^+ / \text{TPA}^+ + \text{Na}^+$ oranının 0,5 olduğu görülmüştür.

Katalizör test sonuçları, bu çalışmada hazırlanan R 314 katalizörünün benzen dönüşümü açısından referans kabul edilen örnekle alınan sonuçlara yakın değerler verdiği ve etilbenzen verimi ve seçiciliği açısından da katalitik başarısının reaksiyon sıcaklığının 425 °C' ye çıkartılmasıyla artırılabilceğini göstermektedir. Bununla birlikte TGA analiz sonuçlarına göre 400 °C' de reaksiyon sırasında R 314 katalizöründe oluşan kok miktarı % 4.8 iken 425 °C ' de bu değerin % 12 ' ye yükseldiği görülmüştür. TGA cihazı kullanılarak gerçekleştirilen amonyak desorpsiyon yöntemine göre R 314 ve R 312 örnekleri için asidik kısım sırasıyla 3.7092×10^{13} ve 3.073×10^{13} molekül / cm² olarak bulunmuştur.

Anahtar kelimeler : Klinoptilolit, ZSM-5, katalizör, alkilasyon, etilbenzen

Bilim Kodu : 603.02.01

ACKNOWLEDGEMENTS

I wish to express my deepest gratitude to my supervisor, Prof.Dr. Işık Önal for his guidance, suggestions and encouragement throughout the course of the study.

I would like to thank Assoc.Prof.Dr.Ayşe Erdem-Şenatalar for providing me the samples of clinoptilolite and ZSM-5.

I wish to thank Assoc.Prof.Dr.Tunç Savaşçı who kindly allowed me to use alkylation catalyst test unit in Petkim and I also wish to thank the members of Research and Development Centre of Petkim for their assistance during the catalytic tests.

I wish to express my sincere thanks to Ms.Kerime Güney for her help and patience in carrying out the chemical analyses.

I am grateful to all members of the Department of Chemical Engineering of both Middle East Technical University and İnönü University for their assistance during this study.

I also wish to thank to Mrs. Naime Sezgi and Mr.Gökhan Şenel for their help in carrying out X-ray diffraction and surface area measurement analyses.

I would like to thank Dr. Bahadır Aydın , Mrs. Saadet Aydın and Mrs. Saime Demir for typing this thesis with care.

Last but not least, I wish to thank my family, particularly my father, Prof. Dr.Kemal Kartal, for his support and guidance throughout the study.



TABLE OF CONTENTS

	Page
ABSTRACT	iii
ÖZ	v
ACKNOWLEDGEMENTS.....	vii
LIST OF TABLES	xiii
LIST OF FIGURES.....	xvi
CHAPTER I : INTRODUCTION.....	1
1.1. The Reasons for Undertaking This Research	1
1.2. Purpose and Scope.....	2
CHAPTER II : ZEOLITES AND THEIR CATALYTIC APPLICATIONS	3
2.1. Description of Zeolites.....	3
2.2. Natural Zeolites and Their Occurances in Turkey	6
2.3. Properties of ZSM-5 Zeolite	9
2.4. Catalytic Properties of Zeolites	10
2.4.1. Shape Selectivity Concept in Zeolites	12
2.4.2. Industrial Catalytic Applications of Zeolites	18
2.5. Ethylbenzene Production History	22
2.5.1. Liquid Phase Alkylation Process	22
2.5.2. Vapor Phase Alkylation Processes	24
2.5.2.1. Yarpet Process.....	24
2.5.2.2. Alkar Process	25

2.5.2.3. Mobil / Badger Process	26
CHAPTER III : LITERATURE REVIEW	30
CHAPTER IV : EXPERIMENTAL WORK	35
4.1. Materials and Methodology for Preparation of Catalyst	35
4.2. Catalyst Preparation.....	35
4.2.1. Pretreatment of Clinoptilolite with HCl Acid.....	35
4.2.2. Synthesis of ZSM-5 Zeolite	36
4.2.3. Preparation of H-Form of ZSM-5 Samples.....	39
4.3. Catalyst Characterization	41
4.3.1. XRD.....	41
4.3.2. IR.....	41
4.3.3. TGA Analysis	42
4.3.4. Chemical Analysis	42
4.3.5. Surface Area Measurement	42
4.4. Catalytic Experiments	43
4.4.1. Catalyst Test Unit.....	43
4.4.2. Catalyst Tests	44
CHAPTER V : RESULTS AND DISCUSSION.....	49
5.1. Effect of HCl Pretreatment on Clinoptilolite Composition and Crystallinity	49
5.2. ZSM-5 Synthesis Results	51
5.2.1. Effect of SiO ₂ / Al ₂ O ₃ Mol Ratio of Clinoptilolite on ZSM-5 Synthesis.....	51
5.2.2. Variation of ZSM-5 Crystallinity with TPA ⁺ / TPA ⁺ + Na ⁺ Ratio	54

5.3. Catalyst Characterization Results	56
5.3.1. XRD.....	56
5.3.2. IR.....	62
5.3.3. TGA.....	62
5.3.4. Chemical Analysis	73
5.4. Catalytic Test Results	74
5.4.1. Comparison of Catalytic Performance of Sample Tested in Benzene Alkylation Reaction.....	74
5.4.2. Effect of Temperature on Benzene Conversion and Ethylbenzene Yield and Selectivity	75
5.4.3. Effect of Temperature on S_T and S_P Selectivities	75
5.4.4. Coking Characteristics of Tested Catalyst Samples	83
 CHAPTER VI : CONCLUSIONS AND RECOMMENDATIONS	 90
 REFERENCES	 92
 APPENDICES	
 APPENDIX A . FLOW DIAGRAMS OF VARIOUS ETHYLBENZENE PRODUCTION PROCESSES	 96
 APPENDIX B . ZSM- 5 SYNTHESIS DATA	 100
B.1. Calculation of Raw Material Amounts for a Specific Starting Batch Composition	 100
B.2. Synthesis Conditions of R 503 Sample.....	105

APPENDIX C .	MEASUREMENT OF VIBRATED BULK DENSITY AND CALCULATION OF REQUIRED AMOUNT OF CATALYSTS	106
C.1.	Measurement of Vibrated Bulk Density	106
C.2.	Calculation of Required Amount of Catalyst.....	107
APPENDIX D .	GAS CHROMATOGRAPHY ANALYSIS RESULTS	108
APPENDIX E .	RATE DATA AND CALCULATION OF S_T AND S_p SELECTIVITIES.....	112
E.1.	Calculation of Reaction Rates.....	112
E.2.	Calculation of S_T and S_p Selectivities	116
APPENDIX F .	X-RAY DIFFRACTION DATA.....	119
APPENDIX G .	AMMONIA DESORPTION DATA	122
APPENDIX H .	SURFACE AREA MEASUREMENT DATA.....	124

LIST OF TABLES

	Page
Table 1. Zeolite Occurance in Turkey	9
Table 2. Molecular Diameters of Selected Molecules	13
Table 3. Pore Size of Various Zeolites	14
Table 4. Industrial Processes Based on Zeolite Catalysts	21
Table 5. Reaction Conditions of $AlCl_3$ Process	23
Table 6. Reaction Conditions of Yarpet Process.....	25
Table 7. Reaction Conditions of Alkar Process	26
Table 8. Reaction Conditions of Mobil / Badger Process	29
Table 9. Conditions for Preparation of H-Form of ZSM-5 Samples	40
Table 10. Composition of Ethylene	44
Table 11. Specification of Benzene.....	44

Table 12. Tested Reaction Conditions	46
Table 13. Temperature Levels Used as a Variable Reaction Parameter	47
Table 14. Variation of SiO ₂ / Al ₂ O ₃ Mol Ratio of Clinoptilolite with HCl Concentration	49
Table 15. Chemical Composition of Natural and HCl Treated Clinoptilolite Samples	50
Table 16. Effect of TPA ⁺ / TPA ⁺⁺ Na ⁺ Ratio on ZSM-5 Crystallinity	56
Table 17. Ammonia Desorption Data of Catalyst Samples (Heating Rate : 15 °C /min)	72
Table 18. Chemical Composition of Tested Catalyst Samples	73
Table 19. TGA Data and Calculated Amount of Coke Present in Catalyst Samples	85
Table B.1. Molecular Weights of Compounds	101
Table B.2. Molar Composition of HCl Treated Clinoptilolite Sample (6H-CL) Used in ZSM-5 Synthesis	102
Table B.3. Composition of Starting Batch Mixture	103

Table D.1. Gas Chromatography Analysis of R 503 Sample Tested at 400 °C and 20 kg /cm ² gauge Pressure	108
Table D.2. Gas Chromatography Analysis of R 314 Sample Tested at 400 °C and 20 kg /cm ² gauge Pressure	109
Table D.3. Gas Chromatography Analysis of R 312 Sample Tested at 400 °C and 20 kg /cm ² gauge Pressure	110
Table D.4. Gas Chromatography Analysis of R 314 Sample Tested at 425 °C and 20 kg /cm ² gauge Pressure	111
Table E.1. Rate of reaction over R 503 Sample at 400 °C and 20 kg /cm ² gauge Pressure	114
Table E.2. Rate of reaction over R 314 Sample at 400 °C and 20 kg /cm ² gauge Pressure	114
Table E.3. Rate of reaction over R 314 Sample at 425 °C and 20 kg /cm ² gauge Pressure	115
Table E.4. Rate of reaction over R 312 Sample at 400 °C and 20 kg /cm ² gauge Pressure	115
Table F.1. X-Ray Data of Reference and As-Synthesized Sample	120

LIST OF FIGURES

	Page
Figure 1. Secondary Building Units and Polyhedra in Zeolite Structure According to Meier.....	4
Figure 2. Channel Structure of Clinoptilolite.....	8
Figure 3. Framework Structure of ZSM-5.....	11
Figure 4. Channel Structure in ZSM-5	11
Figure 5. Reactant Selectivity	15
Figure 6. Product Selectivity	15
Figure 7. Restricted Transition-State Selectivity	17
Figure 8. The Proposed Molecular Traffic Control for ZSM-5	17
A : Sinusoidal Channels	
B : Straight Channels	
Figure 9. Acidic Site in Zeolites.....	20

Figure 10. Reaction Mechanism of Benzene-Ethylene Alkylation over ZSM-5 Catalyst	27	
Figure 11. Apparatus for HCl Treatment of Clinoptilolite.....	37	
Figure 12. Autoclave Used in ZSM-5 Synthesis.....	38	
Figure 13. Catalyst Test Unit.....	45	
Figure 14. X-ray Diffraction Patterns of Natural and HCl Treated Clinoptilolite Samples	52	
Figure 15. Effect of $\text{SiO}_2 / \text{Al}_2\text{O}_3$ Mol Ratio on ZSM-5 Synthesis.....	53	
a. X-ray Diffraction Patterns of the Product Obtained by Utilizing Natural Clinoptilolite Sample ($\text{SiO}_2 / \text{Al}_2\text{O}_3 = 6$)		
b. X-ray Diffraction Patterns of the Product Obtained by Utilizing HCl Treated Clinoptilolite Sample ($\text{SiO}_2 / \text{Al}_2\text{O}_3 = 11$)		
c. X-ray Diffraction Patterns of the Product Obtained by Utilizing HCl Treated Clinoptilolite Sample ($\text{SiO}_2 / \text{Al}_2\text{O}_3 = 27$)		
Figure 16. Effect of $\text{TPA}^+ / \text{TPA}^{++} + \text{Na}^+$ Ratio on ZSM-5 Crystallinity.....	55	
a.0.29	b.0.5	c.0.80
Figure 17. X-ray Diffraction Pattern of Sample R 314	58	
a. As-synthesized Form		
b. After Transforming into H-Form		

Figure 18. X-ray Diffraction Pattern of Sample R 312.....	59
a. As-synthesized Form	
b. After Transforming into H-Form	
Figure 19. X-ray Diffraction Pattern of Sample (R 503) Used as Reference in Catalytic Tests	60
a. As-synthesized Form	
b. After Transforming into H-Form	
Figure 20. X-ray Diffraction Patterns of the Catalyst Samples Tested in Vapor Phase Alkylation Reaction at 400 °C and 20 kg/cm ² gauge Pressure	61
a. R 503	
b. R 314	
c. R 312	
Figure 21. IR Spectrum of As-synthesized Sample.....	63
Figure 22. Thermogravimetric Curve of	65
a. As-synthesized Sample	
b. Sample Calcined at 550 °C for 16 Hours	
Figure 23. Thermogravimetric Curve of HCl Treated Clinoptilolite (6H -CL)...	66
Figure 24. Thermogravimetric Curve of R 312 Before Ammonia Adsorption ..	67
Figure 25. Thermogravimetric Curve of R 314 Before Ammonia Adsorption ..	68
Figure 26. Thermogravimetric Curve of R 312 After Ammonia Adsorption.....	69

Figure 27. Thermogravimetric Curve of R 314 After Ammonia Adsorption	70
Figure 28. Thermogravimetric Curve of R 503 After Ammonia Adsorption	71
Figure 29. Conversion of Benzene over Three Different Catalyst Samples at 400 °C and 20 kg / cm ² gauge Pressure	76
Figure 30. Yield of Ethylbenzene over Three Different Catalyst Samples at 400 °C and 20 kg / cm ² gauge Pressure	77
Figure 31. Selectivity of Ethylbenzene over Three Different Catalyst Samples at 400 °C and 20 kg / cm ² gauge Pressure	78
Figure 32. Effect of Temperature on Benzene Conversion over R 314 Catalyst at 400 °C and 20 kg / cm ² gauge Pressure	79
Figure 33. Effect of Temperature on Ethylbenzene Yield over R 314 Catalyst at 400 °C and 20 kg / cm ² gauge Pressure	80
Figure 34. Effect of Temperature on Ethylbenzene Selectivity over R 314 Catalyst at 400 °C and 20 kg / cm ² gauge Pressure	81
Figure 35. Effect of Temperature on S _T and S _P Selectivities over R 314 Catalyst at 400 °C and 20 kg / cm ² gauge Pressure	82
Figure 36. Thermogravimetric Curve of R 503 Sample After Testing in Benzene Alkylation Reaction at 400 °C and 20 kg / cm ² gauge Pressure	86

Figure 37. Thermogravimetric Curve of R 312 Sample After Testing in Benzene Alkylation Reaction at 400 °C and 20 kg / cm ² gauge Pressure	87
Figure 38. Thermogravimetric Curve of R 314 Sample After Testing in Benzene Alkylation Reaction at 400 °C and 20 kg / cm ² gauge Pressure	88
Figure 39. Thermogravimetric Curve of R 314 Sample After Testing in Benzene Alkylation Reaction at 425 °C and 20 kg / cm ² gauge Pressure	89
Figure A.1. Liquid-Phase AlCl ₃ Process for Ethylbenzene Production.....	96
Figure A.2. Yarpet Process for Ethylbenzene Production	97
Figure A 3. Alkar Process for Ethylbenzene Production	98
Figure A.4. Mobil / Badger Process for Ethylbenzene Production	99
Figure F.1. X-ray Diffraction Pattern of the Sample Used as Reference in Crystallinity Calculations.....	121

CHAPTER I

INTRODUCTION

1.1. The Reasons for Undertaking This Research

Ethylbenzene, a raw material for styrene monomer, has been produced by alkylating benzene with ethylene via liquid phase using AlCl_3 as catalyst or vapor phase using Lewis acids. Several problems, such as corrosion and plugging in process lines have occurred in the processes using these catalysts. To overcome these problems, a new crystalline aluminosilicate zeolite catalyst known as ZSM-5 was developed by Mobil Oil Corporation. ZSM-5 exhibits a high catalytic activity and a low catalytic aging due to coke formation in hydrocarbon reactions in general and in benzene alkylation in particular. These characteristics can be ascribed to its highly siliceous composition and a unique pore structure.

The process of alkylation of benzene with ethylene in the presence of ZSM-5 catalyst prepared by utilizing chemicals such as sodium silicate, sodium aluminate, alumina, silica gel as a source of silica and alumina is under patent protection of Mobil Oil Corporation. In Turkey, ethylbenzene was manufactured via vapor phase alkylation process employing phosphoric acid on kieselguhr catalyst by Yarpet Petrochemical Complex of Petkim. Old catalyst technology of Yarpet Process caused

frequent shut downs due to plugging during operation. Therefore Petkim needs a newly patented catalyst for its own process.

In this work ZSM-5 catalysts for benzene alkylation reaction to obtain ethylbenzene were prepared by utilizing a natural zeolite, found in Western Anatolia in abundant amounts, instead of using chemicals.

1.2. Purpose and Scope

The purpose of this study was to prepare ZSM-5 zeolite catalysts for ethylbenzene production by use of a type of natural zeolite, clinoptilolite, available in this country. This work is not in the domain of Mobil patents since ZSM-5 catalyst samples were prepared by following a different method and their composition differs from Mobil's samples.

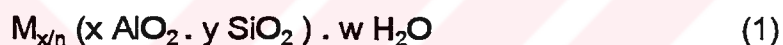
HCl treatment was applied to clinoptilolite sample in order to increase its $\text{SiO}_2 / \text{Al}_2\text{O}_3$ mol ratio to a sufficient value for ZSM-5 synthesis. Hydrothermal reaction was conducted at 180 °C to obtain ZSM-5 zeolite by utilizing HCl treated clinoptilolite, NaOH, TPABr and H_2O as starting materials. After characterizing the solid products obtained by this reaction as ZSM-5 by means of XRD and IR Spectrophotometer, they were transformed into H-form and tested as catalysts in benzene alkylation reaction. TGA analyses were carried out to determine the acidity of the catalyst samples by ammonia desorption and to study the coking characteristics of the tested catalysts. Catalytic performance of catalyst samples prepared in this study was investigated for benzene conversion, ethylbenzene yield and selectivity and effect of temperature on these parameters was also studied.

CHAPTER II

ZEOLITES AND THEIR CATALYTIC APPLICATIONS

2.1. Description of Zeolites

Zeolites are porous crystalline aluminosilicate materials. The structural formula based on the crystal unit cell of zeolite is as follows:



where x and y are the total number of tetrahedra per unit cell, n is the valence of cation M and w is the number of water molecules per unit cell. The ratio of y/x varies usually in the range of 1 to 5 depending upon the structure. However, recently, high silica zeolites in which y/x is 10 to 100, or even higher have been produced.

The three dimensional framework structure of zeolite is built of silicon-oxygen and aluminum-oxygen tetrahedra linked to each other by sharing oxygen atoms. In this framework structure, there are voids and channels containing alkaline and alkaline earth elements as cations and water molecules. Cations are necessary to compensate the negative charge of the framework which results from the existence of aluminum atoms in the structure. The mobility of cations provides for them to undergo ion exchange

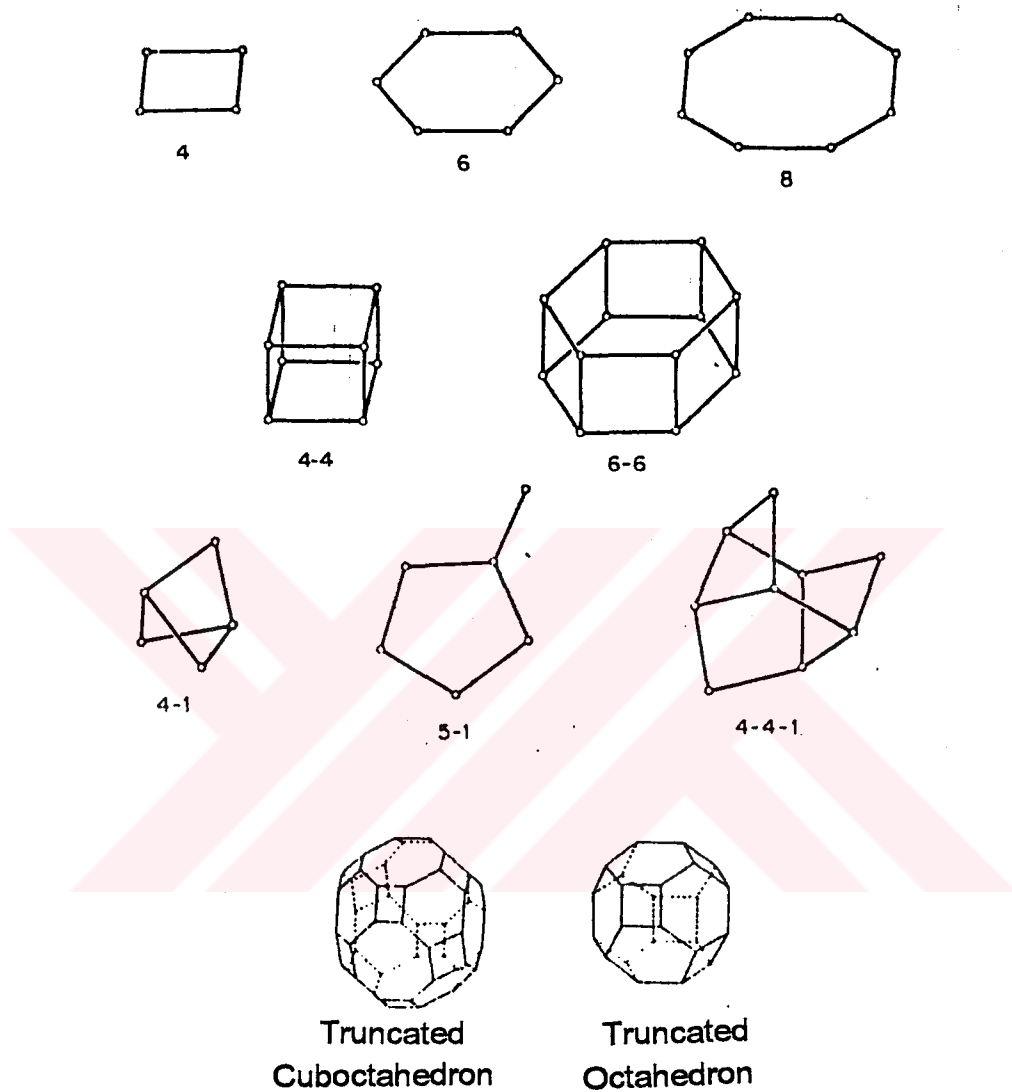


Figure 1 : Secondary Building Units and Polyhedra in Zeolite Structure According to Meier

with other cations. The water molecules in the voids can be removed by heating the zeolite.

The term "molecular sieve" is defined for porous solid materials which exhibit the property of acting as sieves on a molecular scale. At present, the most important molecular sieve effects are shown by crystalline zeolites due to existence of precisely uniform and molecular sized pores ranging from 3 Å to 10 Å in their structure. These pores completely exclude the molecules which are larger than their diameter. Molecular sieving can be total or partial. If it is total, the diffusion of one species into the zeolite may be wholly prevented while the diffusion of a second species occurs. If it is partial, the components of a binary mixture diffuse into the zeolite at different rates depending on the conditions.

Although the basic structural unit in crystalline zeolites is a tetrahedra of SiO_4 and AlO_4 , secondary building units formed by small groupings of linked tetrahedra are needed in visualizing the complex frameworks of them and systematizing their topologies. These secondary building units as proposed by Meier (1967) are shown in Figure 1. They consist of single and double rings of tetrahedra such as single 4-, 6- and double 4-, 6- and 8- rings and some polyhedra such as cubes, hexagonal prisms, or octahedra. Assemblages of these secondary units yields the final framework structure. In the secondary units aluminum or silicon atoms are represented at each corner or termination but the oxygens are not shown. They lie near the midpoints of connecting lines (Barrer, 1982).

2.2. Natural Zeolites and Their Occurances in Turkey

In nature, zeolite minerals exist in both volcanic and sedimentary rocks. The former zeolites exist in small amounts but , zeolites formed by the natural alteration of volcanic ash in alkaline environment in sedimentary rocks occur in large quantities in the world and it seems that the increasing demand for them is satisfied. Although mineral zeolites are known for about 200 years, their identification was made mainly after the development of X-ray diffractometer. In recent years applications and uses of natural zeolites have attracted much attention and considerable progress has been made in use of them in the fields of industry , agriculture and environmental protection. Their applications include gas purification, separation of air components, animal husbandry and poultry, purification of radioactive solutions, etc. These applications are result of two significant properties of zeolites :

1. Adsorptive properties : It is well known that dehydrated zeolites have excellent adsorption properties. Uniform pore structure allows the adsorption of molecules based upon differences in molecular size and shape. Separation of molecules of equal size is also possible because of existence of a strong electrostatic field in their pores due to positive (cation) and negative (aluminum) ions. Molecules are adsorbed according to their degree of polarity.

2. Ion exchange property : Zeolites have superior ion exchange property which is facilitated by their open tectosilicate frameworks. The exchange capacities of zeolites are high and high selectivities toward particular ions are often exhibited. The exchange behavior of nonframework

cations in zeolites depends on the nature of cation, i.e., size and charge of the hydrated cation, the temperature, and the concentration. Cation exchange may produce considerable changes in other properties such as thermal stability, adsorption behavior and catalytic activity. About 40 natural zeolites are known and analcime, chabazite, erionite, clinoptilolite and mordenite are the examples of more common types.

Clinoptilolite is a member the heulandite group of natural zeolites and is isostructural with the zeolite heulandite . But its chemical composition differs from that of heulandite in Si/Al ratio and the exchangeable cations. The thermal stability is also considerably greater than the stability of heulandite .

A major feature of the structure is the 8- and 10- membered channel networks that separated by a dense , gas-impermeable layer of tetrahedra. The channels are elliptical in shape with maximum and minimum internal dimentions of 4.4 Å and 3.0 Å for 8-membered channel and 7.9 Å and 3.5 Å for the 10-membered channel (Figure 2). Ions and molecules with dimensions significantly greater than 10-membered ring are excluded.

The studies on the occurance of natural zeolites in Turkey have been started since 1971 (Ataman ,1977). Table 1 gives the zeolite occurances that have been determined up to now in Turkey. Among these occurances reserve estimation was done only for Bigadiç deposit, which extends about 300 square kilometers, and found to approach 2 billion tons (Erdem-Şenatalar et al.,1990).

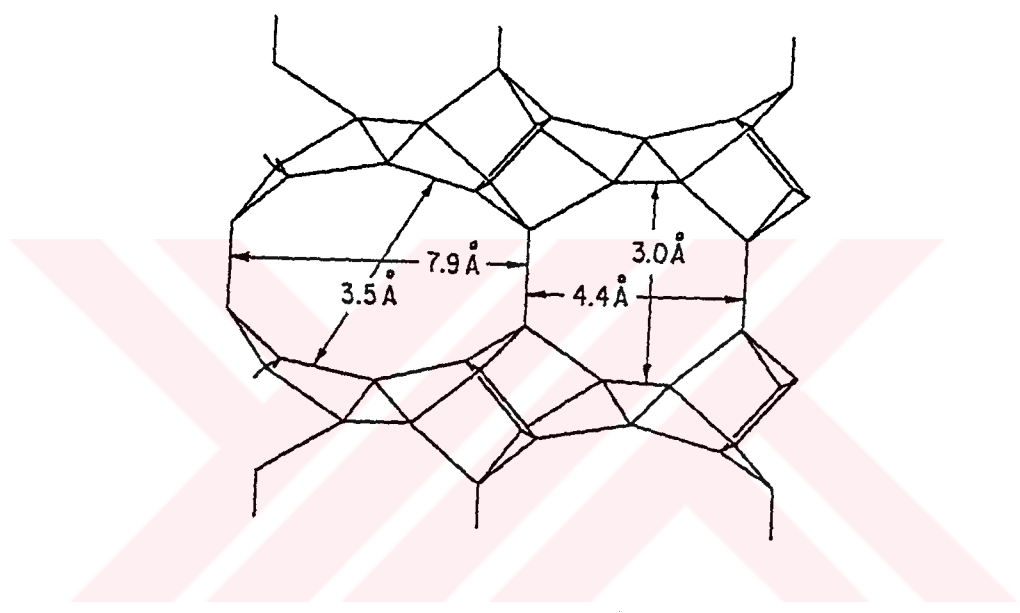


Figure 2 : Channel Structure of Clinoptilolite

Table 1 : Zeolite Occurances in Turkey

Locality	Zeolite Type
Çankırı-Çorum	Analcime
Kalecik-Hasayaz-Çandır-Şabanözü	Analcime
Ankara-Ahiboz	Analcime
Polatlı-Mülk-Oğlakçı-Ayaş	Analcime
Nallıhan-Çayırhan-Beypazarı-Mihalıççık	Analcime
Göynük	Analcime
Gölpazarı	Analcime
Bahçecik	Analcime
Gediz-Emet	Analcime and Clinoptilolite
Emet-Yukarıyoncağa	Clinoptilolite
Kütahya-Şaphane	Clinoptilolite
Akhisar-Gördes	Clinoptilolite
Bigadiç	Analcime and Clinoptilolite
M.Kemalpaşa-Bükköy-Fındıcak	Clinoptilolite
İzmir-Urla	Clinoptilolite
Karamürsel	Clinoptilolite

2.3. Properties of ZSM-5 Zeolite

ZSM-5, a new highly silicious synthetic zeolite, was first synthesized by Mobil Oil Corporation (Argauer and Landolt , 1972). It is a member of a group known as pentasil in which framework structure is formed by eight five-membered rings. These units join through edges to

obtain chains which can be connected to form sheets. Three dimensional framework structure of ZSM-5 was obtained by linking of these sheets as represented in Figure 3.

ZSM-5 has two types of channels both defined by ten-membered oxygen rings of approximately 6 Å diameter. As shown in Figure 4, the sinusoidal channels are nearly circular while the straight ones are elliptical. The size of these channels are between those of large pore zeolites such as faujasite and mordenite and small pore zeolites such as zeolite A (Kokotailo et al., 1978). The unique shape selective property which makes ZSM-5 the most useful industrial catalyst is offered by its channel structure. In addition, it represents a high thermal and acid stability. It can sorb straight chain monomethyl substituted paraffins and monocyclic hydrocarbons at room temperature (Chen and Garwood , 1978) . ZSM-5 has been used as a catalyst in several reactions such as benzene alkylation, xylene isomerization and toluene disproportionation.

2.4. Catalytic Properties of Zeolites

Zeolites have a considerable significance in heterogeneous catalysis in such a way that, they allowed the development of several commercially proven industrial applications. From a catalytic point of view, zeolites have properties which make them different from other porous catalysts (Csicsery , 1984) :

1. They have exchangeable cations .
2. When exchangeable cations are replaced with H^+ , Bronsted acid sites on which reactions proceed, are produced.

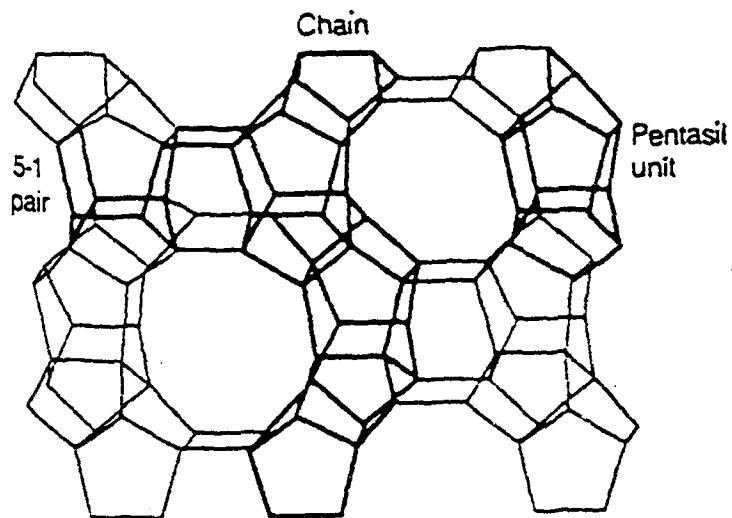


Figure 3 : Framework Structure of ZSM-5

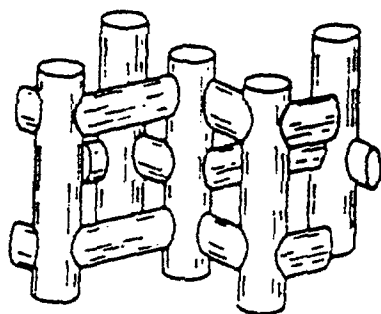


Figure 4 : Channel Structure in ZSM-5

3. They have uniform pores having a diameter of less than 10 Å .

Molecular sieving and shape selectivity properties of zeolites are a result of the third property. It is possible to prepare a zeolite catalyst at different catalytic activity and selectivity levels by modifying its physical and chemical properties such as pore size, cation content and $\text{SiO}_2 / \text{Al}_2\text{O}_3$ ratio.

2.4.1. Shape Selectivity Concept in Zeolites

The term of shape selectivity was first announced by Weisz and Frillette (1960) to describe the catalytic properties of small pore zeolites. After the discovery of medium sized zeolites, application of it has been expanded (Chen and Garwood, 1986) . Shape selectivity exists when the molecular dimensions of reactant and product are close to the pores of zeolites. For shape selectivity to occur, essentially all the active catalytic sites must be in the interior of the pores. The exterior area of crystalline zeolites is about 1 % of the total area, but if diffusion limitations are significant it may be necessary to inactivate exterior sites so that they don't contribute to reaction (Satterfield ,1980). In Table 2, molecular diameters of selected molecules are listed. The diameter of n-butane is 4.3 Å but that of isobutane is 5 Å. The difference between these two diameters is very important in catalytic applications. As shown in Table 3, the pore size of zeolites depends on the number of tetrahedra in the ring. However, the actual pore size is determined by the cations since they occupy the part of a pores.

Table 2 : Molecular Diameters of Selected Molecules (Csicsery, 1984)

Molecule	Kinetic Diameter (Å)
He	2.60
H ₂	2.89
O ₂	3.46
N ₂	3.64
NO	3.17
CO	3.76
CO ₂	3.30
H ₂ O	2.65
NH ₃	2.60
CH ₄	3.80
C ₂ H ₂	3.30
C ₂ H ₄	3.90
C ₃ H ₈	4.30
n-C ₄ H ₁₀	4.30
Cyclopropane	4.23
i-C ₄ H ₁₀	5.00
SF ₆	5.50
Neopentane	6.20
(C ₄ F ₉) ₃ N	10.20
Benzene	5.85
Cyclohexane	6.0

Table 3 : Pore Size of Various Zeolites (Csicsery , 1984)

Number of Tetrahedra in the Ring	Maximum Free Diameter (Å)	Zeolite
6	2.8	
8	4.3	Erionite, A
10	6.3	ZSM-5, Ferrierite
12	8.0	X, Y, Mordenite
18	15	Not yet observed

Four different types of shape selectivities are described:

1. **Reactant Selectivity** : This type of selectivity occurs when the feed contains a mixture of molecules, part of which are small enough, to diffuse into the pores of catalyst (Figure 5). An example of such selectivity can be given as the hydrogenation reaction of propylene, butene and isobutylene using Ca-A zeolite which contains platinum. Linear molecules, propylene and butene, react. Isobutylene, on the other hand, doesn't react.

2. **Product Selectivity** : It occurs when multiple products are formed within the pores of catalyst, only those with the proper shape and size can diffuse out (Figure 6). The bulky molecules formed are either converted to less bulky molecules or they deactivate the catalyst by pore blockage. Alkylation of toluene with methanol over metal oxide modified ZSM-5 is an example of product selectivity. In this reaction, para-xylene is

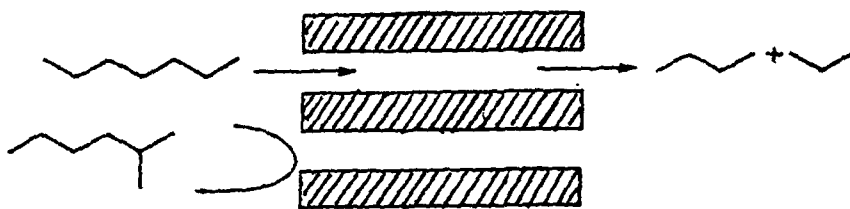


Figure 5 : Reactant Selectivity

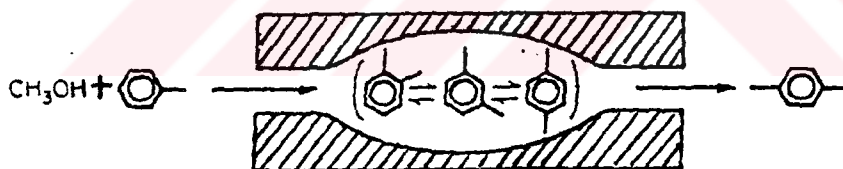


Figure 6 : Product Selectivity

produced as a major product.

3. **Restricted Transition -State Selectivity** : This type of selectivity occurs when certain reactions are hindered because transition state requires large spaces than the available space in the pores of catalyst (Figure 7). Acid-catalysed transalkylation of dialkylbenzenes is an example of such selectivity. In isomerization part of this reaction meta - and para - dialkylbenzenes are produced. In transalkylation part, involved diphenylmethane transition state is collapsed to give 1, 2, 4 - trialkylbenzene and toluene.

4. **Molecular Traffic Control** : This special type of selectivity was first described by Derouane and Gabelica (1980) to explain the absence of counterdiffusion effects in ZSM-5 catalysed reactions. It occurs in zeolites having more than one type of intersecting pore systems in which reactant molecules enter the catalyst through one of the pore systems and the products diffuse out by another pore system. This arrangement minimizes the counterdiffusion effect. For ZSM-5 catalyst the molecular traffic control effect is illustrated in Figure 8. Reactant molecules enter through the sinusoidal channels while the products desorb through the linear channels. The reactions take place at channel intersections where active sites are assumed to be located (Derouane and Gabelica ,1980).

The importance of diffusion in shape selective catalysis can't be overemphasized. In general , one type of molecule will react preferentially and selectively in a shape selective catalyst if its diffusivity is at least one or two orders of magnitude higher than that of competing molecular types. Too large molecules will be absolutely unable to diffuse through the pores. Even

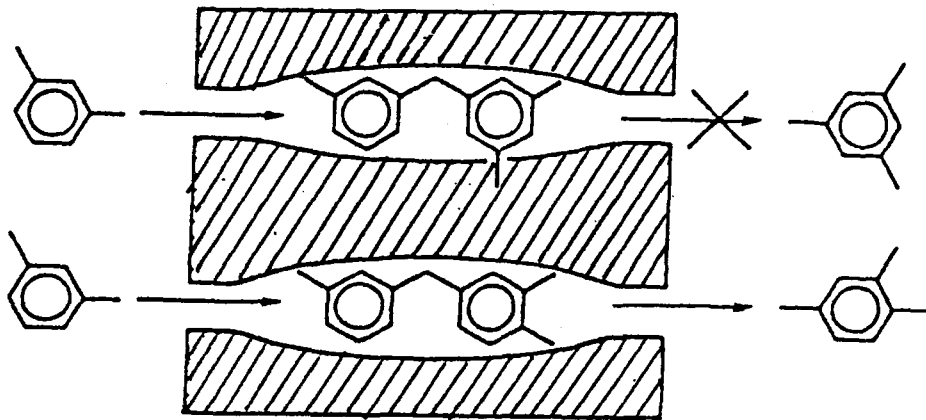


Figure 7: Restricted Transition-State Selectivity

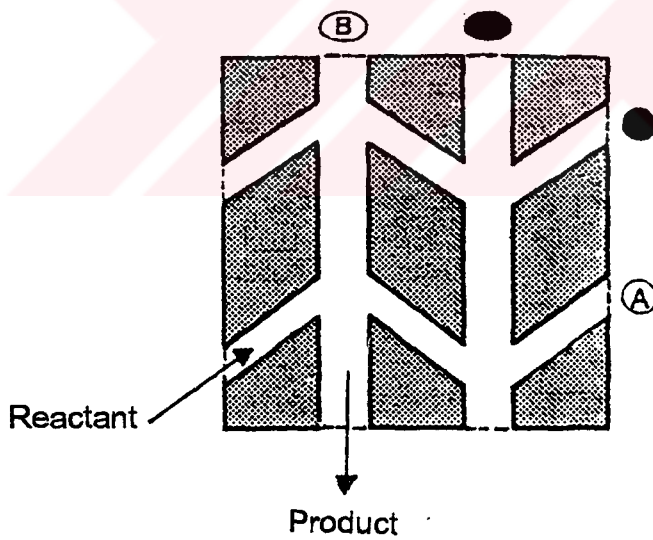


Figure 8: The Proposed Molecular Traffic Control for ZSM-5

A: Sinusoidal Channels

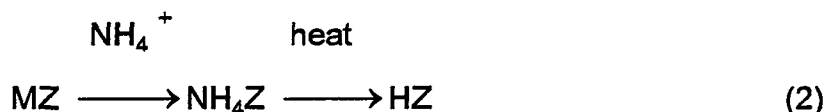
B: Straight Channels

those molecules which react preferentially have smaller diffusivities in shape selective catalysts than in large pore catalysts. For example, normal paraffins have diffusivities at least five orders of magnitude lower in the zeolite KT than in the large pore Y zeolite. Since diffusing molecules are constantly influenced by the zeolite pore wall and collide frequently with it, a Knudsen type diffusion must be involved.

2.4.2. Industrial Catalytic Applications of Zeolites

Growing interest in zeolite catalysis resulted in development of several economically feasible processes. Since industrial applications of zeolites involve acid-catalysed reactions, H-form of them should be prepared to obtain acid sites. If the aluminum remains triple coordinated a neighbouring SiO_4^{4-} will have an excess negative charge which can be balanced by a proton in the form of acidic hydroxyl group known as Bronsted acid sites (Bond, 1974). Figure 9, shows an acidic site in zeolites. Acid sites are introduced into zeolites by various ways (Csicsery, 1976) :

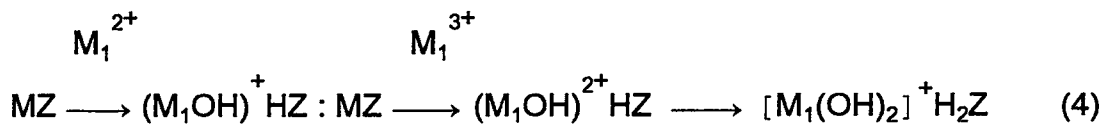
1. By ammonium exchange followed by thermal decomposition for deamination.



2. By acid treatment



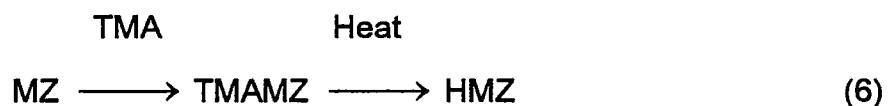
3. By exchange with multivalent cations, such as alkaline earth or rare earth ions.



4. By washing with water



5. By treatment with organic ammonium salts such as TMA followed by thermal decomposition.



Catalytically important zeolites can be reported as zeolite X, zeolite Y, mordenite and ZSM-5 which is the most important catalytic material among them. They have been applied as catalysts in petroleum and

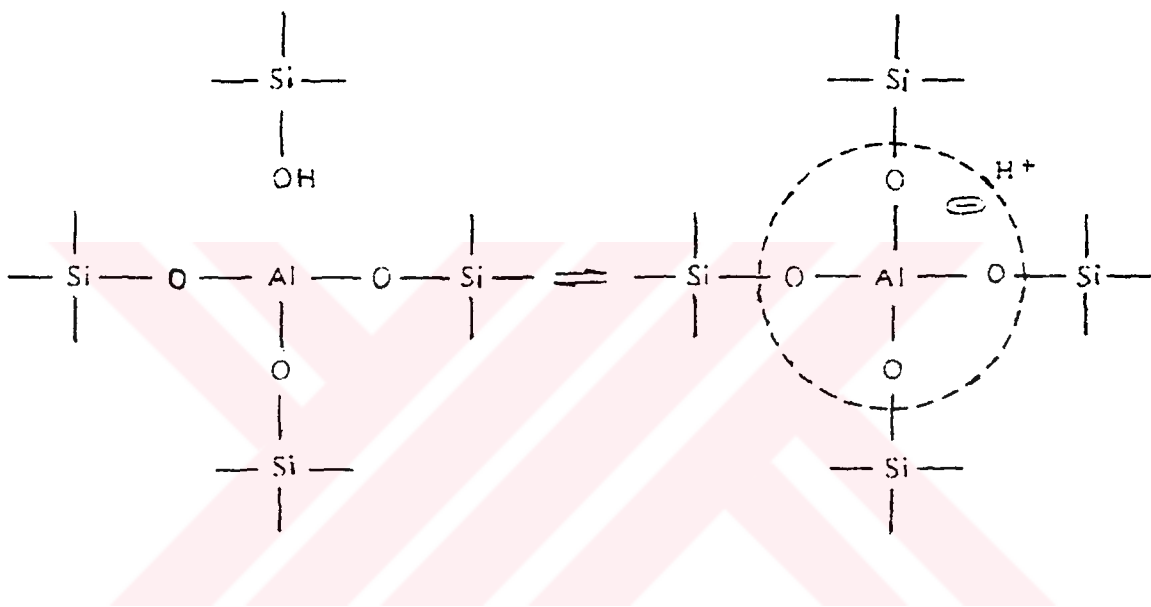


Figure 9 : Acidic Site in Zeolites

chemical industries such as catalytic cracking, hydrocracking, paraffin and olefin isomerization and aromatic alkylation (Bolton, 1976). In Table 4 specific examples of these applications are given.

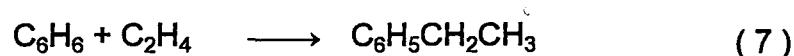
Table 4 : Industrial Processes Based on Zeolite Catalysts

Process	Catalyst
Catalytic Cracking	Zeolite X Zeolite Y
Hydrocracking	Zeolite Y Mordenite Erionite
Dewaxing	ZSM-5
Xylene Isomerization	ZSM-5
Ethylbenzene	ZSM-5
Toluene Disproportionation	ZSM-5
Methanol -to- Gasoline	ZSM-5

2.5. Ethylbenzene Production History

Most of the ethylbenzene has been produced by alkylating benzene with ethylene in the presence of catalysts by liquid or vapor phase.

The main reaction can be written as follows :



Polyethylbenzenes with two to six ethyl groups are produced as a side product and the related reaction is given as :



2.5.1. Liquid Phase Alkylation Process

Liquid - phase alkylation process has been carried out using AlCl_3 catalyst since the 1930s. The reaction proceeds through formation of a catalyst - activated aromatic complex which dissolves the metal halide catalyst and provides the reaction of ethylene with benzene in a polar medium. Three phases of aromatic liquid, ethylene gas and a liquid catalyst complex are present in the reactor and the reaction conditions are given in Table 5.

The amount of polyethylbenzenes can be reduced by using high benzene/ethylene ratios. In addition to an alkylation reactor, a second reactor is necessary for transalkylation of polyethylbenzenes with benzene to

yield ethylbenzene because the alkylation reaction rate is faster than that for transalkylation.

Table 5 : Reaction Conditions of AlCl_3 Process (Mc Ketta et al.,1982)

Parameter	Value
Alkylation	
Reaction Temperature	148 - 177 °C
Reaction Pressure	4.7 - 10 atm
Benzene/Ethylene (mol/mol)	1.5 - 2.5
AlCl_3 / Ethylene (mol/mol)	0.0010 - 0.0025
Transalkylation	
Reaction Temperature	148 - 177 °C
Reaction Pressure	4.7 - 10 atm

Flow diagram of liquid-phase AlCl_3 alkylation process is presented in Figure A.1. The process can be divided into three sections. The first one is reaction section including the benzene purification and catalyst preparation facilities, the alkylation and transalkylation reactors. In the second section, AlCl_3 catalyst is removed from the reaction products by water washing and acid neutralization steps. The third section, the purification, has a series of three distillation columns. The unreacted benzene is separated by the first column. The second one recovers the ethylbenzene from the heavy polyethylbenzenes. The bottom products of the second column are sent to the third column which is used to strip the recyclable polyethylbenzenes from

nonrecyclable residue compounds. Both recycled and fresh benzene must be dried before entering the reactor because water causes corrosion and decrease in catalyst activity.

The highly corrosive nature of AlCl_3 and reaction mixture requires to line the reactors and product handling equipment with corrosion resistant material.

2.5.2. Vapor Phase Alkylation Processes

In Turkey, ethylbenzene was produced for the manufacture of styrene monomer in the alkylation unit of Styrene Monomer Plant of the Yarpet Petrochemical Complex under the licence of UOP. In the world, the Alkar process developed by UOP in the 1960s and Mobil/ Badger process introduced by Mobil Oil Corporation in the 1970s are involved for commercial production of ethylbenzene in vapor phase.

2.5.2.1. Yarpet Process

Although Styrene Monomer Plant was operated between the years of 1976 and 1988, according to ethylene price in the world market, plant operation was stopped in certain periods. Research on improvement of existing ethylbenzene process and development of new catalysts has recently started by Research and Development Centre of Petkim.

The existing ethylbenzene production unit of Styrene Monomer Plant of Petkim is a fixed bed catalytic process in which phosphoric acid on kieselguhr is used as catalyst. The alkylation reaction takes place at high

pressure and low temperature. A single reactor divided into three beds is used for alkylation and transalkylation reactions. A simplified flow diagram presented in Figure A.2 shows that the process can be divided into two sections, a reaction section and a purification section. The reaction section contains the benzene alkylation reactor and the acid settler. Purification section includes the benzene recycle column and ethylbenzene and poly ethylbenzene recovery columns. Typical reaction conditions for ethylbenzene manufacture via the Yarpet process are listed in Table 6.

Table 6 : Reaction Conditions of Yarpet Process

Parameter	Value
Alkylation and Transalkylation	
Reaction Temperature	260 - 290 °C
Reaction Pressure	60 atm
Benzene / Ethylene (mol/mol)	10
Benzene LHSV	1.2 cm ³ /h/cm ³ of catalyst

2.5.2.2. Alkar Process

This process which uses BF₃ supported on a modified anhydrous alumina as a catalyst is a high-pressure and low-temperature process having the possibility to use dilute ethylene streams containing less than 10 % ethylene which are available in many refineries. Table 7 lists the reaction conditions applied in this process. As shown in Figure A.3, the process is divided into two sections of a reaction and a product purification. The

reaction section contains the alkylation reactor, the benzene dehydration column, a gas scrubber to remove aromatics from the effluent reactor gases. The purification section includes the recovery columns of benzene, ethylbenzene and polyethylbenzene and the transalkylation reactor. Alkar process has the advantages of elimination of catalyst recovery system and reduction of corrosion if the entry of water into the process is strictly prevented. However, even small amounts of water hydrolyze the BF_3 catalyst.

Table 7 : Reaction Conditions of Alkar Process (Mc Ketta et al.,1982)

Parameter	Value
Alkylation	
Reaction Temperature	93 - 148 °C
Reaction Pressure	34 atm
Benzene / Ethylene (mol/mol)	5 - 10
BF_3 / Ethylene (mol/mol)	0.0005 - 0.002
Transalkylation	
Reaction Temperature	176 - 232 °C
Reaction Pressure	27 atm

2.5.2.3. Mobil / Badger Process

In this most recent fixed-bed high pressure process, ZSM-5 catalyst is used. ZSM-5 exhibits a high catalytic activity for both alkylation

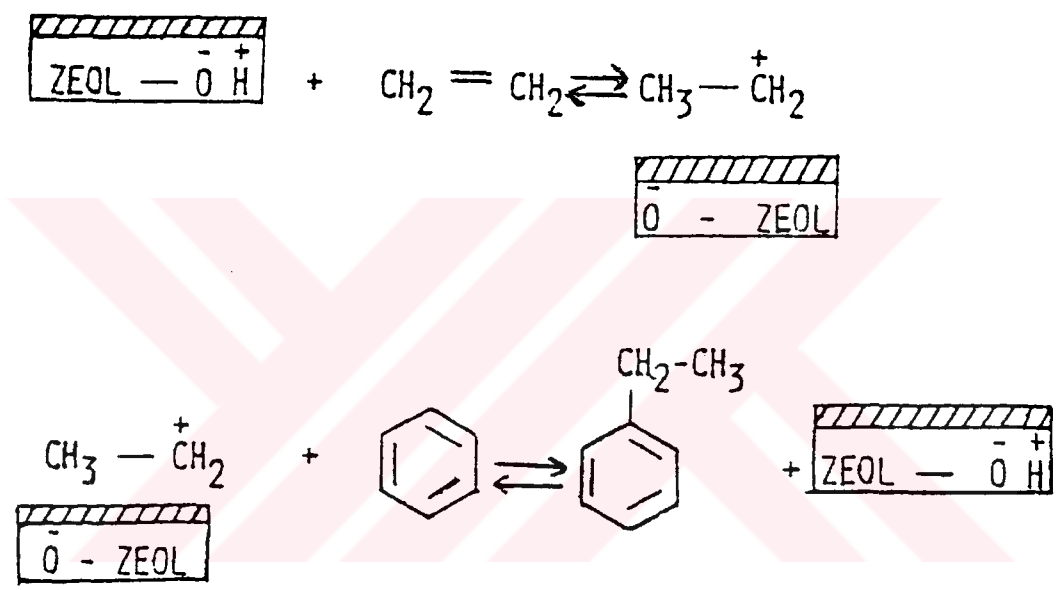


Figure 10 : Reaction Mechanism of Benzene-Ethylene Alkylation over ZSM-5 Catalyst

and transalkylation reactions and a low coking property compared with other zeolite catalysts. Reaction mechanism of this catalyst, shown in Figure 8, is different from those of other processes in such a way that alkylation proceeds through carbonium-ion like mechanism in which ethylene is activated at the Bronsted acid sites of ZSM-5 to make an adsorbed electrophilic species which is readily attacked by benzene (Dwyer, 1981). In Table 8, reaction conditions of this process are given.

Flow diagram of Mobil / Badger process is presented in Figure A.4. The process has two sections namely reaction and purification . The reaction section includes two multibed parallel reactors, a fired heater and a heat recovery equipment. An additional parallel reactor is necessary for regeneration of the catalyst which deactivates as a result of coke formation. Alkylation and transalkylation take place in the same reactor which is different from other processes. In the second section, three distillation columns are present. The first column recovers the unreacted benzene for recycle to the reactor. The bottoms from the benzene recovery column is sent to a product column, where ethylbenzene is taken overhead. A final column serves to recover polyethylbenzenes.

Mobil / Badger process is the latest and the most successful vapor phase process for ethylbenzene manufacture. The important advantages offered by this process are nonpolluting and noncorrosive effluent and product streams, elimination of catalyst recovery and waste treatment facilities and a high energy efficiency provided by the exothermic heat of reaction.

Table 8 : Reaction Conditions of Mobil / Badger Process

(Mc Ketta et.al.,1982)

Parameter	Value
Alkylation and Transalkylation	
Reaction Temperature	398 - 454 °C
Reaction Pressure	13 - 27 atm
Benzene / Ethylene (mol/mol)	5 - 20
Ethylene WHSV	2 - 10 kg/h/kg of catalyst



CHAPTER III

LITERATURE REVIEW

In this section , previous studies on the synthesis of ZSM-5 by utilizing natural zeolites and catalytic application of it in benzene alkylation reaction are reviewed.

Burress (1972) reported first the vapor phase alkylation of benzene with ethylene in the presence of crystalline aluminosilicate zeolite catalyst known as ZSM-5. It was prepared by utilizing sodium silicate, $\text{Al}_2(\text{SO}_4)_3 \cdot x \text{H}_2\text{O}$ (16.7 wt % Al_2O_3), TPABr, H_2SO_4 , NaCl and H_2O at 100 °C for 8 days. Chemical analysis of product indicated that $\text{SiO}_2/\text{Al}_2\text{O}_3$ mol ratio of product was 67. ZSM-5 and Al_2O_3 were blended in proportion to give 65 % ZSM-5 and 35 % Al_2O_3 in the final product. After calcining for 3 hours at 371 °C in air, it was ion exchanged 4 times, one hour each with 5 % NH_4Cl solution at room temperature using 5 cm^3 of solution / g of final product. In Example 1 of this study, at a benzene / ethylene mole ratio of 2.8 40-70 % ethylene conversion was obtained with the inlet temperature being of 400 °C . The selectivity to ethylbenzene increased from 90 % to 95-97 % during 14 days run. When inlet temperature was increased to 412 °C after 12 days conversion decreased about 25 % . The temperature was raised gradually up to 450 °C during 34 days of run. WHSV based on total feed was 7. In Example 2, the catalyst from example 1 was used after regeneration by burning with air to a final bed temperature of 537 °C . This run was

conducted at a WHSV of 42 lb total feed / hr. lb crystalline aluminosilicate with a benzene / ethylene mole ratio of 7.5. At the starting inlet temperature of 316 °C, 30-40 % ethylene conversion was obtained. Then it was raised to 343 °C and finally to 400 °C after 6 days. A maximum ethylene conversion and selectivity were 50 % and 97.5 % respectively during the 7 days of run. After catalyst regeneration at 537 °C , Example 3 was started under the same conditions as in Example 2 , but with an initial inlet temperature of 371 °C. Initial conversion was higher than that obtained in Example 2. Then the inlet temperature was increased to 400 °C , but considerable effect on conversion was'nt observed. Selectivity was 99 % during the first 13 days of the run, then it decreased to 97 % . This run was terminated after 15.5 days. Example 4 started after regeneration of catalyst in the same manner as for Example 3 and with a initial temperature of 400 °C and a WHSV of 42 lb total feed / hr. lb catalyst. The initial ethylene conversion was 80 % and it remained about 70 % for 30 days. During this time the selectivity was in the range of 98.5-99 %. This run was ended after 48 days. The product collected from Example 4 was used in Example 5. It was fed to the reactor starting on the 37th day of the run. Additional ethylene to keep a benzene / ethylene mole ratio at a value of 6.6 was fed to the reactor. Conversion was decreased from 65 to 55 % when recycle feed was used instead of benzene. This may be result of the lower concentration of benzene in the feed. In Example 6 , the run was carried out with catalyst which had been used and regenerated 8 times in the same manner as for Example 3. The initial conditions for this run were similar to those of Example 4 and Example 5. The initial ethylene conversion was around 75 % and dropped to 69 % after 8 days compared to conversion of 80 % for the same periods of Example 4. At this point the pressure of the reactor was raised to 3.4 atm. Ethylene conversion increased from 70 % to 90-95 % and ethylbenzene to

polyethylbenzenes weight ratio increased from 12/1 to 22/1. Conversion remained 90 % for 21 days and at this time the reactor pressure was raised to 18 atm. In Example 7 the feed to Example 6 was changed on the 43rd day to a feedstock containing 18 wt % ethylbenzene. The conversion and selectivity decreased to 85-90 % and 90-92 % respectively. The inlet temperature of the reactor was decreased from 400 °C to 377 °C to increase selectivity to 97 %. This run was terminated on 53rd day. In Example 8, the run was carried out by utilizing fresh H-ZSM-5 catalyst prepared according to Example 1. The conversion obtained was 85-90 % and the selectivity was around 99.5 %. After increasing the pressure of the reactor to 18 atm on 19th day, an increase in conversion to a value of 98 % was observed. It was also observed that reduction of benzene / ethylene mole ratio from 8 to 5 has no noticeable effect on conversion, but selectivity decreased to 98 %. This run continued for 48 days.

Sand and Goto (1988) reported the synthesis of ZSM-5 by using Japanese mordenite and clinoptilolite. Hydrothermal reactions were carried out by reacting two natural zeolites and four aluminum deficient zeolites obtained by HCl treatment with NaOH, TPABr in the temperature range of 135 - 180 °C. A single phase of ZSM-5 wasn't obtained by natural and two aluminum deficient mordenites having different $\text{SiO}_2 / \text{Al}_2\text{O}_3$ mol ratios at 180 °C. Natural clinoptilolite didn't transform into ZSM-5 but aluminum deficient clinoptilolite ($\text{SiO}_2 / \text{Al}_2\text{O}_3 = 19.8$) transformed to a single phase of ZSM-5 in the reaction time period of 80 - 240 hours at 180 °C. Analcime appeared after 240 hours as a coexisting phase with ZSM-5. Single phase of ZSM-5 was obtained in the time period of 4 to 480 hours with the second sample of aluminum deficient clinoptilolite ($\text{SiO}_2 / \text{Al}_2\text{O}_3 = 39.8$). They concluded that in ZSM-5 synthesis the ratio of

$\text{SiO}_2 / \text{Al}_2\text{O}_3$ in the zeolite used as a starting material is the important parameter.

Mavrodinova et al. (1989 . a) have investigated the effect of the structural and chemical characteristics of zeolites in the conversions of toluene , m-xylene and alkylation of benzene with ethylene by comparing two samples of hydrothermally dealuminated faujasite (type Y) and ZSM-5 with a similar Si/Al ratio. The catalytic experiments were conducted at atmospheric pressure with ethylene WHSV of 0.9 hr^{-1} and a molar of benzene / ethylene ratio of 3. At $220 \text{ }^\circ\text{C}$ a higher ethylene conversion were obtained with faujasite catalyst but at $300 \text{ }^\circ\text{C}$ it showed a considerable lower conversion than that exhibited by H-ZSM-5 and deactivated quite rapidly. In the presence of faujasite sample only ethyl- and diethylbenzene were obtained at $220 \text{ }^\circ\text{C}$, however cumene and sec-butylbenzene were the main side products of H-ZSM-5 sample. When temperature raised to $300 \text{ }^\circ\text{C}$ small amounts of cumene was observed with faujasite sample. They concluded on the basis of obtained data that structural characteristics rather than acid center density determined the catalytic behavior of these two catalysts.

Mavrodinova et al. (1989 . b) reported the effect of nonframework Al in the conversion of toluene , m-xylene and alkylation of benzene with ethylene. Catalytic behavior of the two hydrothermally treated type Y samples with highest (46) and lowest (10) content of nonframework Al and ZSM-5 was studied in benzene alkylation reaction at ethylene WHSV of 0.9 hr^{-1} at $250 \text{ }^\circ\text{C}$ and atmospheric pressure. It was observed that the sample having low nonframework Al exhibited higher activity and rate of deactivation. The yields of side aromatics (C_3 - and C_4 - alkylaromatics) were also high. The ZSM-5 catalyst showed, a considerable low ethylene

conversion, but a two or three times higher yield of C₃ - and C₄ - alkylaromatic compounds. They concluded that the rate and type of ethylbenzene reaction taking place on the Y types and ZSM-5 zeolites differed and there was no indication of direct participation of nonframework Al in alkylaromatic conversions.



CHAPTER IV

EXPERIMENTAL WORK

4.1. Materials and Methodology for Preparation of Catalyst

In the preparation of ZSM-5 zeolite catalyst , HCl treated clinoptilolite, tetrapropylammonium bromide (Aldrich , 98 %), sodium hydroxide pellets (Merck , 98 %) and distilled water were used as a starting materials.

ZSM-5 catalyst preparation methodology consists of five steps which can be listed in the following order : Treatment of clinoptilolite with HCl acid, synthesis of ZSM-5, calcination of synthesized ZSM-5, ion exchange of ZSM-5 with ammonium chloride solution and calcination of ammonium exchanged ZSM-5.

4.2. Catalyst Preparation

4.2.1. Pretreatment of Clinoptilolite with HCl Acid

Clinoptilolite sample used in this study was originated from zeolite deposits located in Bigadiç. Prior to pretreatment with HCl, the original sample which was in the form of lumps about 5-10 cm was ground and sieved to

9-16 mesh size. It was treated with HCl acid to increase its $\text{SiO}_2/\text{Al}_2\text{O}_3$ mol ratio in a glass-made apparatus presented in Figure 11. About 70 gram of sieved clinoptilolite was put into zeolite bed and washed with condensed HCl acid which flowed back into flask. The zeolite bed was kept at about $100\text{ }^\circ\text{C}$ by circulating water vapor. After the treatment clinoptilolite was washed with hot and cold distilled water to remove trace of acid and dried at $110\text{ }^\circ\text{C}$ overnight.

To investigate the effect of HCl concentration on $\text{SiO}_2/\text{Al}_2\text{O}_3$ mol ratio of clinoptilolite, 4 M and 6 M HCl acid were used in pretreatment for 4 and 6 hours respectively and the later treatment was found to be sufficient for ZSM-5 synthesis.

4.2.2. Synthesis of ZSM-5 Zeolite

ZSM-5 zeolite tested in benzene alkylation reaction was prepared from a batch composition of $1.2363 \text{ Me}_{2/n}\text{O} / 11 \text{ Na}_2\text{O} / 11 (\text{TPA})_2\text{O} / 3.3328 \text{ Al}_2\text{O}_3 / 90 \text{ SiO}_2 / 2000 \text{ H}_2\text{O} / 22 \text{ Br}$ (Me is exchangeable cations of valence n in clinoptilolite) by hydrothermal crystallization. Prior to synthesis, HCl treated clinoptilolite having $\text{SiO}_2/\text{Al}_2\text{O}_3$ mol ratio of 27 was ground to 100 mesh in an agate mortar and pestle. Then, it was slurried with distilled water and weighted amount of sodium hydroxide (NaOH) was added. Dissolution of NaOH by mixing followed by the addition of tetrapropylammonium bromide (TPABr). After stirring well, the mixture was put into 100 ml autoclaves which were constructed from stainless steel and lined with teflon as given in Figure 12 . The autoclaves were placed in an oven at time zero and hydrothermal reaction was carried out without agitation at $180\text{ }^\circ\text{C}$ under autogeneous pressure for 110 hours . After the reaction was terminated ,

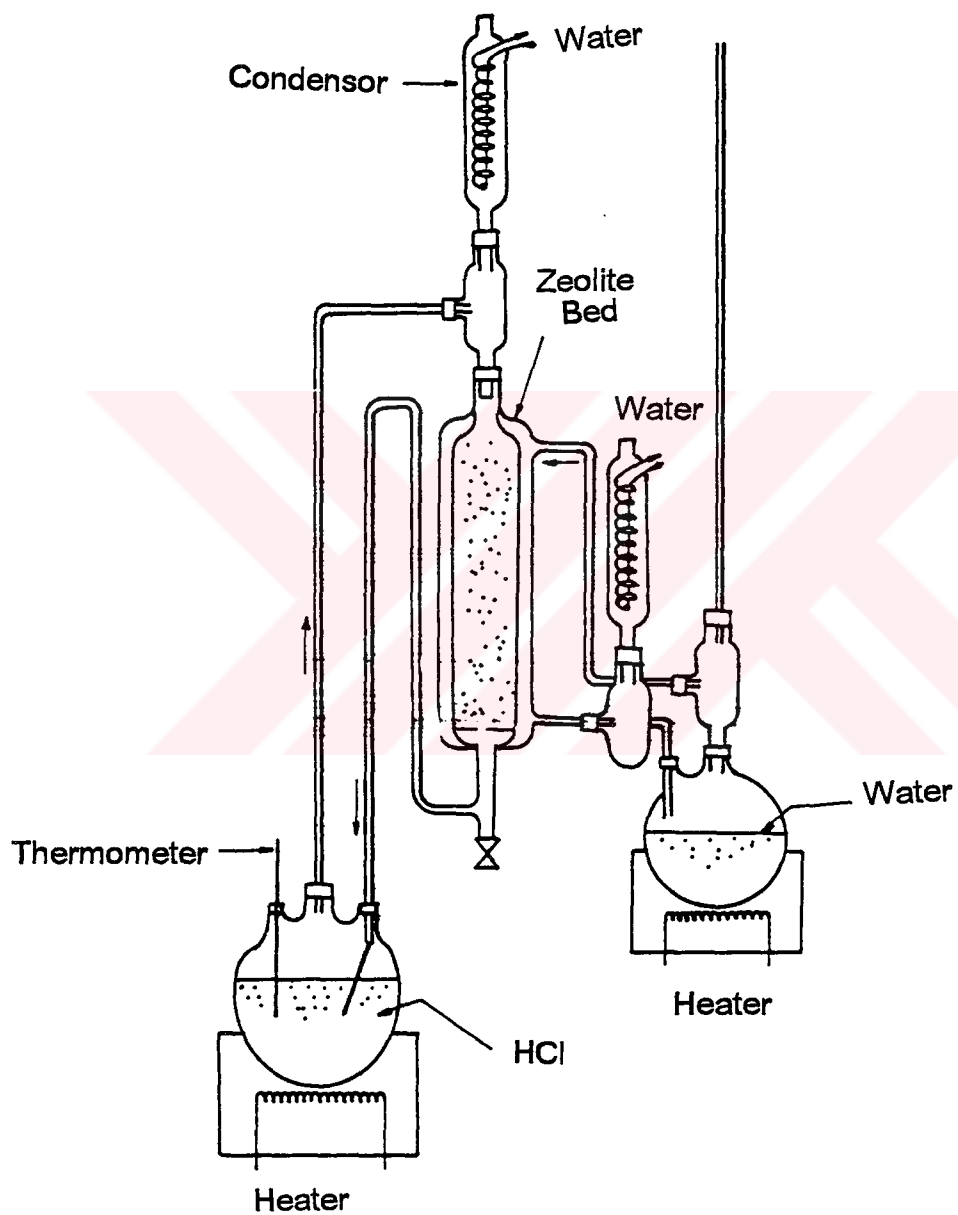


Figure 11 : Apparatus for HCl Treatment of Clinoptilolite

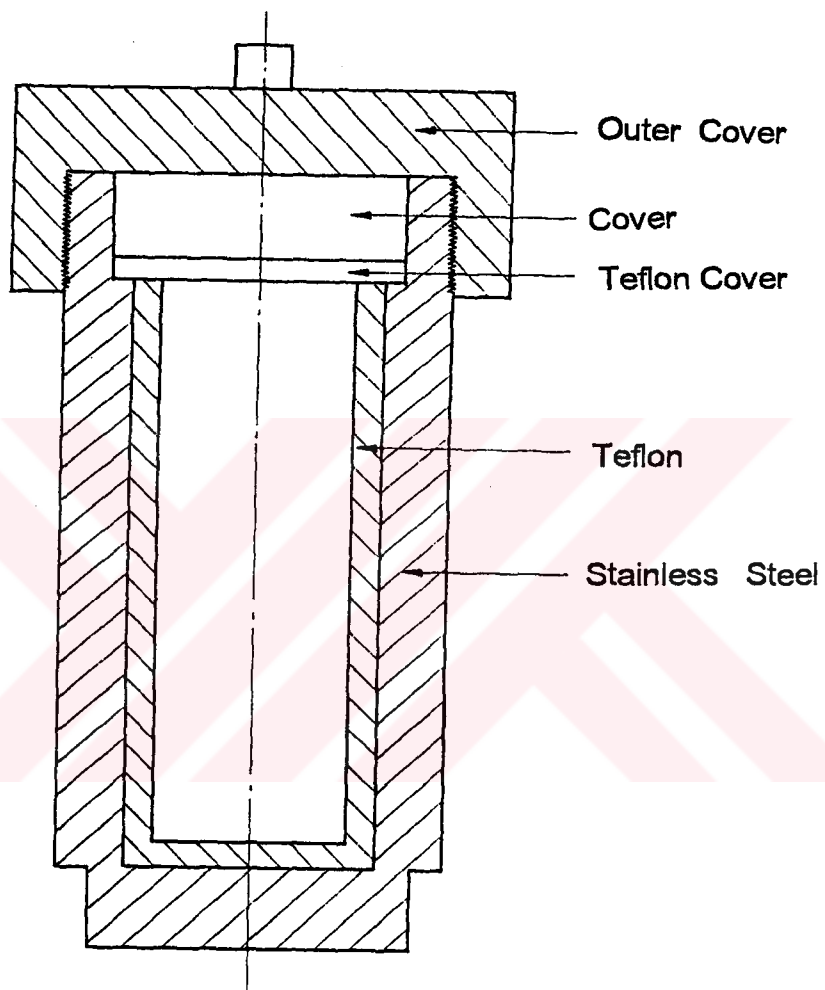


Figure 12 : Autoclave Used in ZSM-5 Synthesis

the autoclaves were removed from oven and cooled by tap water. The solid products obtained were filtered with a Buchner funnel, followed by washing with distilled water to neutrality and then drying at 110 °C overnight. Characterization of synthesized products were done by the methods described in section 4.3.

4.2.3.Preparation of H-Form of ZSM-5 Samples

In Table 9 conditions for preparation of H-form of ZSM-5 samples are given. Sample designated as R 503 was synthesized by Chemical Engineering Department of Istanbul Technical University using patent information (Argauer and Landolt ,1972) and given data. Its synthesis was carried out by use of chemicals such as colloidal silica and aluminum dry gel instead of HCl treated clinoptilolite as reactants. Characterization and transformation into H-form of it were conducted in this study. It was used as a reference sample for catalytic tests of this study.

Synthesized ZSM-5 samples were first calcined in air at 550 °C for 16 hours to remove TPA^+ in the intracrystalline channels. Then, they were subjected to ion exchange with 1 M NH_4Cl solution using 100 cm^3 of solution/g of sample at 80 °C by means of JULABO SW-20 C Shaker. The sample designated as R 312 was ion exchanged for 8 hours however, the samples R 314 and R 503 were ion exchanged for 16 hours. Finally all of them were calcined in air at 550 °C for 3 hours to remove NH_4^+ in the form of NH_3 . In Table 9 H-form preparation conditions of catalyst samples are given.

Table 9 : Conditions for Preparation of H-Form of ZSM-5 Samples

Catalyst Type	Calcination		Ion Exchange			Calcination	
	Temperature (°C)	Time (h)	Concentration (M)	Temperature (°C)	Time (h)	Temperature (°C)	Time (h)
R 312	550	16	1	80	8	550	3
R 314	550	16	1	80	16	550	3
R 503	550	16	1	80	16	550	3

4.3. Catalyst Characterization

Characterization of natural zeolite and prepared ZSM-5 samples were made by using X-ray Diffractometer (XRD) Infrared Spectrophotometer (IR), Thermal Gravimetric Analyzer (TGA), and chemical analysis.

4.3.1. XRD

This is the most widely used technique for zeolite characterization. X-ray powder diffraction patterns of natural zeolite and prepared ZSM-5 samples were obtained by means of PHILLIPS PW 1729 X-Ray Diffractometer using $\text{CuK}\alpha$ radiation. In addition to phase identification, X-ray diffraction patterns of ZSM-5 samples were also used for the calculation of crystallinity which is given (Mintova et al., 1992) as :

$$\text{Crystallinity (\%)} = \frac{\text{Peak area between } 2\theta = 22^\circ - 25^\circ \text{ of the solid product}}{\text{Peak area between } 2\theta = 22^\circ - 25^\circ \text{ of the reference sample}} \times 100 \quad (9)$$

Reference sample used for crystallinity calculations in this study was previously synthesized by Ufuk Gündüz in a M.Sc. study.

4.3.2. IR

In addition to XRD technique, ZSM-5 samples were also characterized by HITACHI 270-30 double beam IR Spectrophotometer.

KBr pellets were made by mixing approximately 1mg of zeolite with 300 mg of KBr.

4.3.3. TGA Analysis

Dehydration property of aluminum deficient clinoptilolite sample was investigated by using Thermogravimetric Analyzer (TGA). Thermogravimetric curves of ZSM-5 sample after its synthesis and calcination at 550 °C for 16 hours were obtained to see whether these conditions are sufficient for calcination by the same analyzer. Desorption of ammonia adsorbed on fresh catalysts at room temperature was studied by DU PONT 951 TGA apparatus in an attempt to investigate the surface acidity of catalyst samples. Ammonia was desorbed into nitrogen stream having a flow rate of 30 ml / min by heating the samples at to a rate of 15 °C / min. Finally coking characteristics of tested catalyst samples were determined by the same apparatus.

4.3.4. Chemical Analysis

Chemical composition of natural clinoptilolite, HCl treated clinoptilolite and ZSM-5 samples was determined by wet chemical methods developed for silicate rocks and minerals (Easton, 1972).

4.3.5. Surface Area Measurement

Since the measurement of the surface area of molecular sieves by nitrogen adsorption using the BET equation is not appropriate due to volume filling adsorption mechanism the estimation of surface area for

zeolites can be made by utilizing a modified BET equations for limited multilayer adsorption, Langmuir equation and the de Boer t-method involving the adsorption of nitrogen in the relative pressure range of 0.1 to 0.15 (Bolton ,1976). In this study, the surface area of prepared ZSM-5 catalysts were measured by means of Micromeritics ASAP 2000 Surface Area Analyzer using Langmuir equation.

4.4. Catalytic Experiments

Candidate catalysts for benzene alkylation reaction were tested for predetermined reaction parameters in a catalyst test unit located at Research and Development Centre of Petkim in Yarımca.

4.4.1. Catalyst Test Unit

As shown in Figure 13 , alkylation catalyst test unit was composed of a reactor placed in a vertical copper tube, a benzene pump, mass flow controller and a receiver. Alkylation of benzene with ethylene was carried out in a fixed bed reactor with a continuous flow system. The reactor was heated to reaction temperature by electrical heater and hold at this temperature during runs by using a temperature controller which is connected to a thermocouple placed in the reactor bed. Benzene was pumped to the system at a rate of $7.2 \text{ cm}^3 / \text{h}$ by BIOTRONIK BT 8100 pump and ethylene flowrate was adjusted to $150 \text{ cm}^3 / \text{h}$ by BROOKS 5850 TR Mass Flowmeter and Mass Flow Controller.

4.4.2. Catalyst Tests

The specifications and composition of raw materials utilized in this study for benzene alkylation reaction are given in Tables 10 and 11.

Table 10 : Composition of Ethylene

Compound	Weight Percent
Ethylene	99.97
Methane	0.01
Ethane	0.01
Acetylene	< 5 ppm

Table 11: Specification of Benzene

Specification	Value
Specific Gravity (60/60 F)	0.8838
Distillation Range	79.4-81.2 °C
Purity	99.96 %
Sulfur	0.1 ppm
Toluene	Negligible
Water	350 ppm

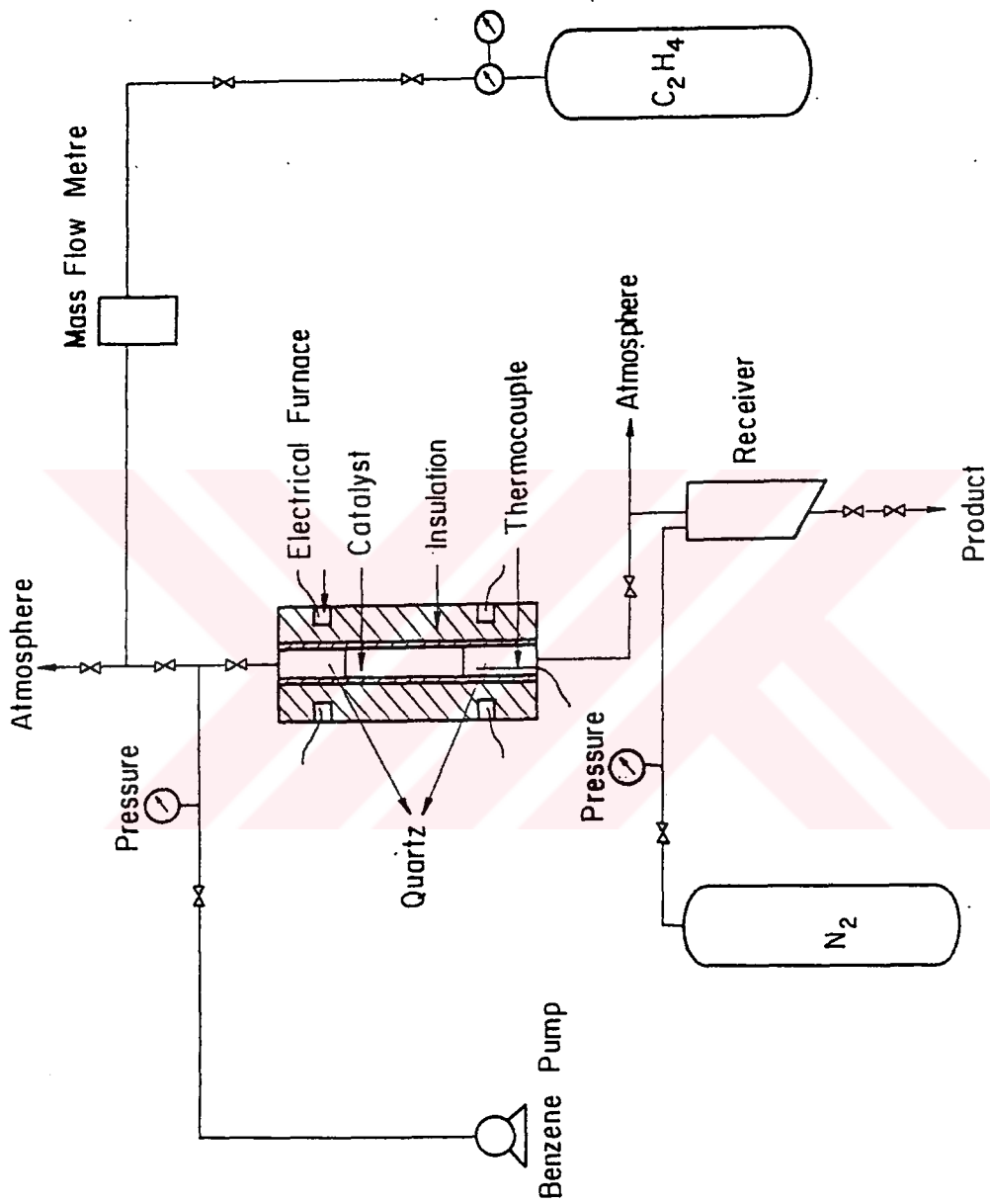


Figure 13: Catalyst Test Unit

Vibrated bulk density of catalysts was measured by using 25 ml graduated cylinder and ENGELSMANN Vibrator to determine the amount of catalyst that should be loaded to the reactor. Details of vibrated density measurement and calculation of catalyst amount are given in Appendix C. Required amount of catalyst was put at the midpoint of cylinder (35 ml) reactor and the lower and the upper portions of it were filled with quartz. Reactants were mixed prior to entering the catalyst bed and passed through the upper portion of reactor which served as a preheater. During a reaction run, product samples collected in the receiver were taken periodically and analyzed by PERKIN-ELMER 900 Gas Chromatograph. Reaction conditions at which catalytic runs were performed are given in Table 12 and the tested reaction parameters are listed in Table 13.

Table 12 : Tested Reaction Conditions

Condition	Value
Benzene LHSV	1.35 hr ⁻¹
Benzene / Ethylene (mol /mol)	13
Catalyst Volume	5.33 cm ³
Reaction Pressure	20 kg/cm ² gauge

Table 13 : Temperature Levels Used as a Variable Reaction Parameter

Catalyst	Temperature (°C)
R 503	400
R 314	400
R 314	425
R 312	400

For the reaction of interest the following definitions are given :

$$\% \text{ Benzene Conversion} = \frac{\text{Moles of Benzene Reacted}}{\text{Moles of Benzene Fed}} \times 100 \quad (10)$$

$$\% \text{ Ethylbenzene Yield} = \frac{\text{Moles of Ethylbenzene Produced}}{\text{Moles of Benzene Fed}} \times 100 \quad (11)$$

$$\text{Ethylbenzene Selectivity wrt Toluene (S}_T\text{)} = \frac{\text{Rate of Ethylbenzene Produced}}{\text{Rate of Toluene Produced}} \quad (12)$$

$$\text{Ethylbenzene Selectivity wrt Polyethylbenzenes}(S_p) = \frac{\text{Rate of Ethylbenzene Produced}}{\text{Rate of Polyethylbenzenes Produced}} \quad (13)$$

$$\text{Ethylbenzene Selectivity} = \frac{\text{Moles of Ethylbenzene Produced}}{\text{Moles of Benzene Reacted}} \times 100 \quad (14)$$



CHAPTER V

RESULTS AND DISCUSSION

5.1. Effect of HCl Pretreatment on Clinoptilolite Composition and Crystallinity

When clinoptilolite was treated with HCl acid, as a result of cation exchange and dealumination, its chemical composition was changed. The natural clinoptilolite was designated as N-CL while the samples treated with 4 and 6 M HCl were designated as 4H-CL and 6H-CL respectively. HCl treatment of clinoptilolite resulted in ion exchange of existing cations by hydrogen ions and hydrolysis of Al-O-Si bonds (Yücel and Çulfaz,1988). As a result, aluminum is extracted from the framework structure and hence $\text{SiO}_2 / \text{Al}_2\text{O}_3$ ratio is increased.

Table 14 : Variation of $\text{SiO}_2 / \text{Al}_2\text{O}_3$ Mol Ratio of Clinoptilolite with HCL Concentration

Sample	HCl Concentration (M)	Time (h)	$\text{SiO}_2 / \text{Al}_2\text{O}_3$ (mol / mol)
N-CL	-	-	6
4H-CL	4	4	11
6H-CL	6	6	27

As illustrated in Table 14, SiO₂ /Al₂O₃ mol ratio of clinoptilolite was increased from 6 to 11 by 4 M HCl treatment for 4 hours, however, 6 M HCl treatment of 6 hours caused to increase this ratio 27 which can be considered high enough for ZSM-5 synthesis.

Table 15 : Chemical Composition of Natural and HCl Treated Clinoptilolite Samples

Component	N-CL	4H-CL	6H-CL
SiO ₂	57.8200	68.3000	76.1000
Al ₂ O ₃	15.9242	10.5037	4.7910
Fe ₂ O ₃	0.6219	0.7463	0.0990
TiO ₂	0.0231	0.0230	0.0100
Na ₂ O	1.6981	0.4447	0.3234
K ₂ O	3.2055	2.2173	0.5302
CaO	3.7500	1.4250	0.4000
MgO	1.9020	0.8230	0.1666
H ₂ O	12.3674	12.3876	12.5127
Total	97.0930	96.5706	94.9329
$\frac{\text{Na}_2\text{O} + \text{K}_2\text{O} + \text{CaO} + \text{MgO}}{\text{Al}_2\text{O}_3}$	1.11	0.74	0.47

Table 15 indicates the chemical composition of natural and aluminum deficient clinoptilolite samples. As can be seen from this table, the exchangeable cations were replaced by hydrogen ion, but

complete decationation was not obtained even treatment with 6 M HCl. Natural clinoptilolite sample lost its 81 % sodium content, 83 % potassium , 90 % calcium and 91 % magnesium content as a result of 6 M HCl treatment. The chemical analysis of zeolites should show a $Me_{2n}O / Al_2O_3$ ratio of unity. A ratio above unity indicates nonzeolitic cations are present and a ratio below unity indicates that cations has been removed from the zeolite framework and replaced by hydrogen ions. N-CL sample has nearly $Na_2O + K_2O + CaO + MgO / Al_2O_3$ ratio of unity. Replacement of hydrogen ions was confirmed for both 4H-CL and 6H-CL sample from their corresponding ratio.

Figure 14 represents the X-ray powder patterns of N-CL, 4H-CL and 6H-CL samples. It is evident from this figure that crystallinity of clinoptilolite samples was affected by HCl treatment. A large intensity loss and broadening of peaks at Bragg angle (2θ) of 9.9° , 22.4° , 26.8° and 30.2° was observed for 6 H-CL sample.

5.2. ZSM-5 Synthesis Results

5.2.1. Effect of SiO_2 / Al_2O_3 Mol Ratio of Clinoptilolite on ZSM-5 Synthesis

ZSM-5 synthesis was carried out by using N-CL, 4H-CL and 6H-CL samples having different SiO_2 / Al_2O_3 mol ratios at $TPA^+ / TPA^+ + Na^+$ ratio of 0.5. When the X-ray diffraction patterns represented in Figure 15 a and b are compared with those in Figure 14 a and b , it is evident that no transformation to ZSM-5 was obtained with the samples of N-CL ($SiO_2 / Al_2O_3 = 6$) and 4H-CL ($SiO_2 / Al_2O_3 = 11$). In other words, the products obtained utilizing these samples by hydrothermal

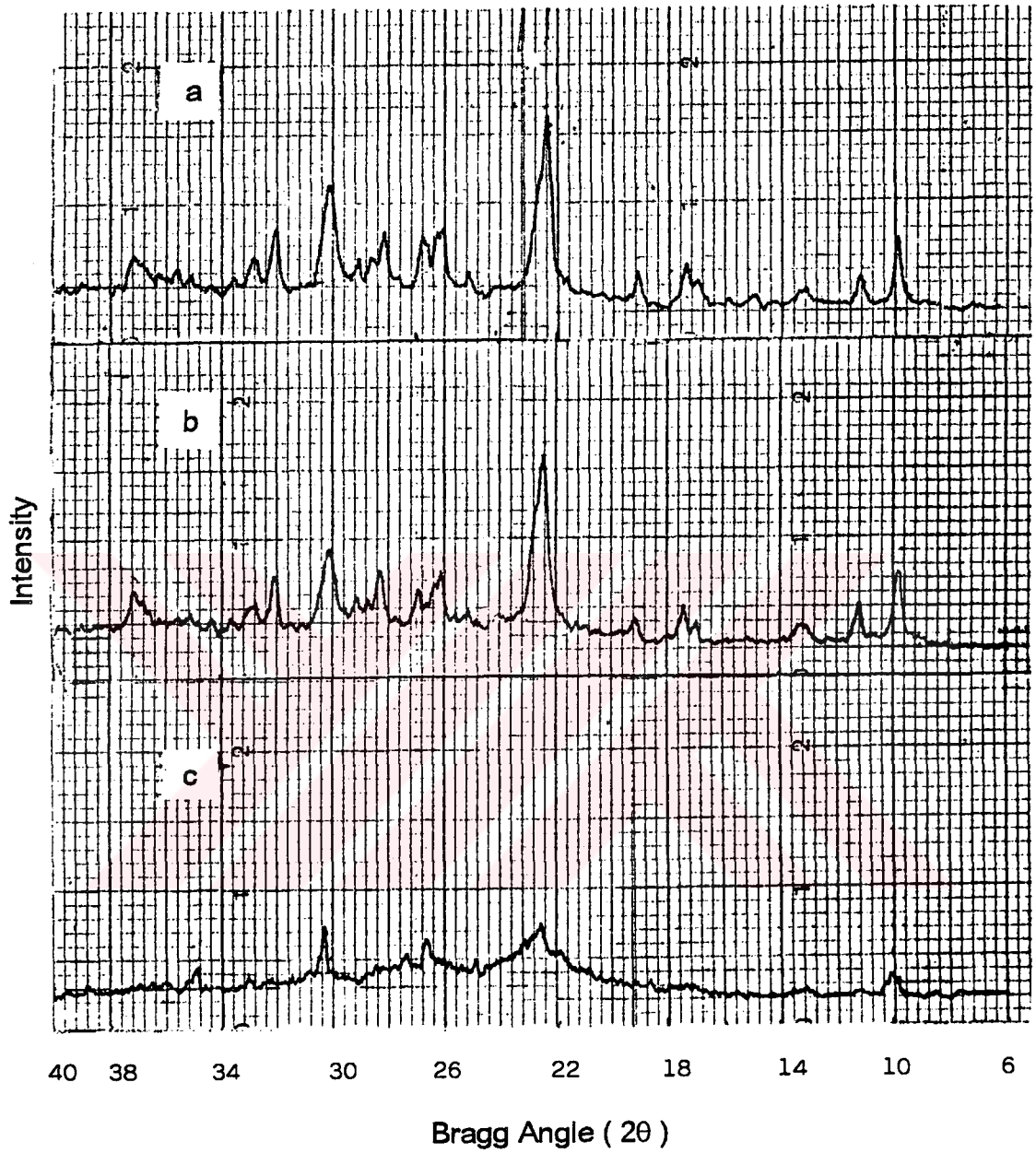


Figure 14 : X-ray Diffraction Patterns of Natural and HCl Treated Clinoptilolite Samples

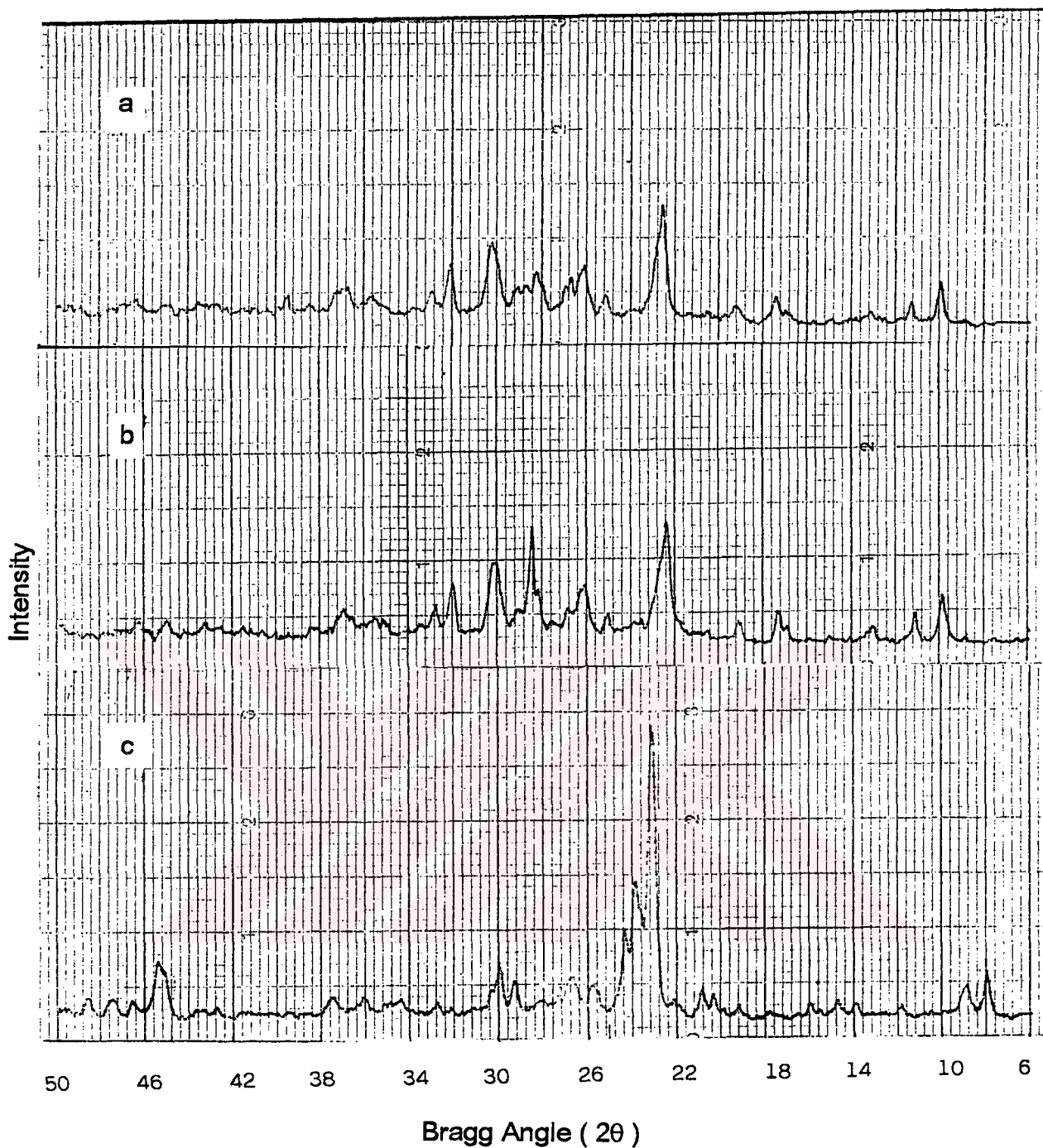


Figure 15 : Effect of $\text{SiO}_2 / \text{Al}_2\text{O}_3$ Mol Ratio on ZSM-5 Synthesis

- a. X-ray Diffraction Patterns of the Product Obtained by Utilizing Natural Clinoptilolite Sample ($\text{SiO}_2 / \text{Al}_2\text{O}_3 = 6$)
- b. X-ray Diffraction Patterns of the Product Obtained by Utilizing HCl Treated Clinoptilolite Sample ($\text{SiO}_2 / \text{Al}_2\text{O}_3 = 11$)
- c. X-ray Diffraction Patterns of the Product Obtained by Utilizing HCl Treated Clinoptilolite Sample ($\text{SiO}_2 / \text{Al}_2\text{O}_3 = 27$)

reaction have the same characteristic peaks of clinoptilolite. The only difference is that, product of 4H-CL sample had a wider peak at $2\theta = 28.4^\circ$. On the other hand 6H-CL ($\text{SiO}_2/\text{Al}_2\text{O}_3 = 27$) sample yielded single phase of a product which was characterized as ZSM-5 in a manner described in section 5.3.1. The corresponding hydrothermal reactions were conducted at 180°C for 110 hours.

5.2.2. Variation of ZSM-5 Crystallinity with $\text{TPA}^+ / \text{TPA}^+ + \text{Na}^+$ Ratio

ZSM-5 synthesis is carried out in the presence of an organic cation which has a structure directing role. Zeolite cages are formed around them during nucleation. Therefore to investigate the effect of organic cation amount on ZSM-5 crystallinity at 3 different values of $\text{TPA}^+ / \text{TPA}^+ + \text{Na}^+$ ratio ZSM-5 samples were synthesized using 6H-CL sample at 180°C for 110 hours and the results are tabulated in Table 16. X-ray diffraction patterns of the samples synthesized at $\text{TPA}^+ / \text{TPA}^+ + \text{Na}^+$ ratios of 0.29 and 0.8 represented in Figure 16 a and c respectively show that, both of the samples have a peak at 44.6° having a high intensity and a new peak at 38.5° . In addition, the former sample exhibits a sharp peak at 26.6° . Peak location and intensities of the sample represented in Figure 16 b are similar to those of the reference sample whose X-ray diffraction pattern given is in Appendix F. The crystallinity of these three samples were calculated by equation 9 reported in section 4.3.1. As shown in Table 16, the highest ZSM-5 crystallinity was obtained when $\text{TPA}^+ / \text{TPA}^+ + \text{Na}^+$ ratio is equal to 0.5.

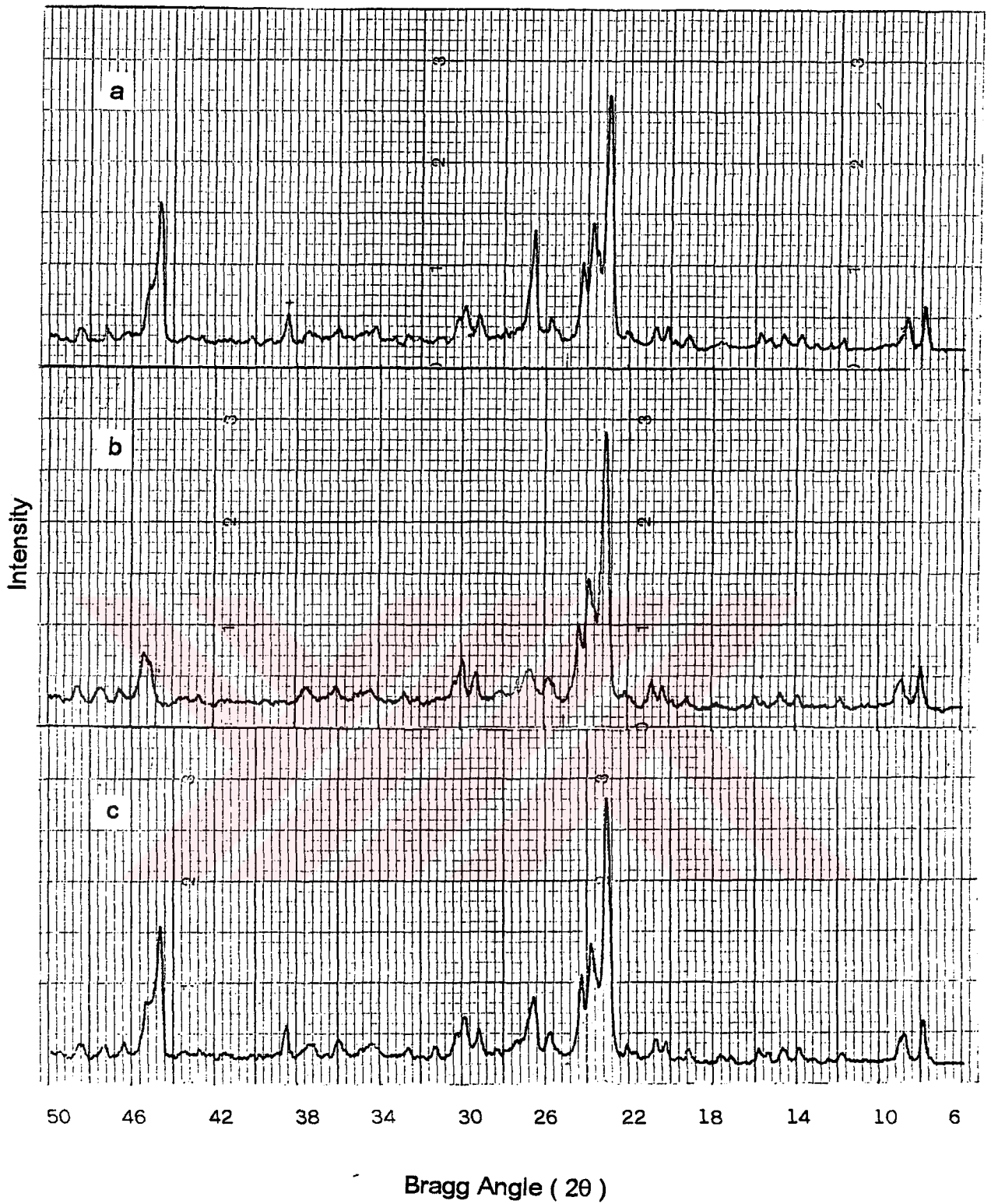


Figure 16 : Effect of TPA⁺ / TPA⁺ + Na⁺ Ratio on ZSM-5 Crystallinity

a. 0.29

b. 0.5

c. 0.80

Table 16 : Effect of $\text{TPA}^+ / \text{TPA}^+ + \text{Na}^+$ Ratio on ZSM-5 Crystallinity

Sample	$\text{TPA}^+ / \text{TPA}^+ + \text{Na}^+$	Crystallinity (%)
R 300	0.29	63
R 310	0.50	74
R 320	0.80	68

5.3. Catalyst Characterization Results

5.3.1. XRD

The solid products of hydrothermal reaction were first analyzed by means of XRD for their phase identification. After identifying them as ZSM-5, the one which has the highest crystallinity was selected to be used in catalyst tests. The X-ray diffraction pattern of this as-synthesized sample is found to be very similar to those of the reference sample and the exact peak locations and calculated relative intensities are listed in Table F.1 in Appendix F . As-synthesized sample was subject to various treatments to transform it into H-form and two different samples (R 312 and R 312) were obtained from it as explained in section 4.2.3. X-ray diffraction patterns of the as-synthesized and R 314 sample are illustrated in Figure 17 a and b respectively. Some modifications took place in the crystal structure during preparation steps of H-form. It is evident that the crystallinity of as-synthesized sample decreases from 73 % to 69 %. The second modification was that the first two peaks at about 7.8° and 9° were intensified due to removal of organic template by calcination in air at 550°C for 16

hours. Another difference between as-synthesized and R 314 samples is that the intensity of the peaks at about 14.0° , 14.8° , 15.6° , 16.0° and 27° is increased, but that of at 27.6° and 30.0° is decreased. The intensity changes can be explained as the consequence of removal of extraframework species present as impurities. In Figure 18 a and b X-ray diffraction patterns of the as-synthesized and R 312 samples are represented respectively. The treatments necessary for converting as-synthesized sample into R 312 lowered its crystallinity from 73 % to 67 %. The modifications observed in the X-ray diffraction pattern of R 312 sample are similar to that of R 314. Figure 19 a and b shows respectively the X-ray diffraction patterns of the reference sample of catalytic tests (R 503) taken after its synthesis and transforming into H-form. Its crystallinity was decreased from 76 % to 73 % after the treatments. Similar to the samples R 312 and R 314, a considerable increase in intensity was observed for the first two peaks nearly occurring at 8.1° and 9.2° for the same reason. Intensification of the peaks at about 14.2° , 15.0° , 15.8° , 16.2° , 18.0° and 28.4° can also be considered to occur due to removal of amorphous species present in its structure.

In Figure 20 the X-ray diffraction patterns of the catalyst samples (R 312, R 314 and R 503) tested at 400°C under 20 kg / cm^2 gauge pressure are shown. The crystallinity of sample R 503 was found as 72 % after the reaction and a decrease in intensity of the first two peaks at 8° and 9.2° was observed. Except for such intensity differences, the X-ray diffraction pattern of R 503 can be considered as unchanged. Similarly intensities of the first two peaks at 8.2° and 9.0° were lowered in sample R 314 and no change in its crystallinity was observed during the reaction. Different from these two samples,

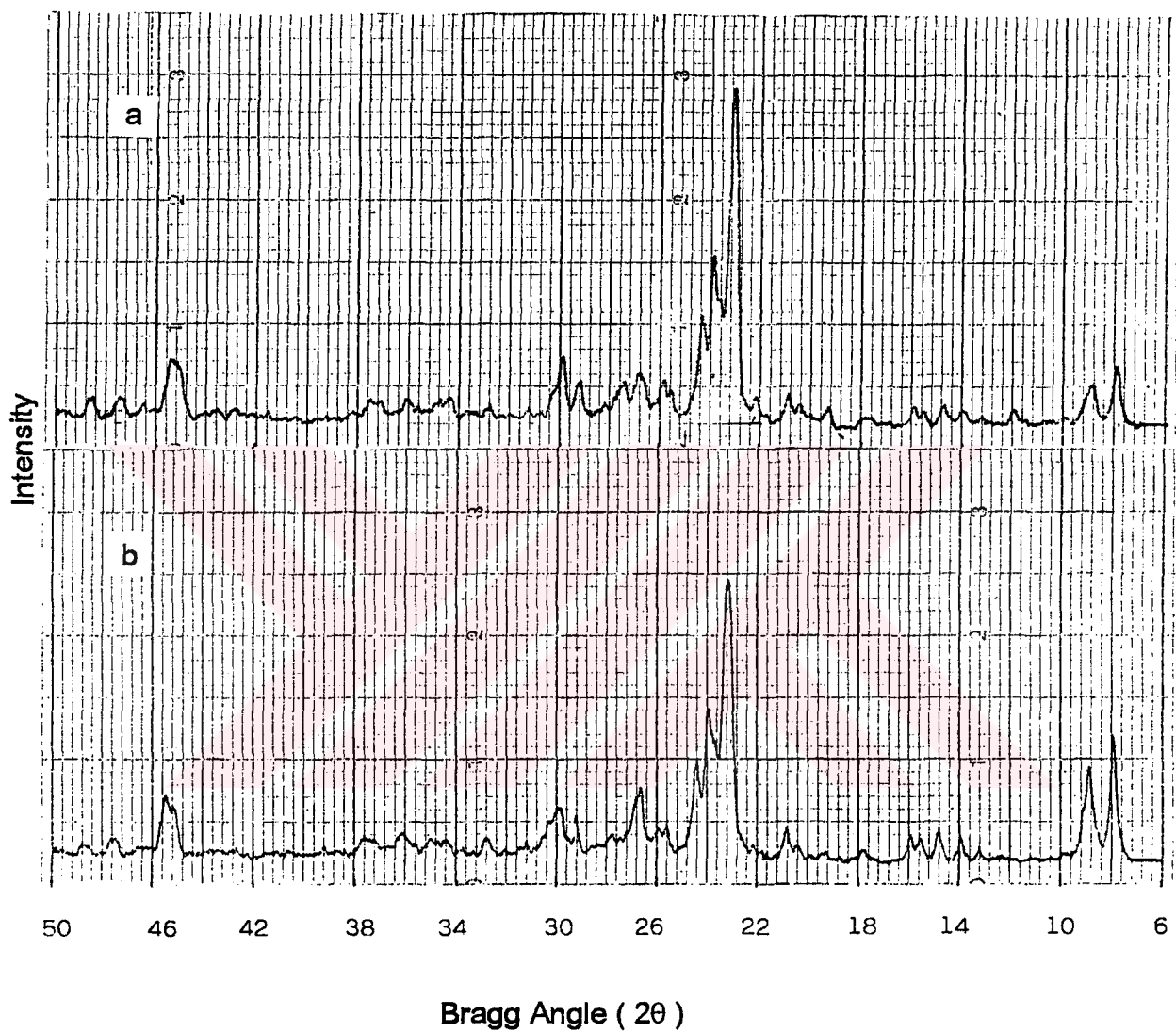


Figure 17 : X-ray Diffraction Pattern of Sample R 314

a. As-synthesized Form

b. After Transforming into H-Form

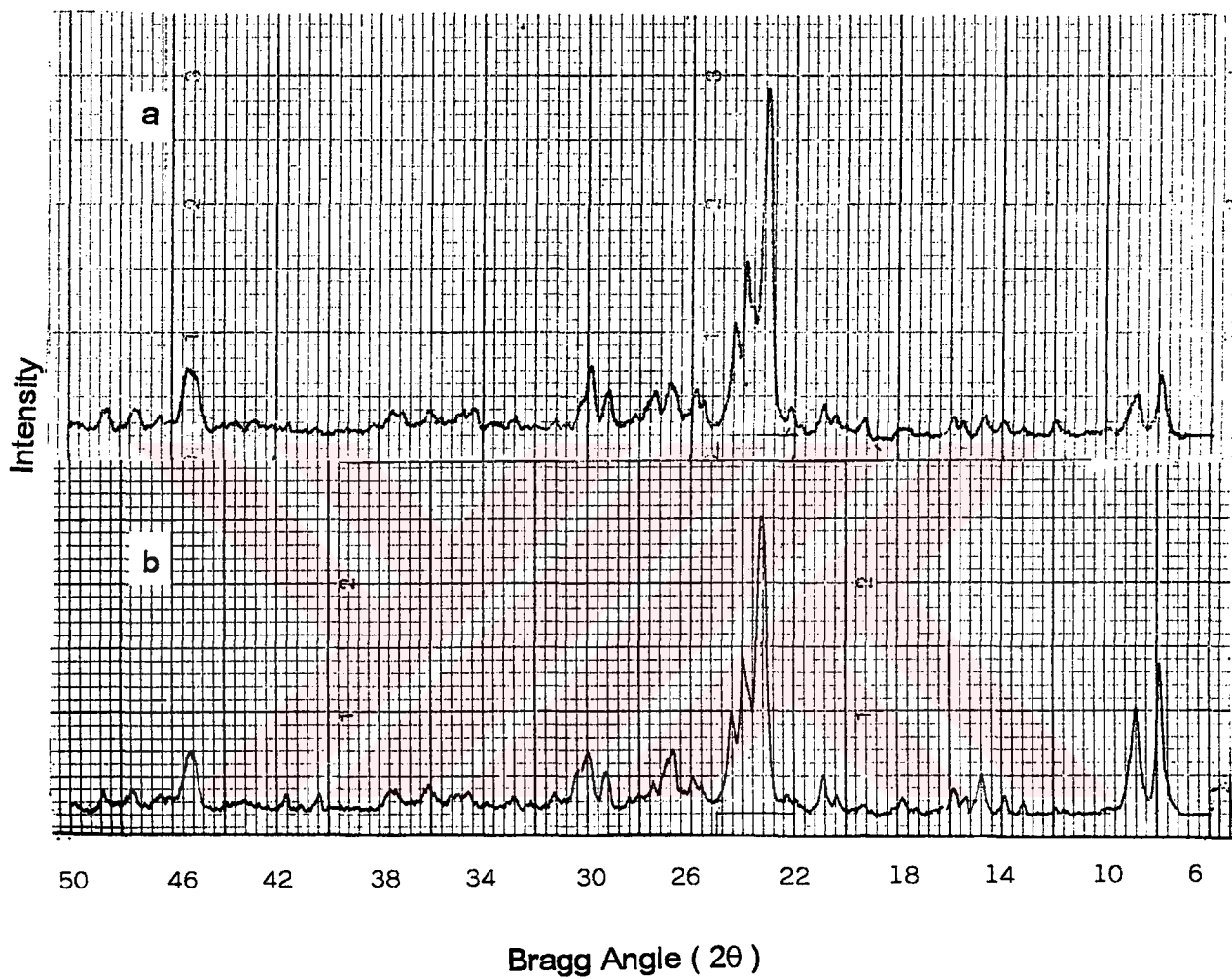


Figure 18 : X-ray Diffraction Pattern of Sample R 312

a. As-synthesized Form

b. After Transforming into H-Form

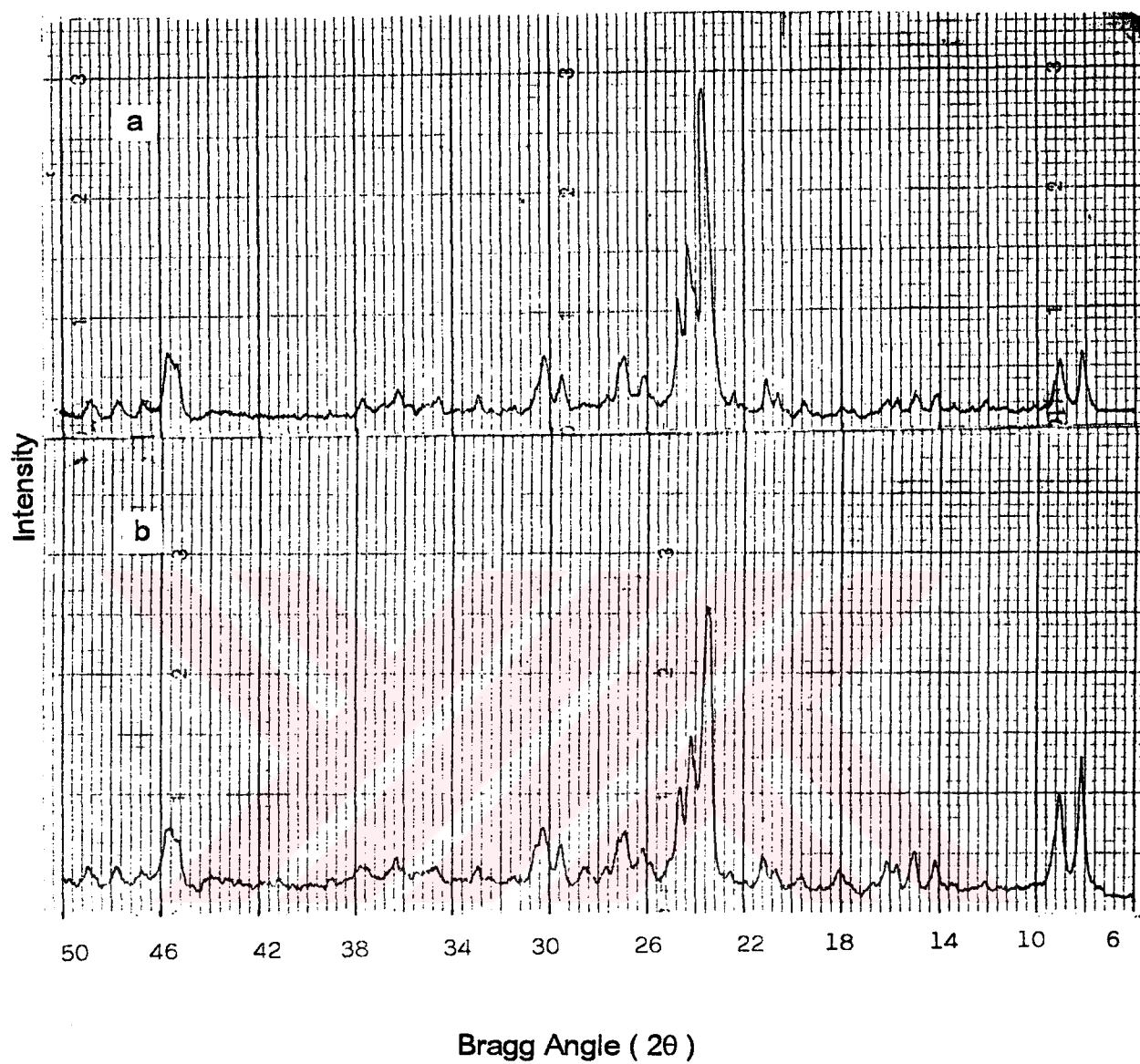


Figure 19 : X-ray Diffraction Pattern of Sample (R 503) Used as Reference

in Catalytic Tests

a. As-synthesized Form

b. After Transforming into H-Form

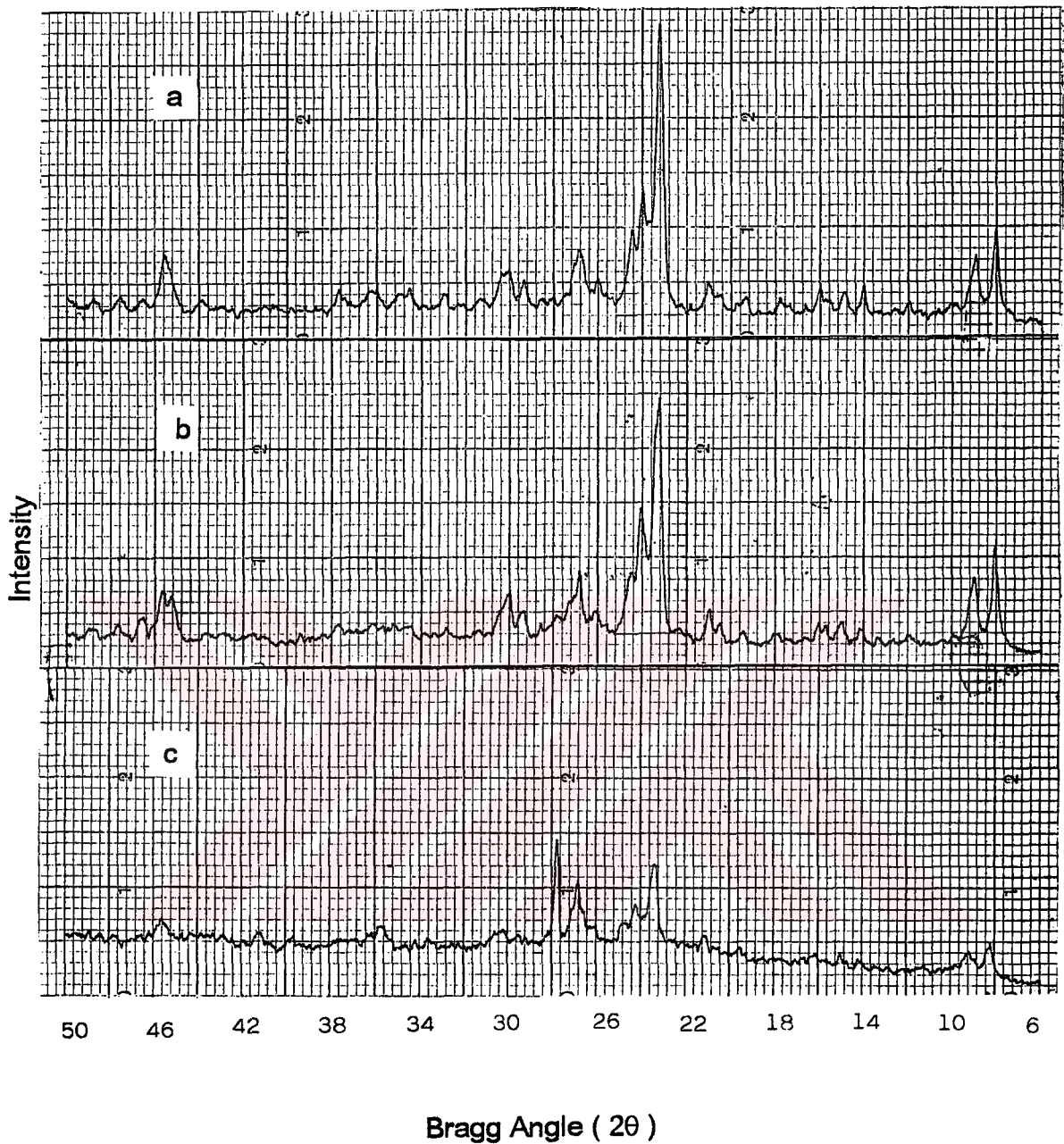


Figure 20 : X-ray Diffraction Patterns of the Catalyst Samples
 Tested in Vapor Phase Alkylation Reaction at 400 °C
 and 20 kg /cm² gauge Pressure
 a. R 503 b. R 314 c. R 312

R 312 lost its crystallinity to such an extent that a large intensity loss of peaks at 8.2° , 9.0° , 23.4° and 26.9° was observed.

5.3.2. IR

Infrared spectrum of sample R 314 at the mid infrared region ($1500-400\text{ cm}^{-1}$) is shown in Figure 21. According to Flanigen (1976), the absorption peaks at 1100, 800-700 and 450 cm^{-1} are characteristic for highly siliceous materials. These bands correspond to asymmetric stretching, symmetric stretching and the bending modes of $(\text{Si,Al})\text{O}_4$ tetrahedra. Jacobs et al.(1981) reported that ZSM-5 has the characteristic absorption bands near 1200 and 550 cm^{-1} which are related to five-membered ring chains and blocks respectively (Jansen et al., 1984) . As shown in Figure 21, both of these bands are observed for the sample.

5.3.3. TGA

Since TPA^+ found in the intracrystalline pores of ZSM-5 can't be removed by ion exchange because of its size, it should be removed by thermal decomposition. In Figure 22 a and b , the thermogravimetric curves of ZSM-5 sample after its synthesis and after calcination at 550°C for 16 hours presented respectively. A considerable weight loss which belongs to TPA^+ decomposition occurred at a temperature range of 600-800 K for as-synthesized sample. Disappearance of this peak in Figure 22 b shows that calcination conditions were sufficient to decompose TPA^+ . The peak occurred at 314 K corresponds to desorption of the water found in the void of the sample.

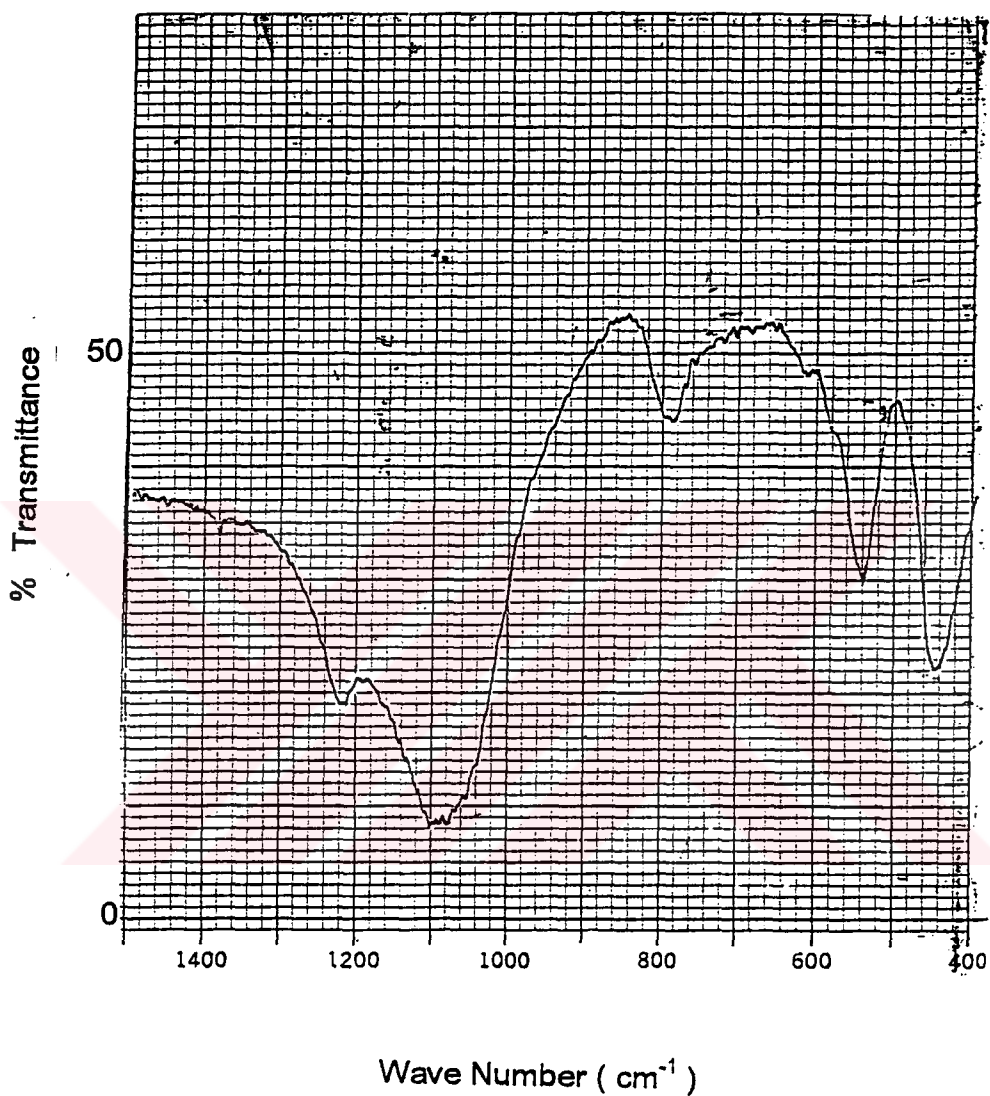


Figure 21 : Infrared Spectrum of As-synthesized Sample

Dehydration property of 6H-CL sample was investigated and it was observed from Figure 23 that, two kinds of water are found in clinoptilolite structure. The first kind evolves up to 400 K and the second kind evolves slowly after 400 K until 1100 K.

Prior to ammonia desorption measurements by TGA apparatus, the catalyst samples (R 312 , R 314 and R 503) were admitted to ammonia atmosphere overnight at room temperature to allow ammonia to adsorb on them. The thermogravimetric curves of samples R 312 and R 314 obtained before ammonia adsorption to investigate the behavior of water in their voids are represented in Figures 24 and 25 respectively. Figures 26 through 28 show the TGA analyses of an ammonia desorption experiment conducted with calcined R 312 , R 314 and R 503 samples. Although they are calcined before ammonia adsorption a noticeable weight loss at a temperature range of 25 - 200 °C was observed for all of them due to desorption of water. Since ammonia solution was used , water present in it was taken by catalyst samples. Ammonia desorption started at 300 and 450 °C for samples R 312 and R 314 respectively, but at 350 - 500 °C for R 503. In Table 17, calculated amount of ammonia adsorbed, number of ammonia molecules per gram of catalyst, surface coverage, number of acid sites together with Langmuir surface area and maximum peak temperature at which ammonia desorption takes place are tabulated . Details of calculations and surface area measurement data are given in Appendix G and H respectively.

Thermal gravimetric analyses were also conducted to determine the coking characteristics which is discussed in section 5.4.5.

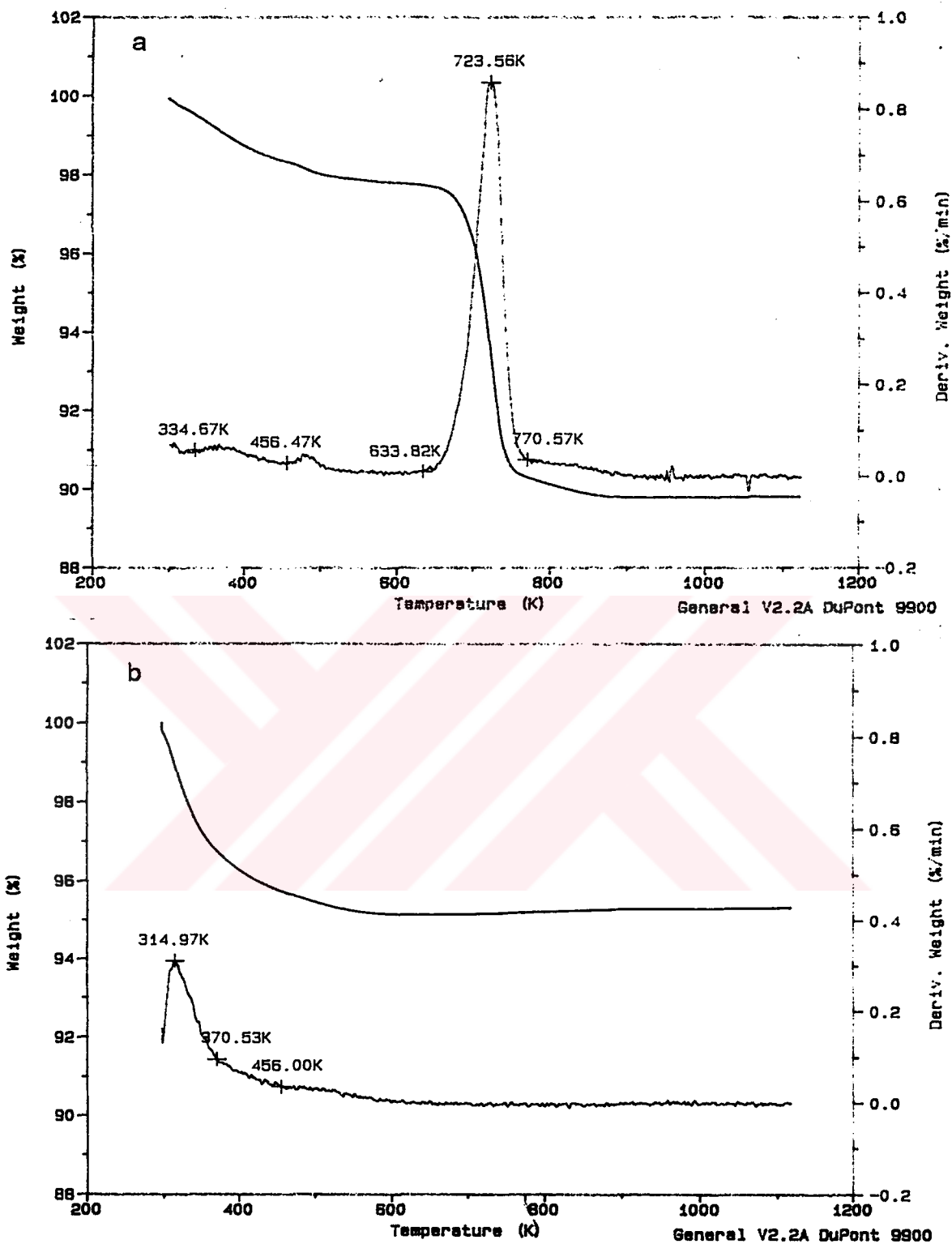


Figure 22 : Thermogravimetric Curve of

a. As-synthesized Sample

b. Sample Calcined at 550 °C for 16 Hours

TGA

Sample: H-CLINOPTILOLITE (6M 6H)
Size: 9.2160 mg
Method: AIR5
Comment: AIR 53 ml/min. HEATING: 5 C/min

File: E:CHE-TGA.02
Operator: PETROLEUM ENG.DEPT.
Run Date: 07/01/92 13:44

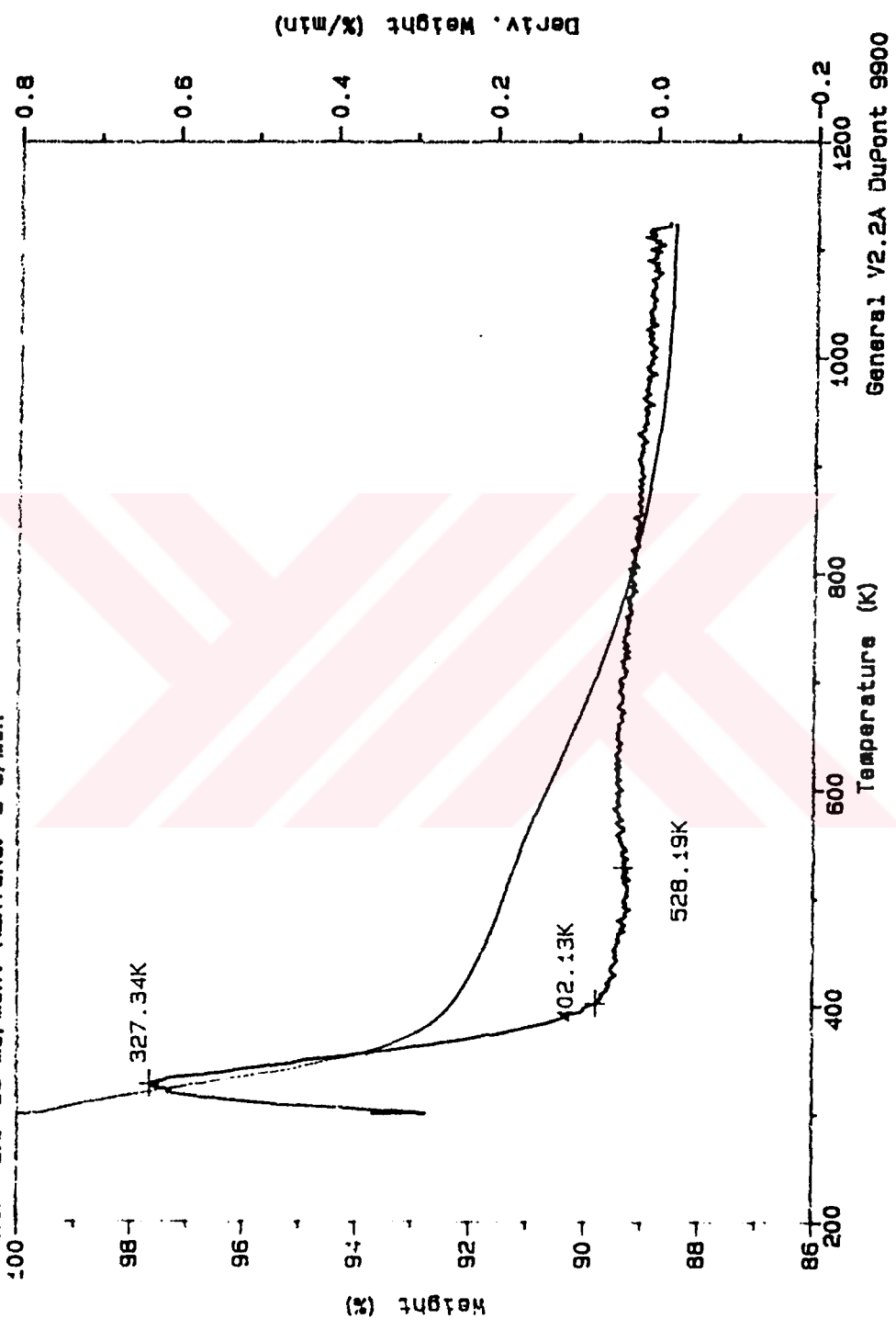


Figure 23 : Thermogravimetric Curve of HCl Treated Clinoptilolite (6H-CL)

Sample: R 312 (H-FORM)
Size: 12.6830 mg
Method: RAMP 10 C/MIN
Comment: GAS: NITROGEN, FLOW RATE: 30 ML/MIN

TGA

File: R312.2
Operator: MIHRICAN
Run Date: 7-Mar-94 10:07

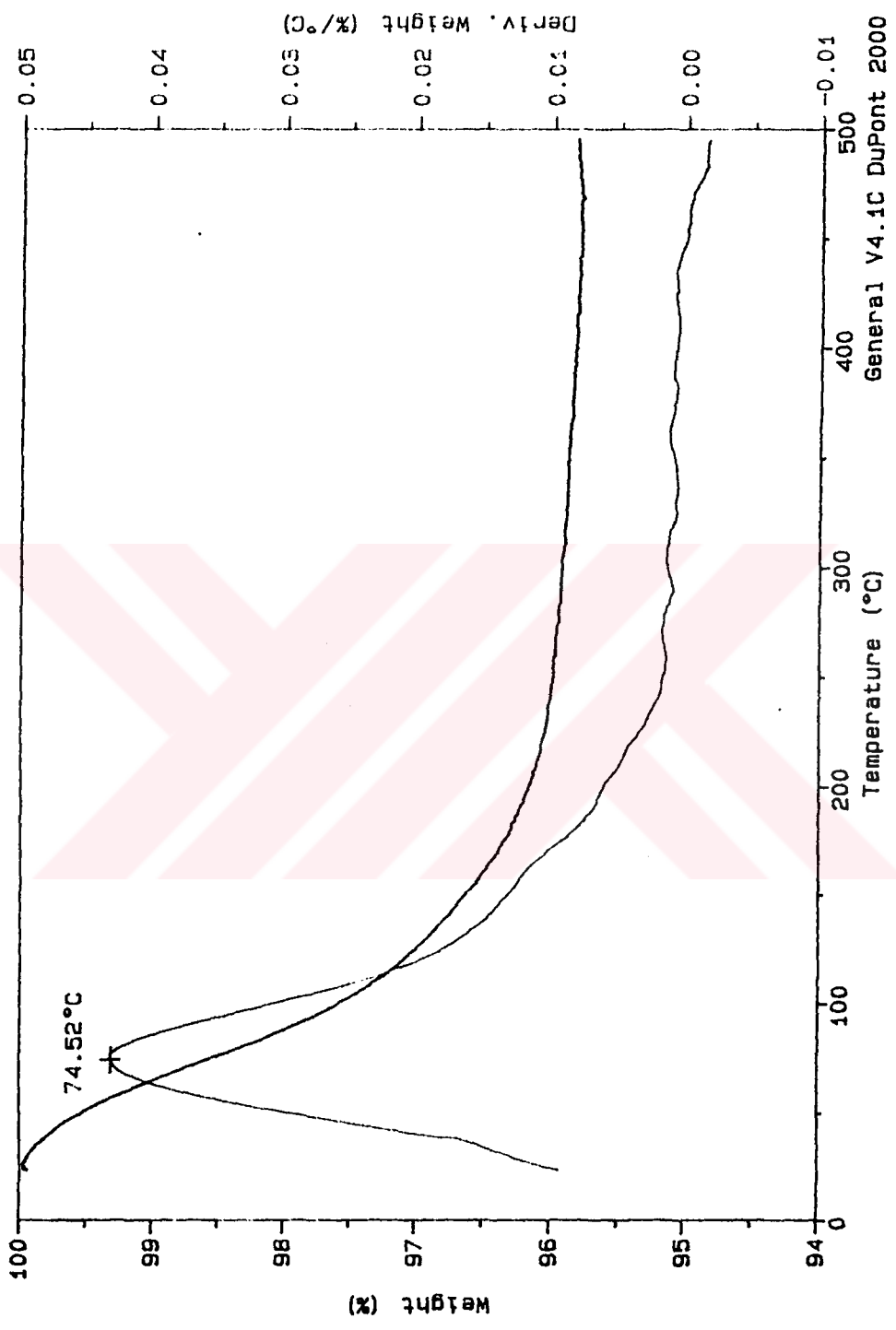


Figure 24 : Thermogravimetric Curve of R 312 Before Ammonia Adsorption

Sample: R 314 (H-FORM)
Size: 10.2460 mg
Method: RAMP 10 C/MIN
Comment: GAS: NITROGEN, FLOW RATE: 30 ML/MIN

TGA

File: R314.2
Operator: MIHRICAN
Run Date: 7-Mar-94 08:22

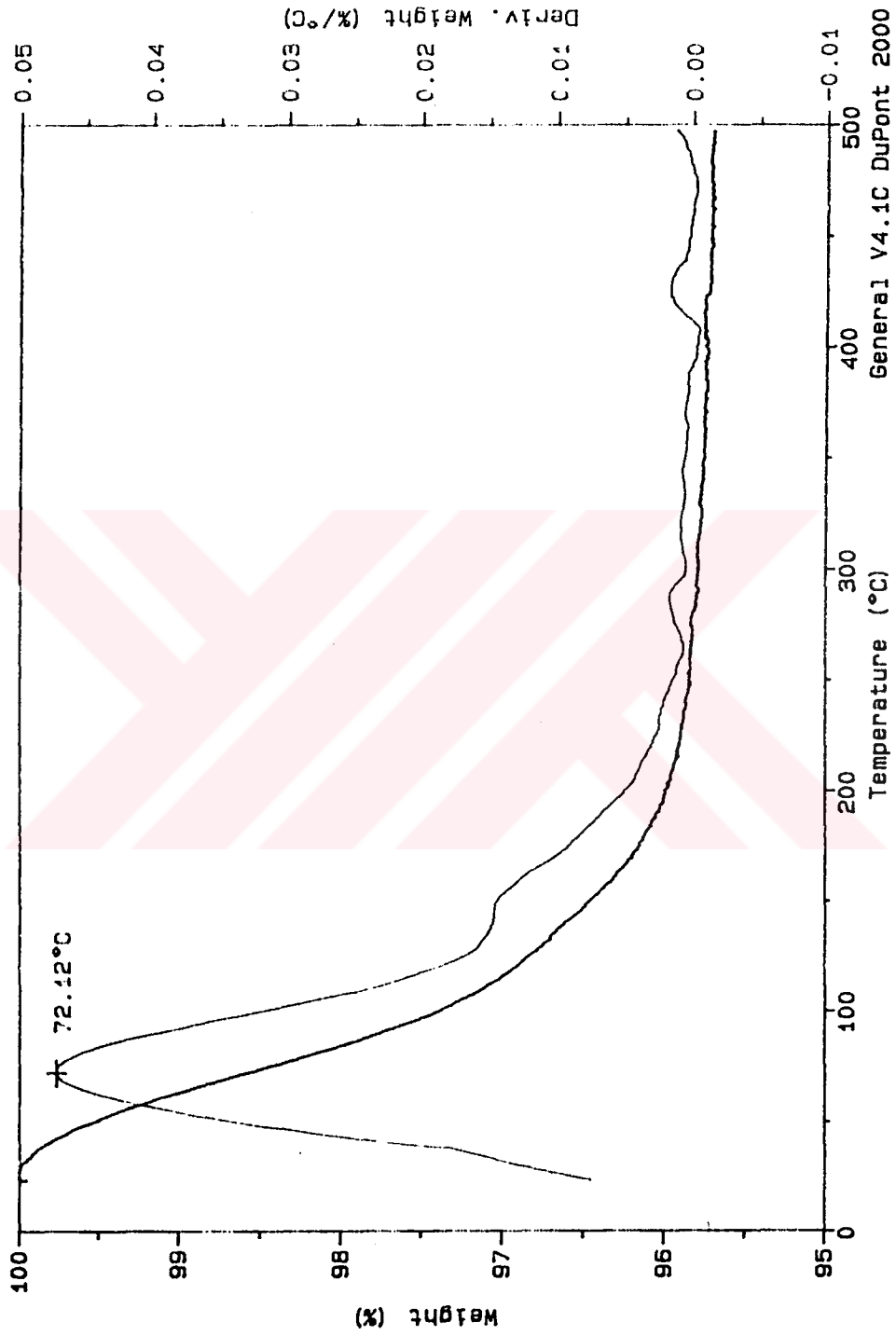


Figure 25: Thermogravimetric Curve of R 314 Before Ammonia Adsorption

Sample: R 312
 Size: 11.3780 mg
 Method: RAMP 15 C/MIN
 Comment: GAS: NITROGEN, FLOW RATE: 30 ML/MIN
 File: R312.3
 Operator: MIHRICAN
 Run Date: 8-Mar-94 09:50

TGA

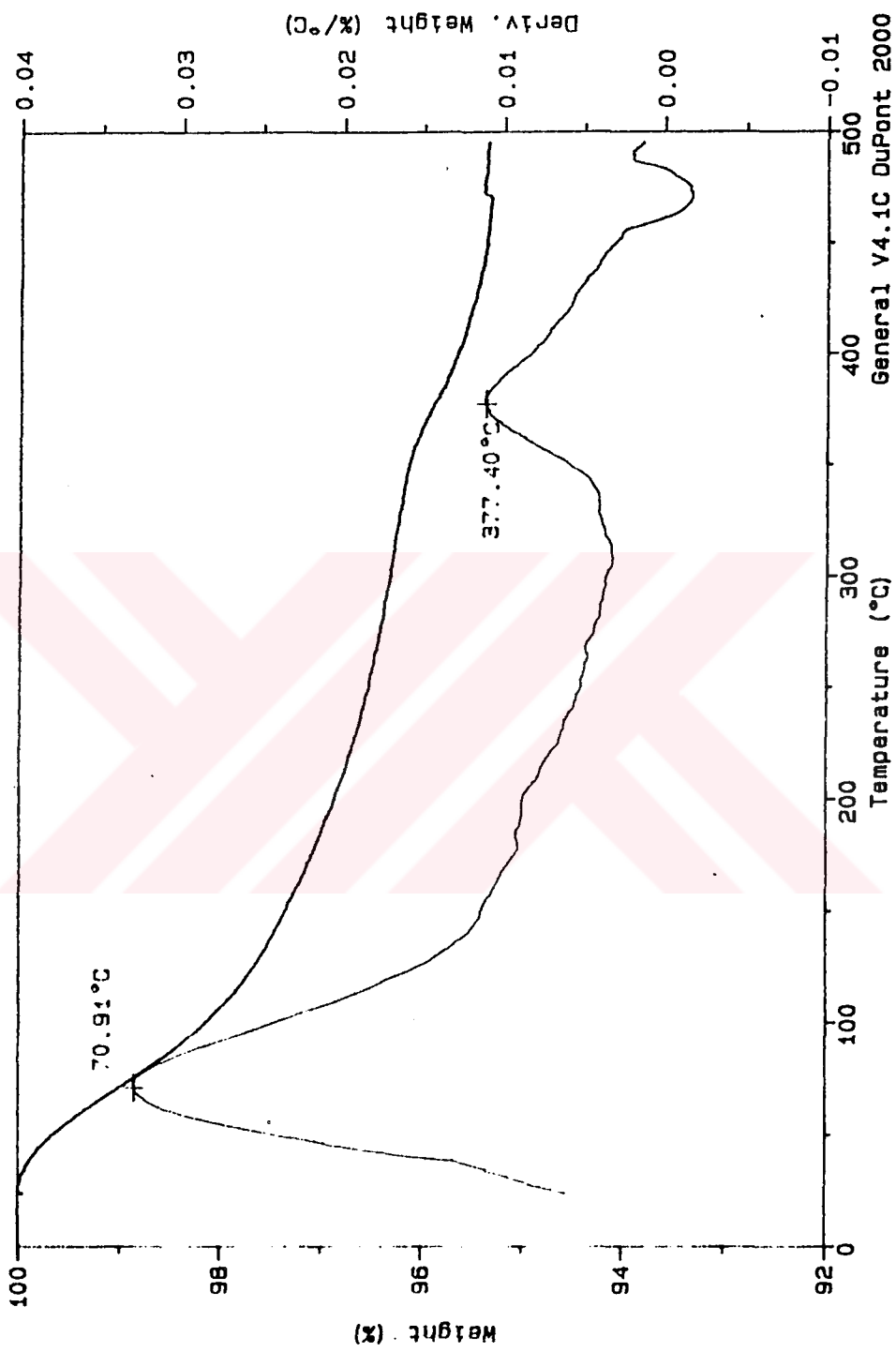


Figure 26: Thermogravimetric Curve of R 312 After Ammonia Adsorption

Sample: R 314

Size: 8.9430 mg

Method: RAMP 15 C/MIN

Comment: GAS: NITROGEN, FLOW RATE: 30 ML/MIN

TGA

File: R314.3

Operator: MIHRICAN

Run Date: 8-Mar-94 11:22

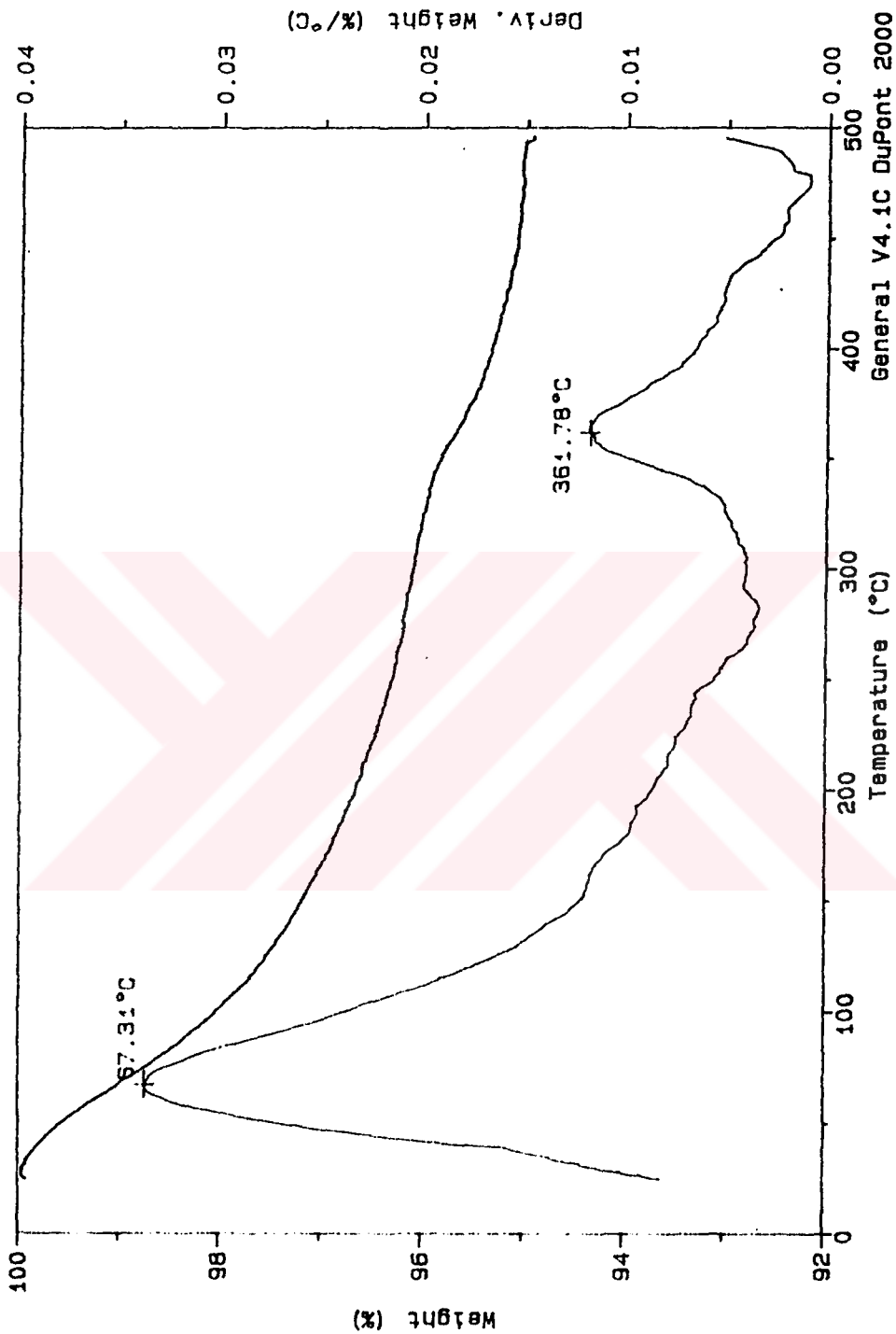


Figure 27: Thermogravimetric Curve of R 314 After Ammonia Adsorption

Sample: R 503
 Size: 31.3660 mg
 Method: RAMP 15 C/MIN
 Comment: GAS: NITROGEN, FLOW RATE: 30 ML/MIN
 File: R503.2
 Operator: MIHRICAN
 Run Date: 8-Mar-94 07:53

TGA

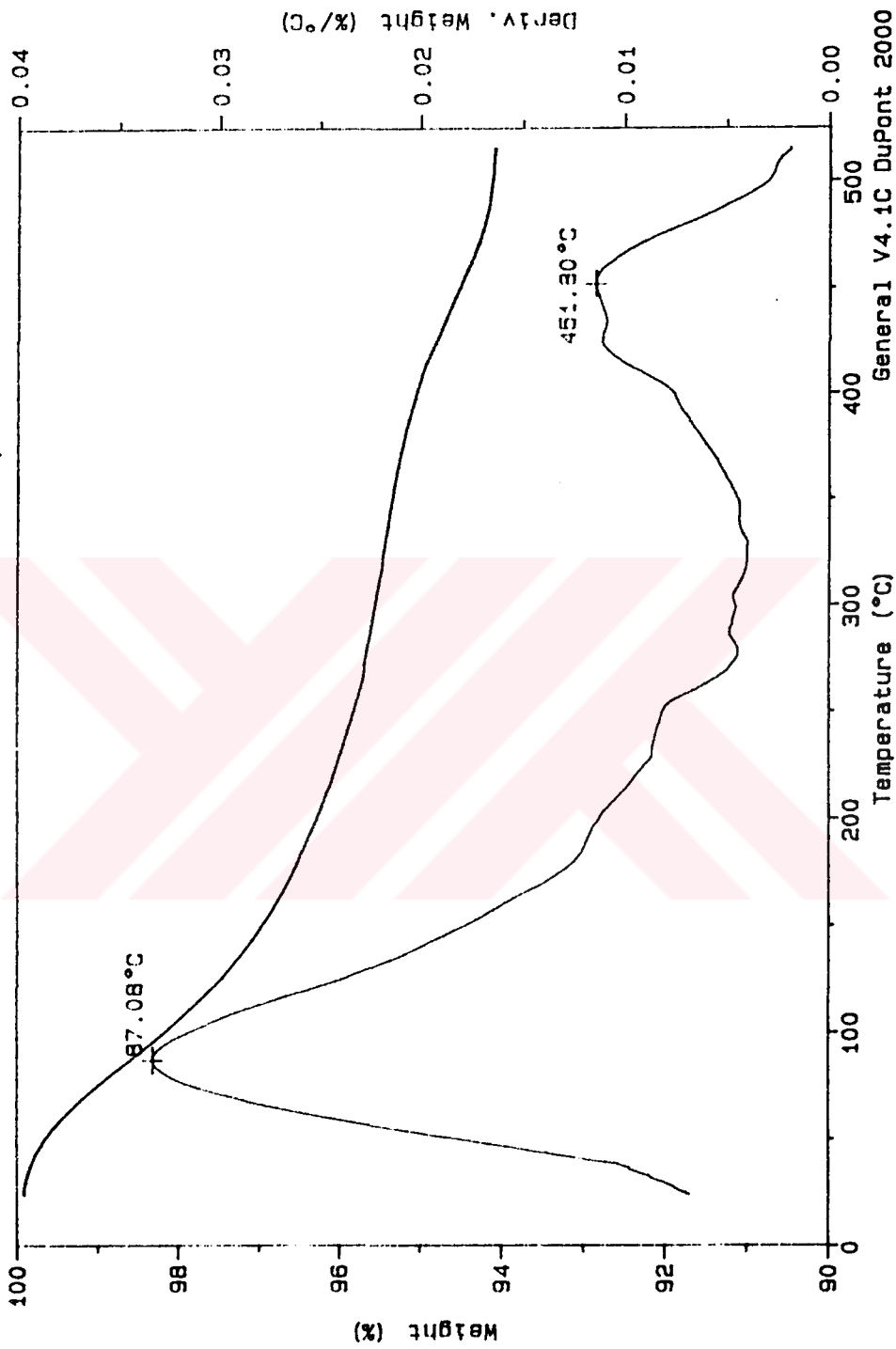


Figure 28 : Thermogravimetric Curve of R 503 After Ammonia Adsorption

Table 17 : Ammonia Desorption Data of Catalyst Samples (Heating Rate : 15 °C / min)

Catalyst	Amount of Ammonia Adsorbed (g / g _{catalyst})	Number of Ammonia Molecules Adsorbed (Molecule / g _{catalyst})	Surface Coverage (θ)	Langmuir Surface Area (m ² / g _{catalyst})	Number of Acid Sites (molecule / cm ²)	Maximum Peak Temperature (°C)
R 503	5.333 x 10 ⁻³	1.8885 x 10 ²⁰	0.075	328	5.7576 x 10 ¹³	451
R 314	3.75 x 10 ⁻³	1.3279 x 10 ²⁰	0.048	358	3.7092 x 10 ¹³	361
R 312	3.437 x 10 ⁻³	1.2172 x 10 ²⁰	0.039	396	3.073 x 10 ¹³	377

5.3.4. Chemical Analysis

Chemical compositions of catalysts tested are given in Table 18. As shown from this table, all samples have nearly the same $\text{SiO}_2 / \text{Al}_2\text{O}_3$ ratio. Samples R 312 and R 314 differ in their total alkaline content. Since sample R 503 was synthesized by use of chemicals as a silica and alumina source instead of using HCl treated clinoptilolite, it doesn't contain cations such as Ca^{+2} , Mg^{+2} , K^+ , Ti^{+3} and Fe^{+3} . $\text{Na}_2\text{O} + \text{K}_2\text{O} + \text{CaO} + \text{MgO} / \text{Al}_2\text{O}_3$ ratio of the samples shows that cations were replaced by hydrogen ions .

Table 18 : Chemical Composition of Tested Catalyst Samples

Component	R 312	R 314	R 503
SiO_2	82.7000	82.9400	84.0800
Al_2O_3	5.1400	5.0120	4.8600
Fe_2O_3	0.2125	0.2123	-
TiO_2	0.0225	0.0250	-
Na_2O	0.5391	0.5121	0.6065
K_2O	0.5543	0.5061	-
CaO	0.0000	0.0000	-
MgO	0.4347	0.4347	-
H_2O	7.3186	7.0533	7.6923
Total	96.9217	96.6962	97.2388
$\text{Na}_2\text{O} + \text{K}_2\text{O} + \text{CaO} + \text{MgO}$	0.50	0.49	0.20
Al_2O_3			
$\text{SiO}_2 / \text{Al}_2\text{O}_3$	27	28	29

5.4. Catalytic Test Results

5.4.1. Comparison of Catalytic Performance of Sample Tested in Benzene Alkylation Reaction

Vapor phase benzene alkylation reaction at 400 °C and under 20 kg / cm² gauge pressure were carried out in the presence of 3 different catalyst samples. Ethylbenzene was the main product and toluene, sec-butylbenzene and para-diethylbenzene were produced as a side products. Gas chromatography analysis results are given in Appendix D. Figures 29 and 30 show the benzene conversion and ethylbenzene yield obtained . As expected , R 503 sample gave the highest benzene conversion and ethylbenzene yield compared with R 312 and R 314. This is because it has a high number of acid sites and crystallinity and possesses only sodium as cation. It exhibited a different catalytic behavior than other two samples in such a way that as reaction proceeds both benzene conversion and ethylbenzene yield increase. Sample R 314 gives the highest initial benzene conversion which is close to the theoretical value of 7.68 % and the highest initial ethylbenzene yield. However, both of them decreased up to 50th hours of reaction time and after then they remained unchanged during the rest of the reaction . R 312 sample showed the lowest catalytic performance in terms of benzene conversion and ethylbenzene yield. The difference in the initial performance can be attributed to existence of a low number of active sites in R 312 sample. Its X-ray diffraction pattern of it taken after reaction (Figure 20) indicates there is a considerable loss of crystallinity and as depicted in Table 19 it has the highest amount of coke compared with the other two samples. These are considered to be the causes of low catalytic performance of R 312. Figure 31 indicates that as reaction

proceeds S_T selectivity of R 503 increases and reaches to a value of about 6 % at the end of the reaction. In contrast , R 314 has a maximum 2 % S_T selectivity during the reaction. R 312 didn't yield toluene. In the case of S_P selectivities, both R 314 and R 503 exhibited nearly equal S_P values at the beginning of the reaction. A decrease did occur for R 314 sample during the reaction time, whereas S_P selectivity of R 503 sample increased slightly. Although initial S_P selectivity of R 312 was lower at the beginning of the reaction, it increased from 9 % to 14 % at the end of the reaction.

5.4.2. Effect of Temperature on Benzene Conversion and Ethylbenzene Yield and Selectivity

R 314 sample was tested in vapor phase benzene alkylation reaction at 400 and 425 °C under 20 kg / cm² gauge pressure to see the effect of temperature on benzene conversion and ethylbenzene yield. As indicated in Figure 32 the highest initial conversion was obtained at 400 °C . After observing a sharp decrease up to a certain reaction time at 400 °C, it remained unchanged at about 6 %. Benzene conversion decreased slightly from 6.5 % to 6 % during reaction time at 425 °C. It is evident that increase in temperature has no a considerable effect on benzene conversion.

Figures 33 and 34 show the effect of temperature on ethylbenzene yield and selectivity respectively. It is obvious from these that as temperature increases both yield and selectivity increase.

5.4.3 . Effect of Temperature on S_T and S_P Selectivities

As shown in Figure 35 both S_T and S_P selectivities were higher at

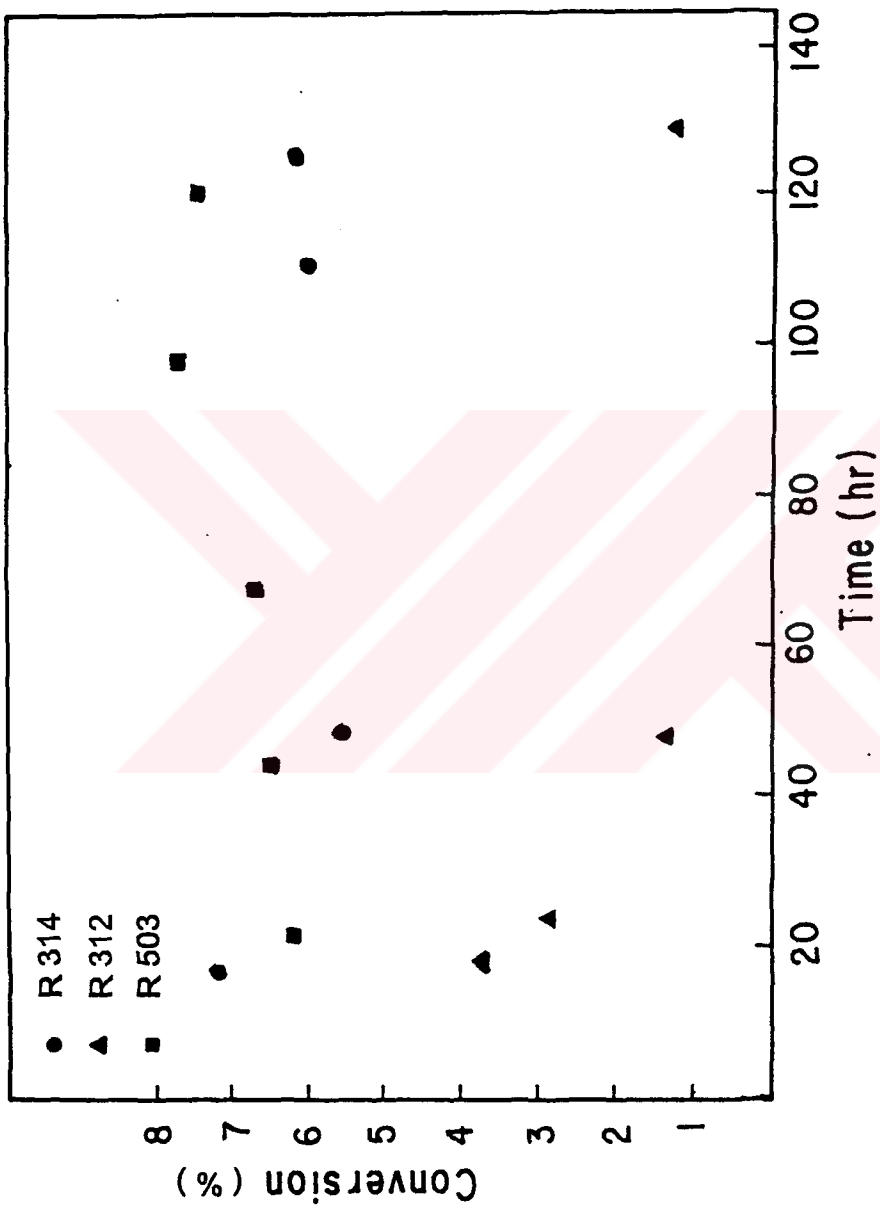


Figure 29: Conversion of Benzene over Three Different Catalyst Samples at 400 °C and 20 kg / cm² gauge Pressure

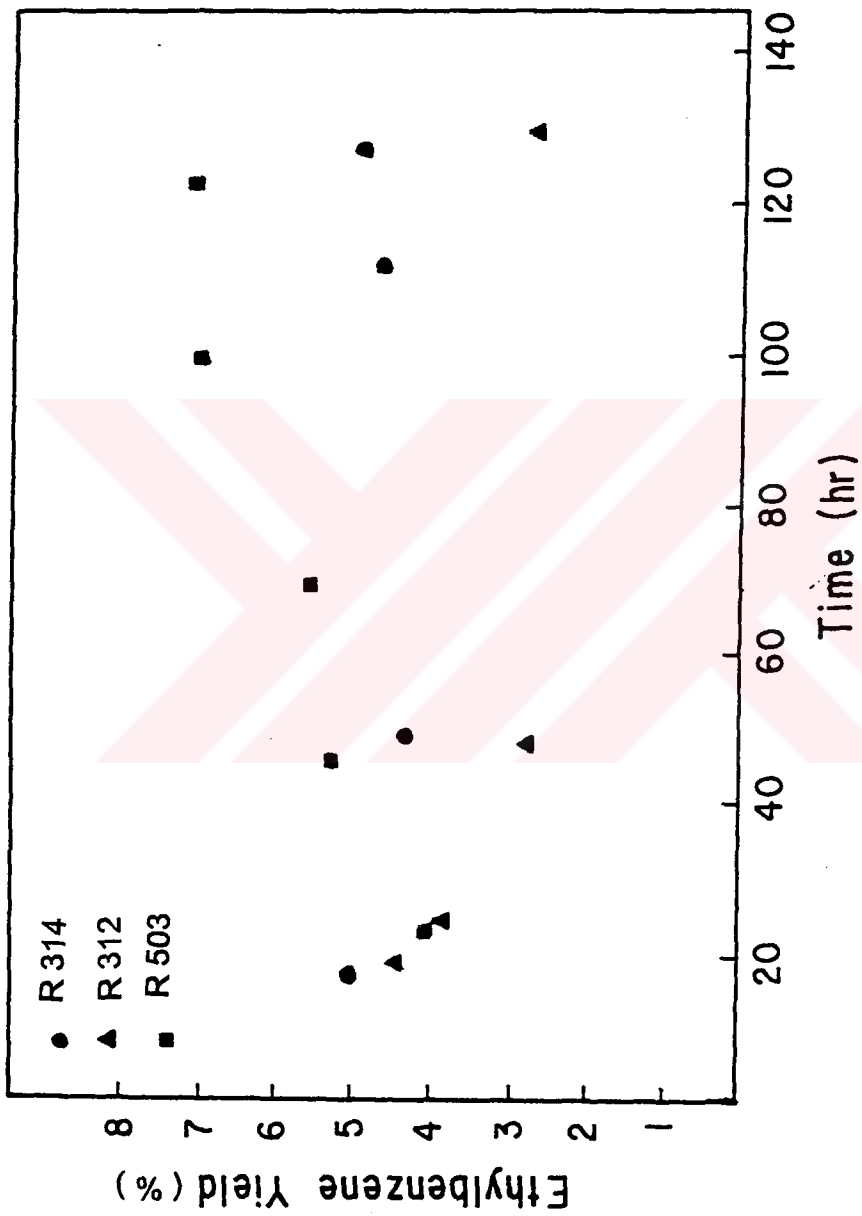


Figure 30: Yield of Ethylbenzene over Three Different Catalyst Samples at 400 °C and 20 kg / cm² gauge Pressure

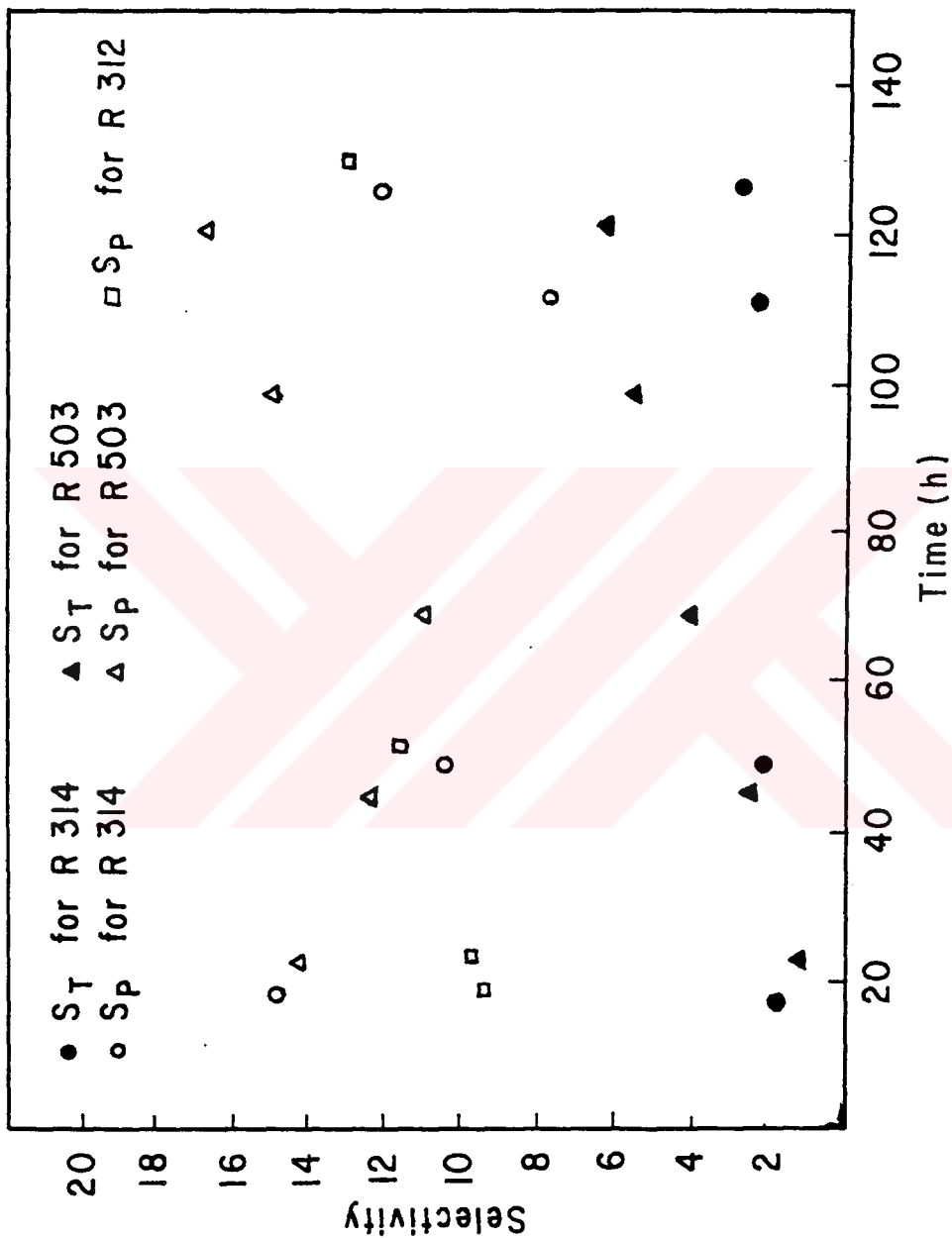


Figure 31 : Selectivity of Ethylbenzene over Three Different Catalyst
 Samples at 400 °C and 20 kg / cm² gauge Pressure

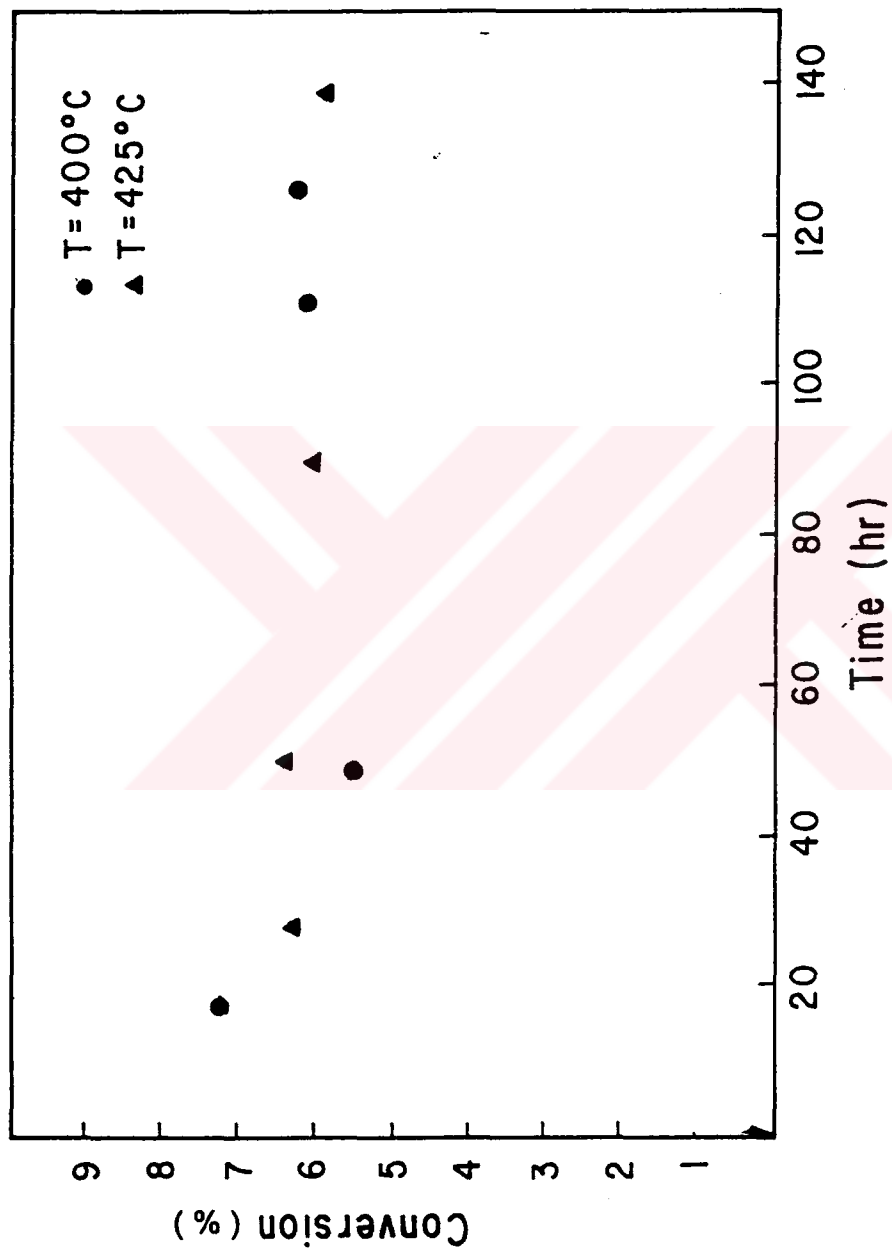


Figure 32 : Effect of Temperature on Benzene Conversion over R 314
 Catalyst under 20 kg / cm² gauge Pressure

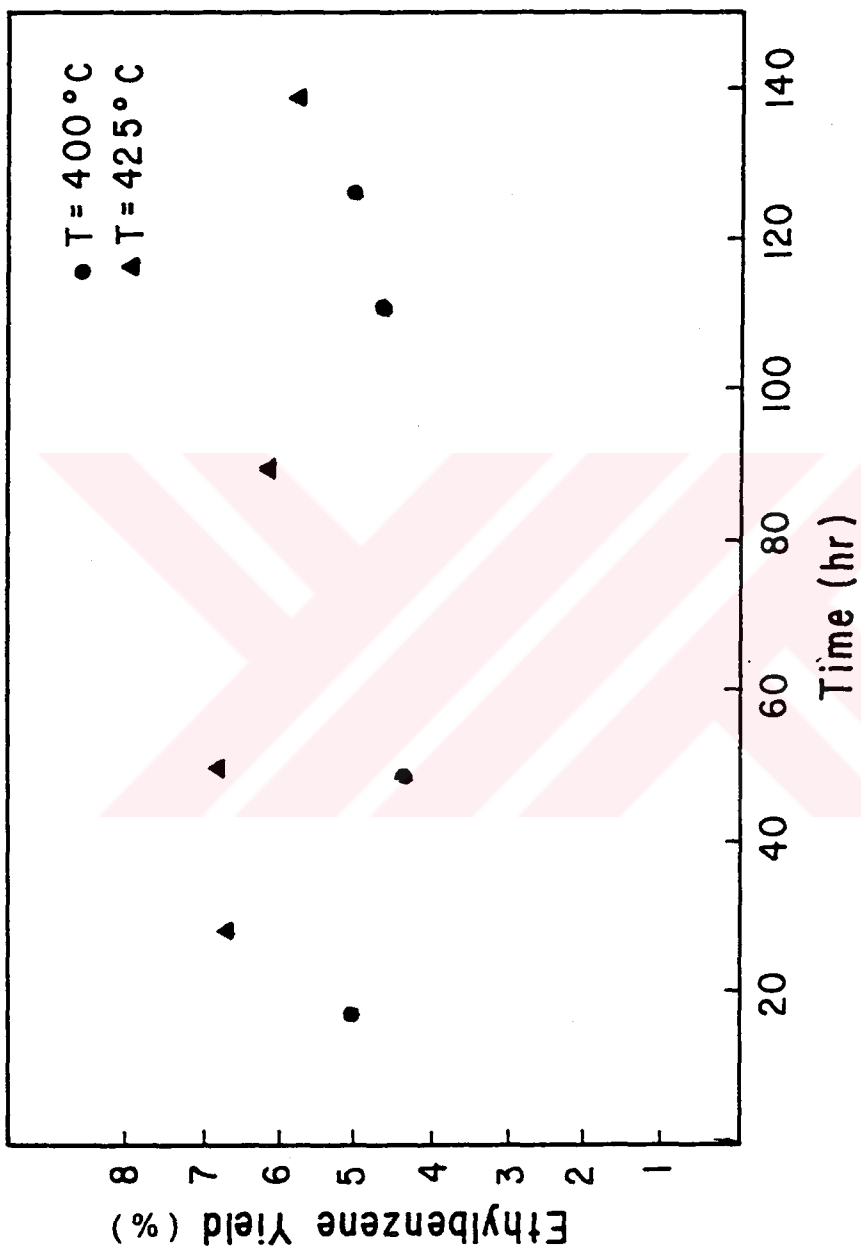


Figure 33 : Effect of Temperature on Ethylbenzene Yield over R 314 under 20 kg / cm² gauge Pressure

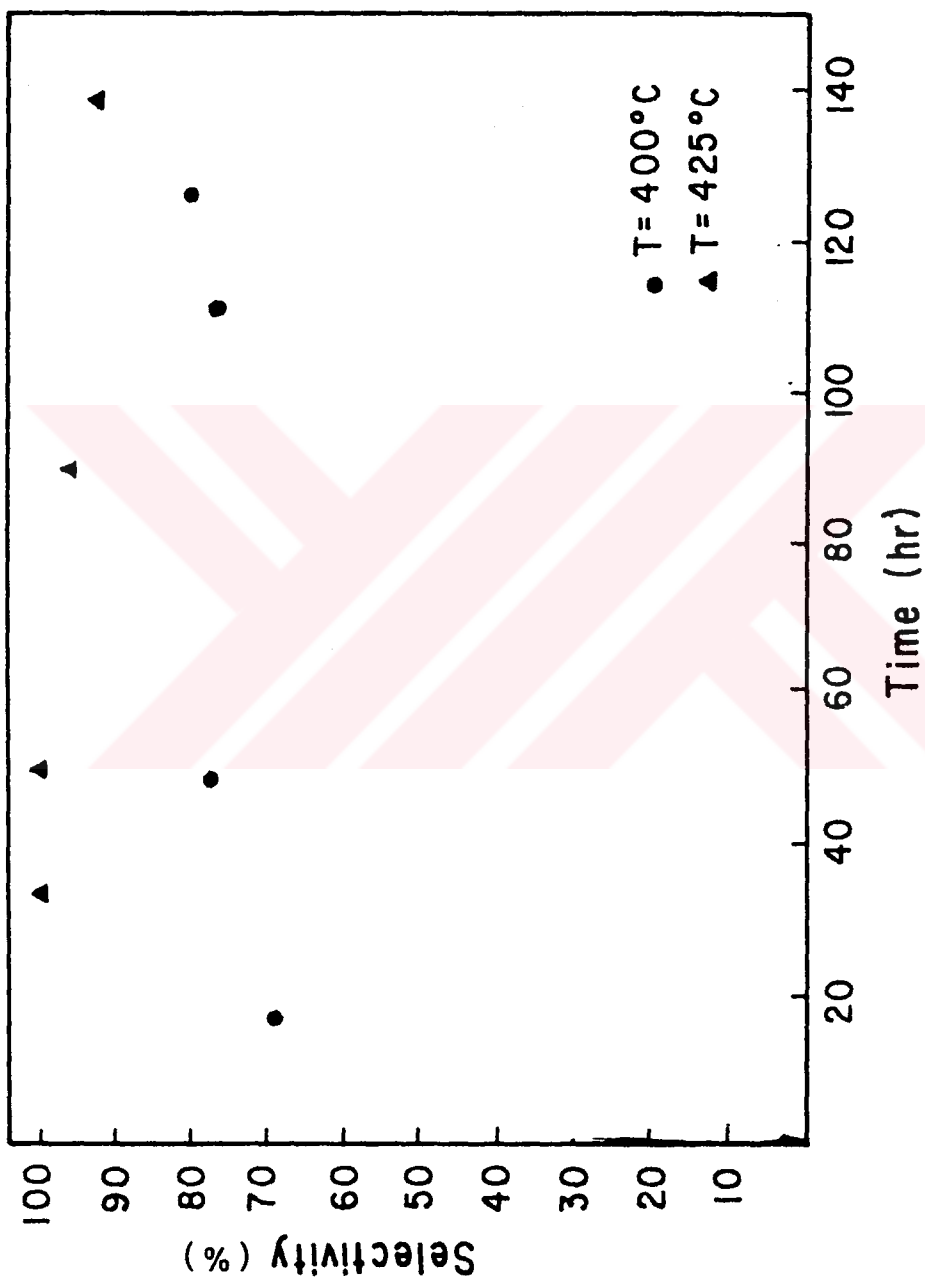


Figure 34 : Effect of Temperature on Ethylbenzene Selectivity over R 314
under 20 kg / cm² gauge Pressure

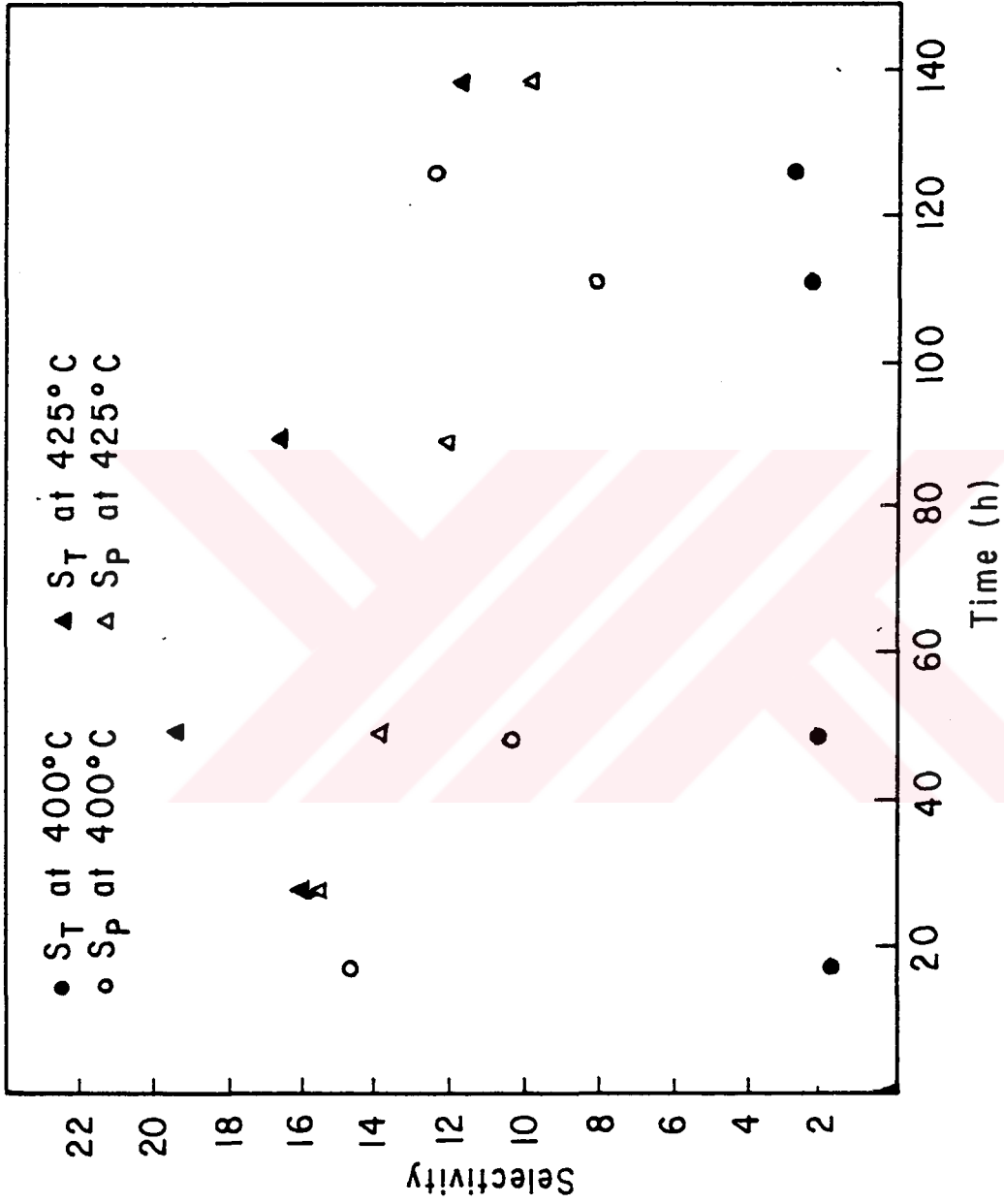


Figure 35 : Effect of Temperature on S_T and S_P Selectivities over R 314 under 20 kg / cm² gauge Pressure

the beginning of the reaction at 425 °C, but then they dropped gradually during reaction. At 400 °C very low (2%) S_T selectivity was obtained. S_P selectivity which was 15 % initially decreased to 10 % during the reaction time.

5.4.4. Coking Characteristics of Tested Catalyst Samples

Tested catalyst samples were analyzed by TGA apparatus in 50 ml / min air flow to determine their coking properties. The thermogravimetric curves obtained by heating the samples to 400 °C at a rate of 10 °C /min and between 400-700 °C at 3 °C /min are represented in Figures 36 through 39. As shown in these figures all catalyst samples had a weight loss at a temperature range of 100-300 °C because of removal of water present in their voids and hydrocarbons adsorbed on their surface during reaction. The second considerable weight loss occurred between 400-700 °C due to burning the coke formed in catalyst structure as reaction proceeds. The amount of coke found in catalyst samples together with temperature levels tested and the peak temperature at which coke was burnt are tabulated in Table 19. As depicted from this table, R 503 sample tested at 400 °C contained 7 % coke, but R 314 sample had only 4.8 % coke at the same temperature. The temperatures at which the coke started to burn and the peak temperature observed were close for these two samples. The highest amount of coke was found in R 312 sample and for that reason it had the lowest catalytic performance. Reaction temperature strongly affects the coke formation and as temperature increases the amount of coke formed increases.

Sample R 314 has the lowest amount of coke at 400 °C compared with other two samples. Sample R 503 showed the highest benzene conversion, ethylbenzene yield and selectivity at 400 °C, but its coke content was higher than R 314 sample. The reason for that is considered to be the presence of high number of acid sites in R 503 sample. As a result of a noticeable crystallinity loss and the presence of high amount of coke in sample R 312, it showed the lowest catalytic performance in benzene conversion, and ethylbenzene yield amount the samples tested. But it didn't yield toluene as a side product and had the higher S_p selectivity than R 314 sample.



Table 19: TGA Data and Calculated Amount of Coke Present in Catalyst Samples

Catalyst	Temperature Levels Tested (°C)	Amount of Coke (%)	Temperature at which Coke Started to Burn (°C)	Maximum Peak Temperature (°C)
R 312	400	16	455	610
R 314	400	4.8	440	522
R 314	425	12	455	565
R 503	400	7	440	517

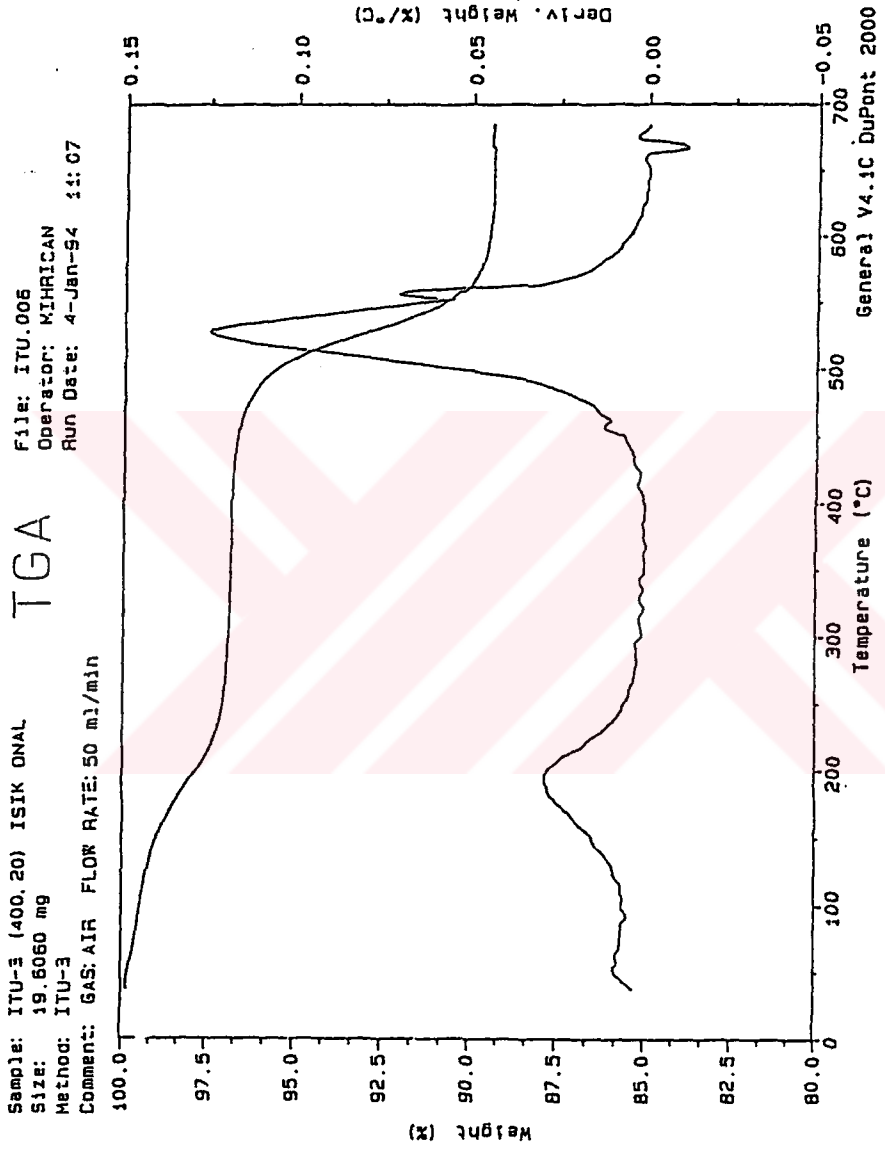


Figure 36 : Thermogravimetric Curve of R 503 Sample After Testing in Benzene Alkylation Reaction at 400 °C and 20 kg / cm² gauge Pressure

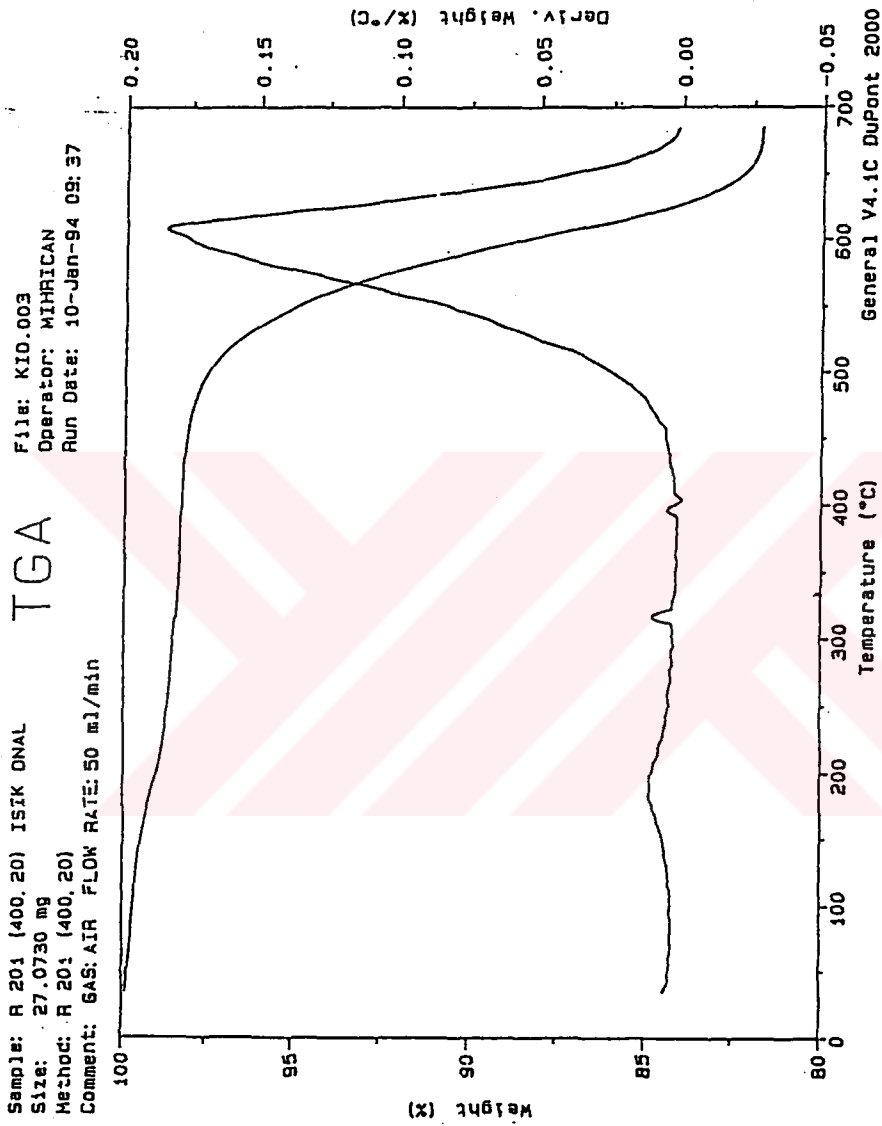


Figure 37 : Thermogravimetric Curve of R 312 Sample After Testing in Benzene
 Alkylation Reaction at 400 °C and 20 kg / cm² gauge Pressure

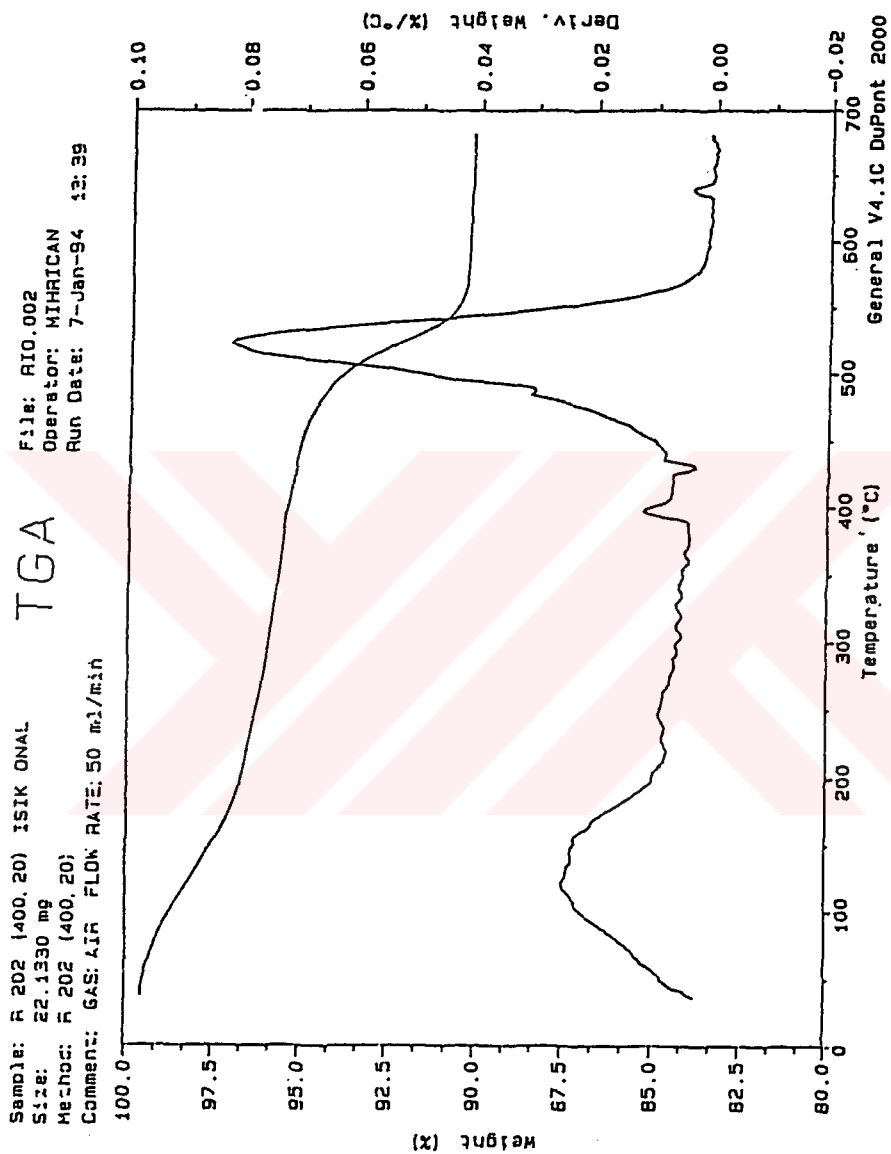


Figure 38 : Thermogravimetric Curve of R 314 Sample After Testing in Benzene
 Alkylation Reaction at 400 °C and 20 kg / cm² gauge Pressure

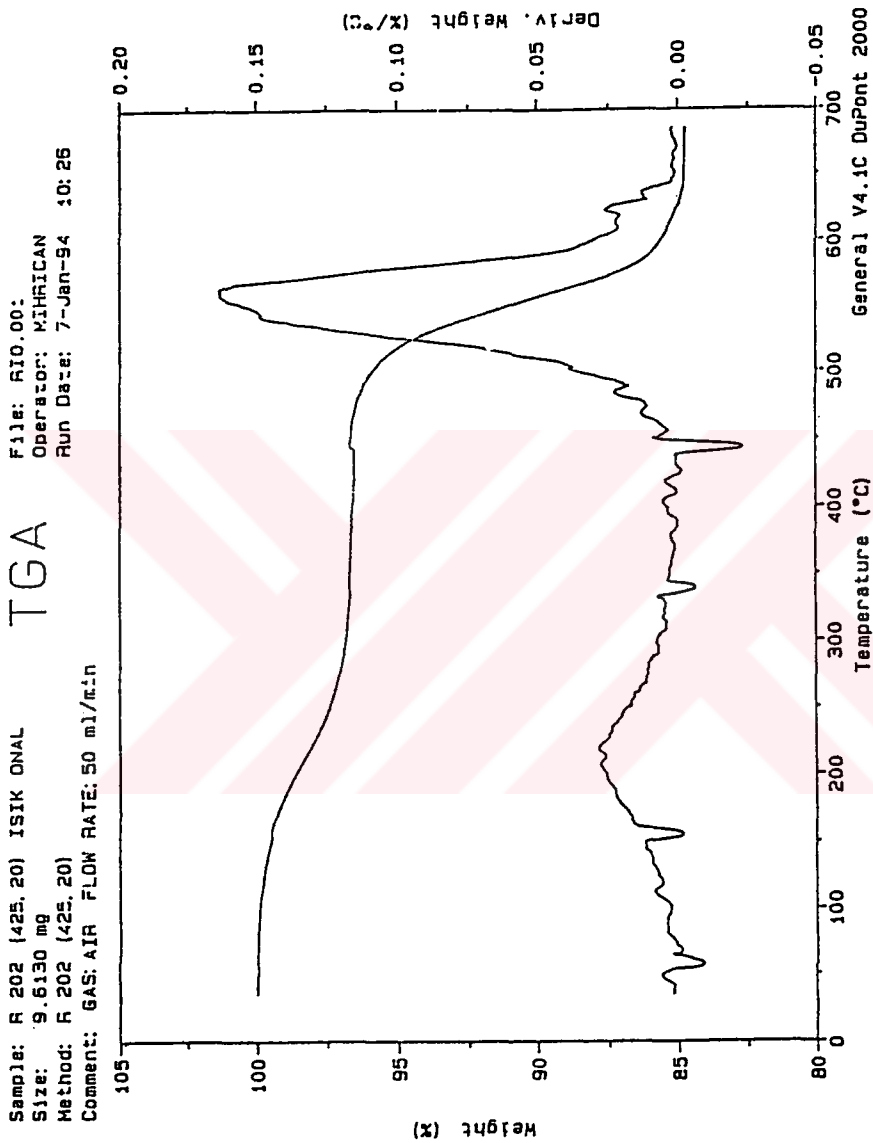


Figure 39 : Thermogravimetric Curve of R 314 Sample After Testing in Benzene Alkylation Reaction at 425 °C and 20 kg / cm² gauge Pressure

CHAPTER VI

CONCLUSIONS AND RECOMMENDATIONS

The purpose of this study was to obtain zeolite catalysts which contain ZSM-5 phase by utilizing clinoptilolite which was subjected to HCl treatment, NaOH, TPABr and H₂O at 180 °C for ethylbenzene production. After transforming ZSM-5 samples into H-form they were tested as catalysts in benzene alkylation reaction.

It was observed that SiO₂/Al₂O₃ mol ratio of clinoptilolite was an important parameter in ZSM-5 synthesis.

The optimum TPA⁺ / TPA⁺⁺ + Na⁺ ratio was found to be 0.5 for ZSM-5 crystallinity.

The catalyst sample prepared in this study (R 314) exhibited catalytic performance in terms of benzene conversion close to that of reference sample. It was observed that increasing the reaction temperature to 425 °C made improvements on its ethylbenzene yield and selectivity. Coke formed in the structure of this sample was strongly affected by temperature. It was seen from the results of TGA analyses that high temperature favored the formation of coke.

Catalyst test results indicated the possibility of using natural zeolites in the synthesis of ZSM-5 and preparing the catalyst samples for benzene alkylation reaction.

The catalyst tests can be conducted at different pressures to investigate the effect of pressure on benzene conversion, ethylbenzene yield and selectivity.

This work can be extended by performing kinetic modelling for selected catalysts.



REFERENCES

Argauer, R.J., and Landolt, G.R., 1972. US Patent 3 702 886

Ataman, G., 1977. " Batı Anadolu Zeolit Olusumları ", Yer Bilimleri ,
Vol. 3 , No. 1-2 , pp. 85-94.

Barrer, R.M., 1982. Hydrothermal Chemistry of Zeolites, Academic Press,
London.

Bolton, A.P., 1976. " Molecular Sieve Zeolites ", Experimental Methods in
Catalytic Research, ed. R.B. Anderson, P.T. Dowson, Academic
Press, NY, Vol. 2 , pp. 1-43.

Bond, G.C., 1974. Heterogeneous Catalysis: Principles and Applications,
Clarendon Press, Oxford.

Burres, G.T., 1972. US Patent 3 751 506

Chen, N.Y., and Garwood, W.E., 1978. " Some Catalytic Properties of
ZSM-5, a New Shape Selective Zeolite ", Journal of Catalyst ,
Vol. 52 , pp. 453-458.

Chen, N.Y., and Garwood, W.E., 1986. " Industrial Application of Shape
Selective Catalysis ", Catal. Rev.Sci. Eng. , Vol. 28 , pp. 185-264.

Csicsery, S.M., 1984. " Shape - Selective Catalysis in Zeolites", Zeolites ,
Vol. 4 , pp. 202-213.

Derouane, E.G., and Gabelica, Z., 1980. " A Novel Effect of Shape
Selectivity : Molecular Traffic Control in Zeolite ZSM-5 ",Journal of
Catalyst , Vol. 65 , pp. 486-489.

————— , 1992. " Endüstri Mineralleri Alt Komisyonu Raporu",
Altıncı Beş Yıllık Kalkınma Planı , DPT. 2300 - ÖİK : 407.

Dwyer, F.G., 1981. " Mobil / Badger Ethylbenzene Process Chemistry
and Catalytic Implications ", Chem. Adv. , Vol. 5 , pp. 39-50.

Easton, A.J., 1972. Chemical Analysis of Silicate Rocks , Elsevier
Publishing Company, Amsterdam.

Erdem-Şenatalar, A., Sirkecioğlu, A., Esenli, F., and Kumbasar, R. H., 1990.
"Mineralogical and Chemical Properties of Bigadiç Clinoptilolite:
Variation of Ammonium Ion Exchange Capacity with Zeolite
Content " , presented at International Earth Sciences Congress
on Aegean Regions, İzmir.

Flanigen, E.M., 1976. " Structural Analysis by Infrared Spectroscopy ",
Zeolite Chemistry and Catalysis , ed. J.A. Rabo, American
Chemical Society, Washington , pp. 80-116.

- Goto, Y. and Sand, L.B., 1988. " Crystallization of ZSM-5 from Natural Japanese Mordenite and Clinoptilolite ", Occurance, Properties and Utilization of Natural Zeolites, ed. D. Kallo, H.S. Sherry, Akademiai Kiado, Budapest , pp. 161-169.
- Gündüz, U. ,1987. " Synthesis and Characterization of Silicalite ", M.S. Thesis in Chemical Engineering, Middle East Technical University, Ankara .
- Jansen, J.C., Van Der Gaag, J., Bekkum, H. V., 1984. " Identification of ZSM-type and Other 5-ring Containing Zeolites by IR Spectroscopy ", Zeolites, Vol.4, pp. 369-372.
- Kokotailo, G.T., Lawton, S.L., and Olsan, D.H., 1978 . "Structure of Synthetic Zeolite ZSM-5 ", Nature , Vol. 272 , pp. 437-438.
- Mavrodinova, V., Penchev, V., Lohse, U., and Stach, H., 1989. a. "Factors Influencing the Conversions of Alkylaromatic Hydrocarbons on High-Silica Zeolites : Part I. Structure and Density of the Active Centres", Zeolites , Vol. 9, pp. 197-202.
- Mavrodinova, V., Penchev, V., Lohse, U., and Gross, T., 1989. b. "Factors Influencing the Conversions of Alkylaromatic Hydrocarbons on High-Silica Zeolites : Part II. Presence of Extralattice Al. ", Zeolites , Vol. 9, pp. 203- 207.
- Mc Ketta, J.J. et al. (Ed.), 1982. Encyclopedia of Chemical Process Design , Marcel Dekker, New York, pp. 77- 87.

- Meier, W.M., 1968. Molecular Sieves, Society for Chemical Industry, London.
- Mintova, S., Valtchev, V., Vultcheva, E., and Veleva, S., 1992. "Crystallization Kinetics of Zeolite ZSM-5", Zeolites, Vol. 12, pp. 210-215.
- Satterfield, C.N., 1980. Heterogeneous Catalysis in Practice, McGraw- Hill, NY.
- Yücel, H., and Çulfaz, A., 1988. "Characterization of Clinoptilolites of Western Anatolia", Occurance, Properties and Utilization of Natural Zeolites, ed. D. Kallo, H.S. Sherry, Akademiai Kiado, Budapest, pp. 99 -108.
- Ward, J.W., 1976. "Shape - Selective Catalysis", Zeolite Chemistry and Catalysis, ed. J.A. Rabo, American Chemical Society, Washington, pp. 118-284.



APPENDICES

APPENDIX A

FLOW DIAGRAMS OF VARIOUS ETHYLBENZENE PRODUCTION PROCESSES



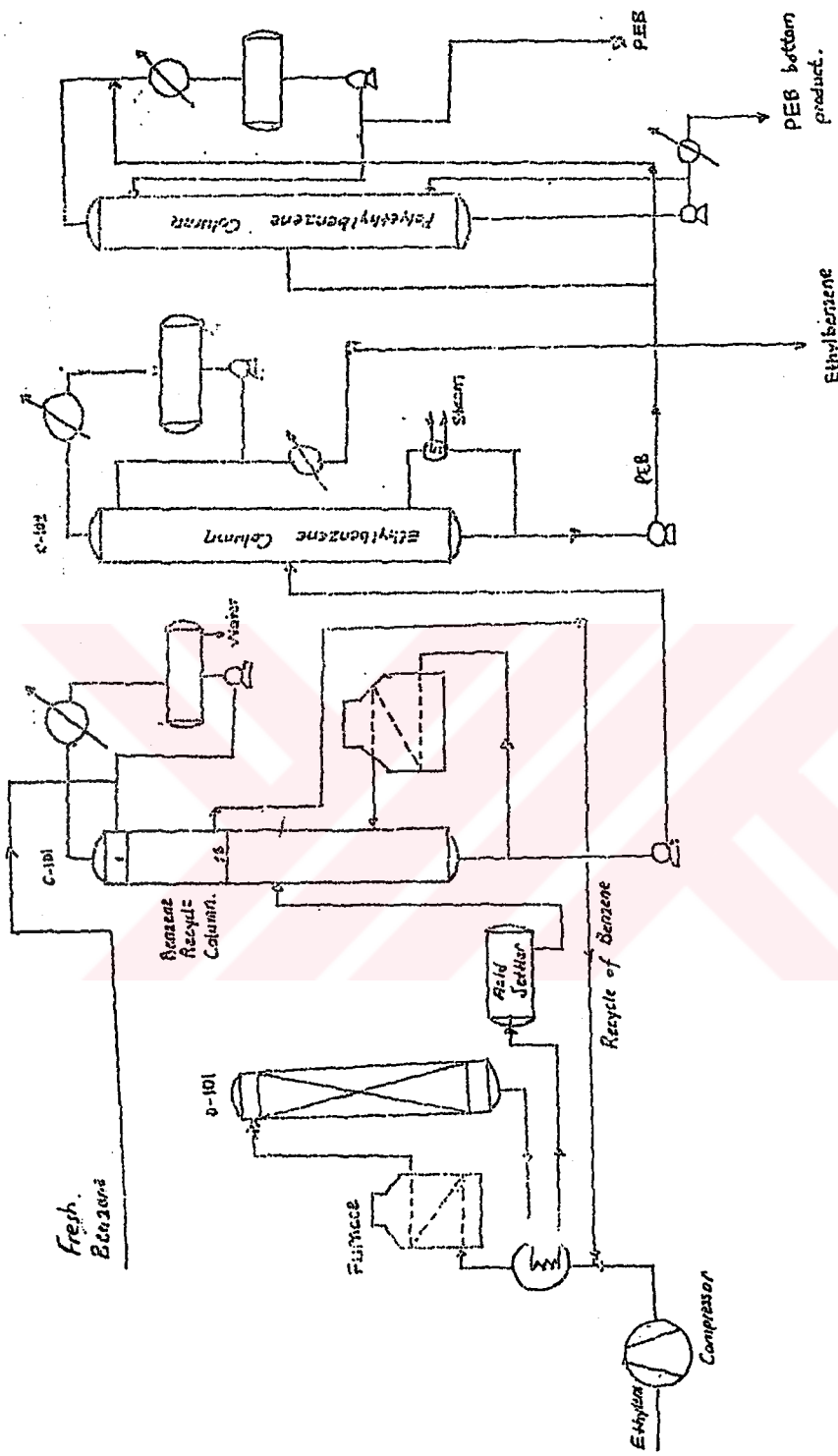


Figure A.2 : Yarpet Process for Ethylbenzene Production

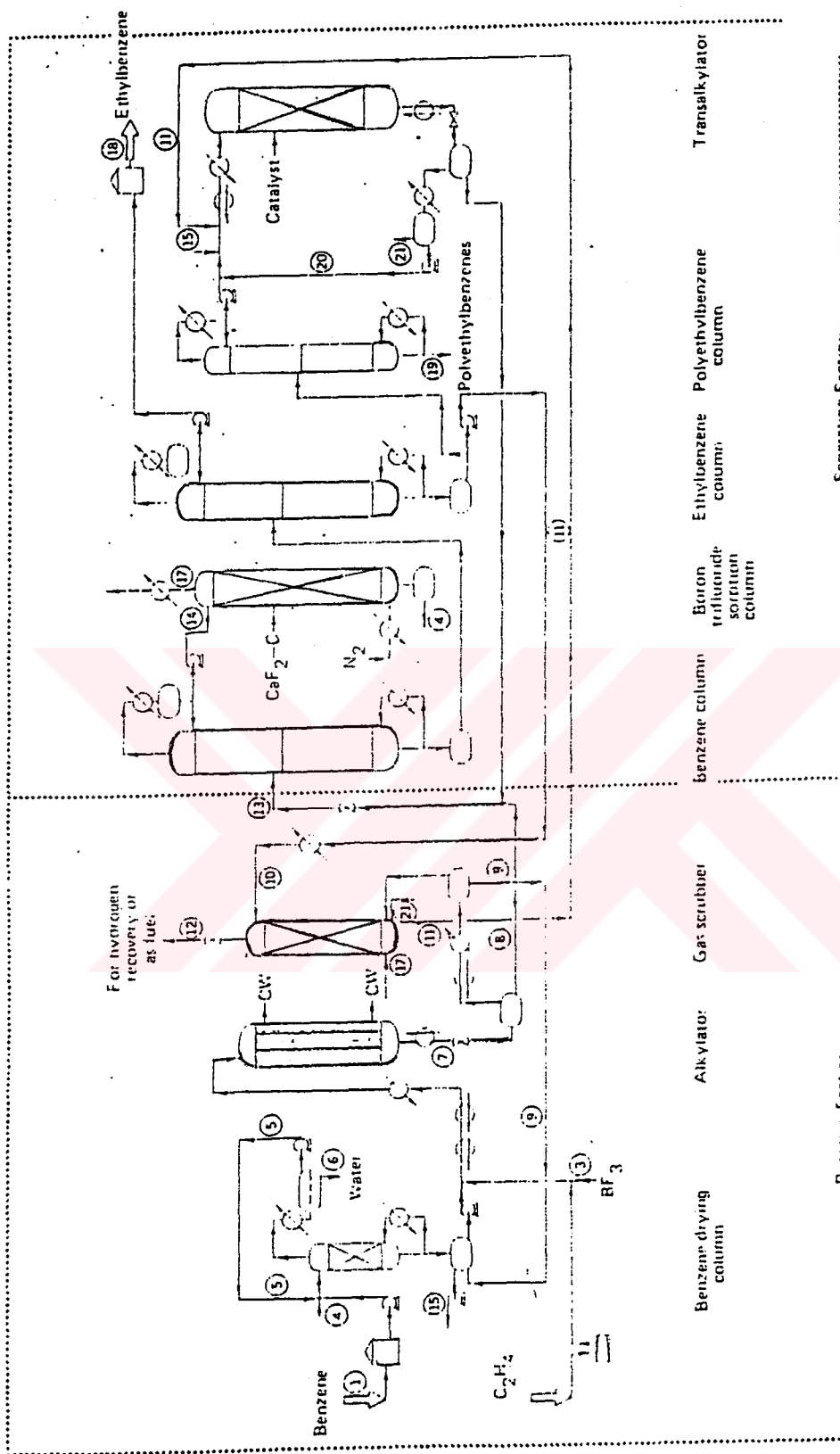


Figure A.3 : Alkar Process for Ethylbenzene Production

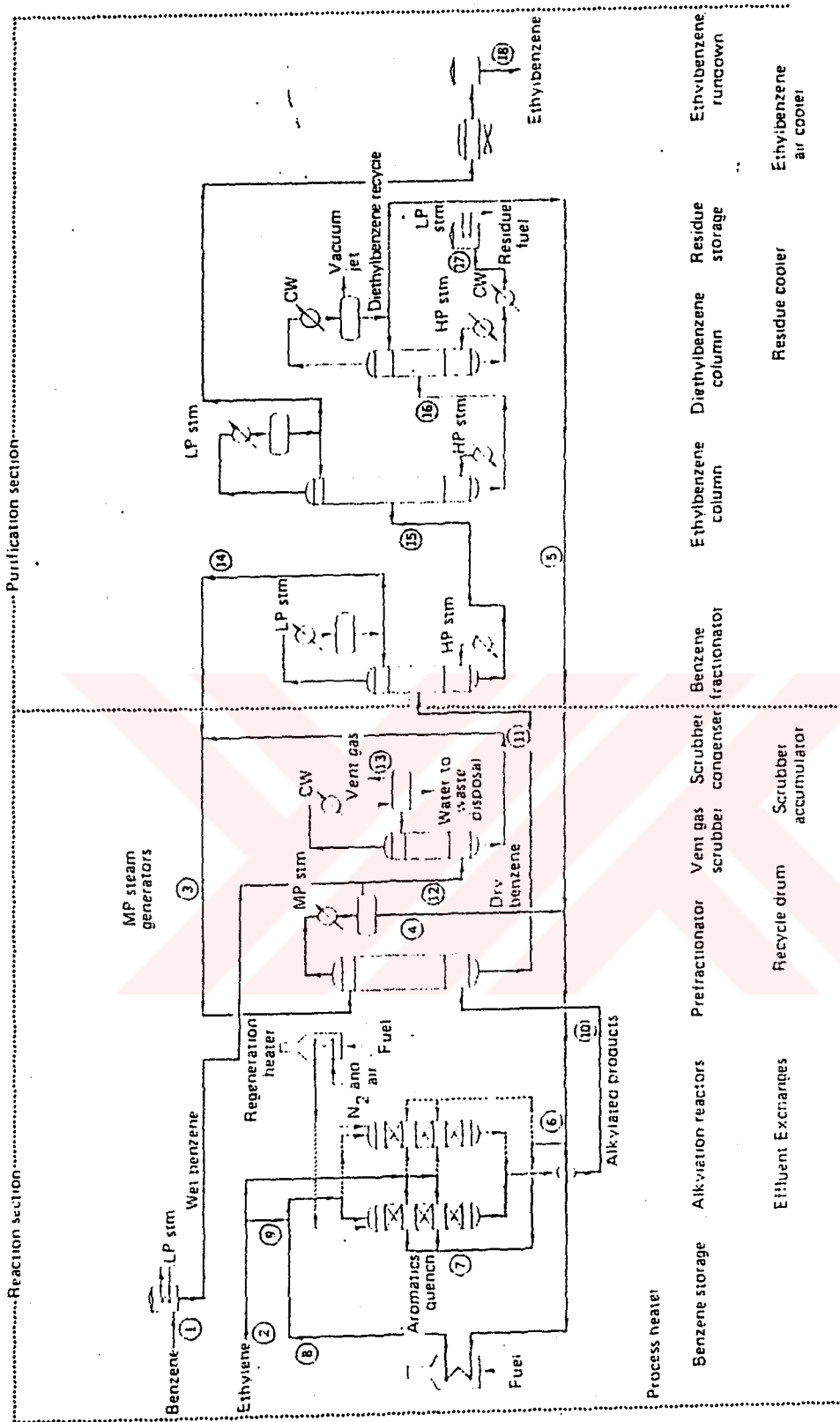


Figure A.4 : Mobil / Badger Process for Ethylbenzene Production

APPENDIX B

ZSM- 5 SYNTHESIS DATA

B.1. Calculation of Raw Material Amounts for a Specific Starting Batch Composition

The molecular weights of compounds used for the calculation of raw material amounts necessary for a specific starting batch composition are listed in Table B.1.

From given batch equation the required moles of compounds for ZSM-5 synthesis are :

$$\text{SiO}_2 = 90 \text{ mol} \qquad \text{Na}_2\text{O} = 11 \text{ mol} \qquad \text{H}_2\text{O} = 2000 \text{ mol}$$

The moles of $(\text{TPA})_2\text{O}$ can be calculated as follows :

$$\text{TPA}^+ / \text{TPA}^+ + \text{Na}^+ = 0.5 \qquad (\text{B.1})$$

$$\text{Na}^+ = 11 \text{ mol Na}_2\text{O} \left(\frac{2 \text{ mol Na}^+}{1 \text{ mol Na}_2\text{O}} \right) = 22 \text{ mol Na}^+$$

From equation B.1

$$\text{TPA}^+ = \text{Na}^+ = 22 \text{ mol} . \text{ Then,}$$

$$(\text{TPA})_2\text{O} = 22\text{mol TPA}^+ \left(\frac{1 \text{ mol } (\text{TPA})_2\text{O}}{2 \text{ mol TPA}^+} \right) = 11 \text{ mol}$$

$$\text{TPABr} = 22 \text{ mol TPA}^+ \left(\frac{1 \text{ mol TPABr}}{1 \text{ mol TPA}^+} \right) = 22 \text{ mol}$$

$$\text{Br} = 22 \text{ mol TPABr} \left(\frac{1 \text{ mol Br}}{1 \text{ mol TPABr}} \right) = 22 \text{ mol}$$

Table : B.1 : Molecular Weights of Compounds

Compound	Molecular Weight
SiO ₂	60.0848
Al ₂ O ₃	101.9612
Fe ₂ O ₃	159.6922
TiO ₂	79.8988
Na ₂ O	61.9790
K ₂ O	94.2034
CaO	56.8744
MgO	40.3114
TPA ion ((CH ₃ CH ₂ CH ₂) ₄ N)	186.3599
TPABr	266.2639
(TPA) ₂ O	388.7192
NaOH	39.9970
H ₂ O	18.0000

T.C. YÜKSEKÖĞRETİM VE
DOKÜMANTASYON

Table B.2 : Molar Composition of HCl Treated Clinoptilolite
Sample (6H-CL) Used in ZSM-5 Synthesis

Component	Mass Percent	Mole
SiO ₂	76.1000	1.2665
Al ₂ O ₃	4.7910	0.0469
Fe ₂ O ₃	0.0990	0.0006
TiO ₂	0.0100	0.0001
Na ₂ O	0.3234	0.0052
K ₂ O	0.5302	0.0056
CaO	0.4000	0.0070
MgO	0.1666	0.0041
H ₂ O	12.5127	0.6951

Batch composition calculations based on 90 mol of SiO₂ :

$$\text{Al}_2\text{O}_3 = (90) (0.0469) / (1.2665) = 3.3328 \text{ mol}$$

$$\text{Fe}_2\text{O}_3 = (90) (0.0006) / (1.2665) = 0.0426 \text{ mol}$$

$$\text{TiO}_2 = (90) (0.0001) / (1.2665) = 0.0071 \text{ mol}$$

$$\text{K}_2\text{O} = (90) (0.0056) / (1.2665) = 0.3979 \text{ mol}$$

$$\text{CaO} = (90) (0.0070) / (1.2665) = 0.4974 \text{ mol}$$

$$\text{MgO} = (90) (0.0041) / (1.2665) = 0.2913 \text{ mol}$$

So batch composition becomes :

0.0426 Fe₂O₃ / 0.0071 TiO₂ / 0.3979 K₂O / 0.4974 CaO / 0.2913 MgO /
11Na₂O / 11 (TPA)₂ O / 3.3328 Al₂O₃ / 90 SiO₂ / 2000 H₂O / 22 Br

Table B.3 : Composition of Starting Batch Mixture

Component	Mole	Mass	Mass fraction
SiO ₂	90.00	5407.6320	0.1112
Al ₂ O ₃	3.332	339.8162	0.0069
Fe ₂ O ₃	0.0426	6.8028	0.00014
TiO ₂	0.0071	0.5672	0.00001
Na ₂ O	11.00	681.7690	0.0140
K ₂ O	0.3979	37.4835	0.0007
CaO	0.4974	28.2893	0.0006
MgO	0.2913	11.7427	0.0002
(TPA) ₂ O	11.00	4275.9112	0.0879
Br	22.00	1757.8880	0.0361
H ₂ O	2000.00	36000	0.7405

Basis : 100 g of starting mixture

Zeolite Requirement :

$$\text{SiO}_2 \text{ required} = (100) (0.1112) = 11.12 \text{ g}$$

$$\text{Zeolite required} = (11.12) / (0.7610) = 14.6123 \text{ g}$$

NaOH Requirement :

$$\text{Na}_2\text{O required} = (100) (0.0140) = 1.4 \text{ g}$$

$$\text{Na}_2\text{O from zeolite} = (14.6123) (0.003234) = 0.0472 \text{ g}$$

$$\text{Na}_2\text{O added} = \text{Na}_2\text{O required} - \text{Na}_2\text{O from zeolite}$$

$$\text{Na}_2\text{O added} = 1.4 - 0.0472 = 1.352 \text{ g}$$

$$\text{NaOH required} = \frac{(1.3528) (2) (22.9897) (39.9970)}{(61.9790) (22.9897)} = 1.7460 \text{ g}$$

TPABr Requirement :

$$(\text{TPA})_2\text{O required} = (100) (0.0879) = 8.79 \text{ g}$$

$$\text{TPABr required} = \frac{(8.79) (2) (186.3599) (226.2639)}{(388.7192) (186.3599)} = 12.0420 \text{ g}$$

H₂O Requirement :

$$\text{H}_2\text{O added} = \text{H}_2\text{O required} - (\text{H}_2\text{O from zeolite} + \text{H}_2\text{O from NaOH})$$

$$\text{H}_2\text{O required} = (100) (0.7405) = 74.05 \text{ g}$$

$$\text{H}_2\text{O from zeolite} = (14.6123) (0.125127) = 1.8284 \text{ g}$$

$$\text{H}_2\text{O from NaOH} = 1.7460 \left(\frac{18}{(2) (39.9970)} \right) = 0.3928 \text{ g}$$

$$\text{H}_2\text{O added} = 74.05 - (1.8284 + 0.3928) = 71.8288 \text{ g}$$

B.2. Synthesis Conditions of R 503 Sample

Starting Materials : Colloidal Silica
Aluminum Dry Gel
NaOH
TPABr
TPAOH
H₂O

Batch Composition : 6 Na₂O / 6 TPABr / 2 TPAOH / 2 Al₂O₃ /
100 SiO₂ / 2500 H₂O

Reaction Temperature : 170 °C

Reaction Time : 120 hours

TPA⁺ / TPA⁺ + Na⁺ : 0.4

APPENDIX C

MEASUREMENT OF VIBRATED BULK DENSITY AND CALCULATION OF REQUIRED AMOUNT OF CATALYSTS

C.1. Measurement of Vibrated Bulk Density

Vibrated bulk density of tested catalyst samples was measured as follows :

1. Empty graduated cylinder (25 ml) was weighted.
2. 1.00 ± 0.1 g of sample to be tested was weighted and poured slowly through a funnel in a graduated cylinder.
3. Graduated cylinder was placed inside the retaining ring on the vibrator which is adjusted to 500 cycles of vibration.
4. Volume of compacted sample was read.
5. Graduated cylinder containing compacted sample was weighted.
6. Vibrated bulk density (d_c) of sample was calculated as :
 - a : Weight of graduated cylinder (g)
 - b : Weight of graduated cylinder containing compacted sample (g)
 - c : Volume of compacted sample (cm^3)

$$d_c, \text{ g/cm}^3 = (b - a) / c \quad (\text{C.1})$$

C.2. Calculation of Required Amount of Catalyst

$$\text{Benzene LHSV} = 1.35 \text{ cm}^3 \text{ benzene} / \text{cm}^3 \text{ catalyst. /h} \quad (\text{C.2})$$

$$\text{Entering volumetric flow rate of benzene (} V_{bo} \text{)} = 7.2 \text{ cm}^3 / \text{h}$$

By using equation C.2 volume of the catalyst (V_c) can be calculated as:

$$V_c = 7.2 / 1.35 = 5.33 \text{ cm}^3$$

Bulk densities (d_c) of R 312, R 314 and R 503 samples were found by use of equation C.1 to be :

$$d_c(\text{R 312}) = 0.769 \text{ g} / \text{cm}^3$$

$$d_c(\text{R 314}) = 0.769 \text{ g} / \text{cm}^3$$

$$d_c(\text{R 503}) = 0.870 \text{ g} / \text{cm}^3$$

Then, the amount of catalyst (M) that should be loaded to the reactor was found as follows :

$$M_i = (d_{ci}) (V_{ci}) \quad (\text{C.3})$$

$$M_{\text{R 312}} = (0.769) (5.33) = 4.09 \text{ g}$$

$$M_{\text{R 314}} = (0.769) (5.33) = 4.09 \text{ g}$$

$$M_{\text{R 503}} = (0.870) (5.33) = 4.63 \text{ g}$$

APPENDIX D

GAS CHROMATOGRAPHY ANALYSIS RESULTS



Table D.1. : Gas Chromatography Analysis of R 503 Sample Tested at 400°C and
20 kg /cm² gauge Pressure

Component	Feed (wt %)	Product (wt %)									
		Time (h)									
		22.5	29	45	52	69	76	93	99	117	121
Non-aromatics	0.92	0.11	0.09	0.15	0.16	0.15	0.13	0.15	0.20	0.14	0.11
Benzene	99.08	90.54	91.30	90.31	90.06	90.18	90.62	89.97	89.09	89.05	89.34
Toluene	-	4.09	3.28	2.47	2.00	1.59	1.43	1.46	1.38	1.22	1.25
Ethylbenzene	-	4.81	4.91	6.40	7.01	7.22	7.16	7.96	8.58	8.54	8.62
Sec-butylbenzene	-	0.34	0.29	0.44	0.50	0.48	0.42	0.33	0.35	0.60	0.32
Para-diethylbenzene	-	0.10	0.13	0.23	0.26	0.38	0.23	0.12	0.39	0.44	0.35

Table D.2. : Gas Chromatography Analysis of R 314 Sample Tested at 400°C and
20 kg /cm² gauge Pressure

Component	Feed (wt %)	Product (wt %)												
		Time (h)												
		17	23	41	49	65	71	89	95	111	126			
Non-aromatics	0.92	0.08	0.10	0.12	0.05	0.11	0.10	0.10	0.08	0.12	0.16			
Benzene	99.08	89.47	88.30	90.34	91.10	94.40	93.63	95.24	94.69	90.54	90.45			
Toluene	-	3.36	3.32	2.90	2.46	1.37	1.44	1.25	1.19	2.34	2.20			
Ethylbenzene	-	6.51	7.05	5.65	5.67	3.67	4.20	3.15	3.52	6.04	6.49			
Sec-butylbenzene	-	0.22	0.75	0.67	0.44	0.39	0.47	0.19	0.44	0.73	0.37			
Para-diethylbenzene	-	0.35	0.47	0.31	0.27	0.05	0.15	0.06	0.07	0.23	0.32			

Table D.3. : Gas Chromatography Analysis of R 312 Sample Tested at 400°C and
20 kg /cm² gauge Pressure

Component	Feed (wt %)	Product (wt %)											
		Time (h)											
		18	24	42	48	66	70	86	89.5	105.5	112	129.5	
Non-aromatics	0.92	1.06	1.11	0.98	1.20	0.98	0.92	0.95	0.89	1.00	1.11	1.26	
Benzene	99.08	92.78	93.71	95.26	95.10	95.87	95.84	95.99	96.12	95.99	95.33	95.27	
Toluene	-	-	-	-	-	-	-	-	-	-	-	-	
Ethylbenzene	-	5.39	4.59	3.40	3.33	2.87	2.94	2.81	2.76	2.77	3.26	3.17	
Sec-butylbenzene	-	0.24	0.19	0.09	0.09	0.07	0.07	0.07	0.05	0.05	0.06	0.07	
Para-diethylbenzene	-	0.52	0.42	0.26	0.27	0.20	0.22	0.17	0.18	0.18	0.23	0.22	

Table D.4. : Gas Chromatography Analysis of R 314 Sample Tested at 425°C and
20 kg /cm² gauge Pressure

Component	Feed (wt %)	Product (wt %)												
		Time (h)												
		21	28	44	50	67	74	90	97	114	121	139.5		
Non-aromatics	0.92	0.15	0.16	0.16	0.18	0.50	0.53	0.55	0.52	0.53	0.65	0.60		
Benzene	99.08	91.02	90.47	91.11	90.29	88.30	88.95	90.62	87.75	87.48	91.78	90.84		
Toluene	-	0.54	0.46	0.42	0.38	0.91	0.76	0.40	0.72	0.61	0.20	0.53		
Ethylbenzene	-	7.80	8.22	7.89	8.36	9.21	8.86	7.60	9.85	9.96	6.69	7.09		
Sec-butylbenzene	-	0.41	0.46	0.38	0.48	0.68	0.53	0.61	0.78	1.02	0.52	0.63		
Para-diethylbenzene	-	0.07	0.22	0.03	0.30	0.39	0.36	0.21	0.37	0.39	0.15	0.30		

APPENDIX E

RATE DATA AND CALCULATION OF S_T AND S_p SELECTIVITIES

E.1. Calculation of Reaction Rates

The reactor used in the catalytic tests is considered to be a differential reactor. By knowing the volumetric flow rate through the catalyst bed and the weight of catalyst the rate of reaction per unit mass of catalyst can be calculated using design equation which is written on benzene as follows :

$$-r_b = F_{bo} - F_b / W \quad (E.1)$$

where

r_b : Rate of benzene , gmol of benzene reacted / h. g catalyst

F_{bo} : Entering molar flow rate of benzene , cm^3 / h

F_b : Molar flow rate of benzene at exit , cm^3 / h

W : Weight of catalyst , g

Calculations are made by considering R 314 catalyst as an example at a 49th of the reaction time .

Entering volumetric flow rate of benzene (V_{bo}) = $7.2 \text{ cm}^3 / \text{h}$

Entering volumetric flow rate of ethylene (V_{eo}) = $150 \text{ cm}^3 / \text{h}$

$$\text{Entering mass flow rate of benzene } (m_{bo}) = d_b \cdot V_{bo} \quad (\text{E.2})$$

$$\text{Entering mass flow rate of ethylene } (m_{eo}) = d_e \cdot V_{eo} \quad (\text{E.3})$$

$$\text{Total entering mass flow rate} = m_{bo} + m_{eo} \quad (\text{E.4})$$

where d_b and d_e are the densities of benzene and ethylene respectively.

$$m_{bo} = (7.2)(0.867) = 6.2424 \text{ g/h}$$

$$m_{eo} = (150)(0.001148) = 0.1722 \text{ g/h}$$

$$\text{Entering molar flow rate of benzene } (F_{bo}) = m_{bo} / 78 \quad (\text{E.5})$$

$$\text{Entering molar flow rate of ethylene } (F_{eo}) = m_{eo} / 28 \quad (\text{E.6})$$

$$F_{bo} = 6.2424 / 78 = 0.08 \text{ gmol/h}$$

$$F_{eo} = 0.1722 / 28 = 6.15 \times 10^{-3} \text{ gmol/h}$$

$$\text{Total entering mass flow rate} = 6.2424 + 0.1722 = 6.4146 \text{ g/h}$$

Total entering mass flow rate should be equal to total mass flow rate at exit.

$$\text{Weight \% of benzene in product stream} = 91.10 \quad (\text{From Table D.2})$$

$$\begin{aligned} \text{Mass flow rate of benzene at exit } (m_b) &= (6.4146)(0.9110) \\ &= 5.8437 \text{ g/h} \end{aligned}$$

$$\text{Molar flow rate of benzene at exit } (F_b) = m_b / 78$$

$$F_b = 5.8437 / 78 = 0.0749 \text{ gmol/h}$$

$$\text{Weight of catalyst} = 4.09 \text{ g}$$

Then rate of reaction becomes ,

$$-r_b = 0.08 - 0.0749 / 4.09 = 1.24 \times 10^{-3} \text{ gmol /h.g catalyst}$$

Table E.1. : Rate of Reaction over R 503 catalyst at
400°C and 20 kg /cm² gauge Pressure

Time (h)	-r _b (gmol /h.g catalyst)
22.5	1.19 x 10 ⁻³
45	1.23 x 10 ⁻³
69	1.26 x 10 ⁻³
99	1.45 x 10 ⁻³
121	1.41 x 10 ⁻³

Table E.2. : Rate of Reaction over R 314 catalyst at
400°C and 20 kg /cm² gauge Pressure

Time (h)	-r _b (gmol /h.g catalyst)
17	1.57 x 10 ⁻³
49	1.24 x 10 ⁻³
111	1.35 x 10 ⁻³
126	1.37 x 10 ⁻³

Table E.3. : Rate of Reaction over R 314 catalyst at
425°C and 20 kg /cm² gauge Pressure

Time (h)	-r _b (gmol /h.g catalyst)
28	1.36 x 10 ⁻³
50	1.40 x 10 ⁻³
90	1.33 x 10 ⁻³
139.5	1.29 x 10 ⁻³

Table E.4. : Rate of Reaction over R 312 catalyst at
400°C and 20 kg /cm² gauge Pressure

Time (h)	-r _b (gmol /h.g catalyst)
18	9.04 x 10 ⁻⁴
24	7.17 x 10 ⁻⁴
48	4.38 x 10 ⁻⁴
129.5	4.03 x 10 ⁻⁴

E.2. Calculation of S_T and S_P Selectivities

Definition of S_T and S_P selectivities are given as follows :

$$S_T = r_{eb} / r_t \quad (E.7)$$

$$S_P = r_{eb} / r_p \quad (E.8)$$

where

r_{eb} : Rate of ethylbenzene , gmol / h. g catalyst

r_t : Rate of toluene , gmol / h. g catalyst

r_p : Rate of polyethylbenzenes , gmol / h. g catalyst

Since the reactor used in the catalytic tests is considered to be a differential reactor and the corresponding rate equations in terms of product flow rates can be written as follows :

$$r_{eb} = F_{eb} / W \quad (E.9)$$

$$r_t = F_t / W \quad (E.10)$$

$$r_p = F_p / W \quad (E.11)$$

where

F_{eb} : Molar flow rate of ethylbenzene , cm^3 / h

F_t : Molar flow rate of toluene , cm^3 / h

F_p : Molar flow rate of polyethylbenzenes , cm^3 / h

W : Weight of catalyst , g

Then , S_T and S_P selectivities becomes :

$$S_T = F_{eb} / F_t \quad (E.12)$$

$$S_P = F_{eb} / F_p \quad (E.13)$$

Calculations are made by considering R 314 catalyst as an example at a 49th of the reaction time .

$$\text{Total entering mass flow rate} = 6.2424 + 0.1722 = 6.4146 \text{ g / h}$$

(From equation E.4)

Total entering mass flow rate should be equal to total mass flow rate at exit.

$$\text{Weight \% of ethylbenzene in product stream} = 5.67 \text{ (From Table D.2)}$$

$$\text{Weight \% of toluene in product stream} = 2.46 \text{ (From Table D.2)}$$

$$\text{Weight \% of Sec-butylbenzene in product stream} = 0.44 \text{ (From Table D.2)}$$

$$\text{Weight \% of Para-diethylbenzene in product stream} = 0.27 \text{ (From Table D.2)}$$

$$\begin{aligned} \text{Mass flow rate of ethylbenzene at exit (} m_{eb} \text{)} &= (6.4146) (0.0567) \\ &= 0.3637 \text{ g / h} \end{aligned}$$

$$\begin{aligned} \text{Mass flow rate of toluene at exit (} m_t \text{)} &= (6.4146) (0.0246) \\ &= 0.1577 \text{ g / h} \end{aligned}$$

$$\begin{aligned} \text{Mass flow rate of polyethylbenzenes at exit (} m_p \text{)} &= (6.4146) (7.1 \times 10^{-3}) \\ &= 0.0455 \text{ g / h} \end{aligned}$$

$$\begin{aligned} \text{Molar flow rate of ethylbenzene at exit (} F_{eb} \text{)} &= 0.3637 / 106.168 \\ &= 3.425 \times 10^{-3} \text{ gmol / h} \end{aligned}$$

$$\begin{aligned} \text{Molar flow rate of toluene at exit (} F_t \text{)} &= 0.1577 / 92.141 \\ &= 1.711 \times 10^{-3} \text{ gmol / h} \end{aligned}$$

$$\begin{aligned}\text{Molar flow rate of polyethylbenzenes at exit (} F_p \text{)} &= 0.0455 / 134.222 \\ &= 3.389 \times 10^{-4} \text{ gmol / h}\end{aligned}$$

Then from equation E.12

$$S_T = 3.425 \times 10^{-3} / 1.711 \times 10^{-3} = 2$$

Similarly from equation E.13

$$S_p = 3.425 \times 10^{-3} / 3.389 \times 10^{-4} = 10$$



APPENDIX F

X-RAY DIFFRACTION DATA

Bragg Equation gives the relationship of the distance between planes in a crystal and the angle at which the reflected radiation has a maximum intensity for a given wavelength λ .

$$\lambda = 2d\sin\theta \quad (\text{F.1})$$

where d is the distance between the layers of crystal, θ is diffraction angle and λ is the wavelength of the radiation which is 1.542 \AA for $\text{CuK}\alpha$ radiation. The X-ray diffractometer gives the intensity of radiation versus diffraction angle (2θ).

X-ray diffraction pattern of reference sample used in crystallinity calculations is indicated in Figure F.1. and the calculated X-ray data of this and as-synthesized sample are tabulated in Table F.1.

Table F.1. : X-ray Diffraction Data of Reference Sample and
As-synthesized Sample

Reference Sample		As-synthesized Sample	
d (Å)	I / I ₀ x 100	d (Å)	I / I ₀ x 100
11.0420	13.5	11.1815	17.7
9.8172	8.1	9.9273	11.1
4.5483	6.7	4.6187	4.6
4.3496	7.4	4.2267	9.2
4.2467	8.1	3.8306	100
3.8144	100	3.7200	50
3.7047	48.6	3.6449	32.5
3.6449	27	3.4371	12.9
3.4241	10.8	3.2995	14.8
3.3237	10.2	3.2291	12.5
3.2995	12.4	3.0557	12.5
3.0455	13.5	2.9760	19.6
2.9760	14.8	1.9960	18.5
1.9960	20.0		

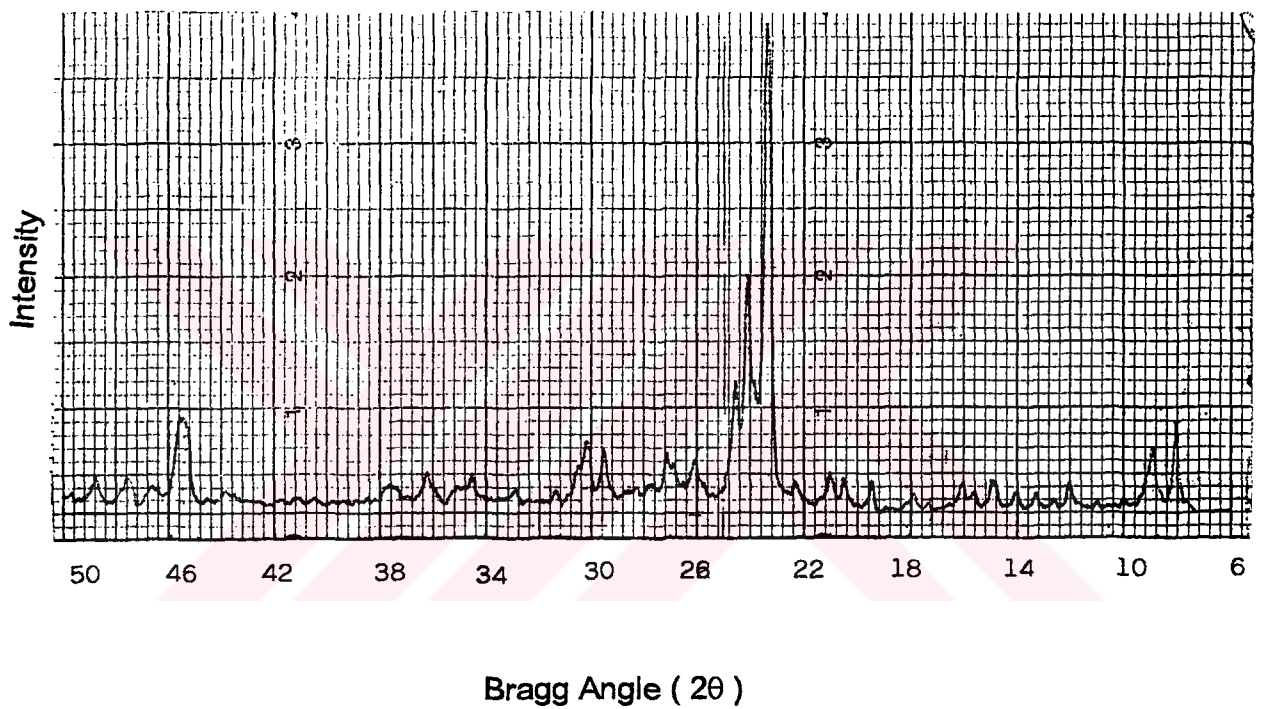


Figure F.1. : X-ray Diffraction Pattern of the Sample Used as Reference in Crystallinity Calculations

APPENDIX G

AMMONIA DESORPTION DATA

Number of acid sites was calculated by considering R 314 catalyst as an example below :

$$\text{Langmuir Surface Area } (A_s) = 358 \text{ m}^2 / \text{g}_{\text{catalyst}}$$

$$\text{Cross sectional area of one ammonia molecule } (A) = 13 \text{ \AA}^2$$

Number of molecules (n) necessary for monolayer coverage can be found as follows :

$$n = A_s / A \quad (\text{G.1})$$

$$n = 358 / 13 \times 10^{-20} = 2.7538 \times 10^{21}$$

$$\% \text{ weight loss} = 95.5 - 95.125 = 0.375 \% \quad (\text{From Figure 27})$$

$$\text{Amount of ammonia adsorbed} = (8.9430) (3.75 \times 10^{-3}) = 0.0335 \text{ g}$$

Amount of ammonia adsorbed

$$\text{per gram of catalyst} = 0.0335 / 8.9430 = 3.75 \times 10^{-3} \text{ g} / \text{g}_{\text{catalyst}}$$

$$\begin{aligned}\text{Moles of ammonia adsorbed} &= 3.75 \times 10^{-3} / 17 \\ &= 2.2058 \times 10^{-4} \text{ mol} / \text{g}_{\text{catalyst}}\end{aligned}$$

$$\begin{aligned}\text{Number of ammonia molecules adsorbed} &= (2.2058 \times 10^{-4}) (6.02 \times 10^{23}) \\ &= 1.3279 \times 10^{20}\end{aligned}$$

$$\text{Surface Coverage} = 1.3279 \times 10^{20} / 2.7538 \times 10^{21} = 0.048$$

$$\begin{aligned}\text{Number of acid sites} &= 1.3279 \times 10^{20} / (358) . (100)^2 \\ &= 3.7092 \times 10^{13} \text{ molecules} / \text{cm}^2\end{aligned}$$



APPENDIX H

SURFACE AREA MEASUREMENT DATA



SAMPLE DIRECTORY/NUMBER: DATA1 /297
 SAMPLE ID: R 503
 SUBMITTER: Ozlem E.KARTAL
 OPERATOR: Isa DEMIRCI OGLU
 UNIT NUMBER: 1
 ANALYSIS GAS: Nitrogen

START 06:22:03 09/29/92
 COMPL 08:45:20 09/29/92
 REPR 09:25:29 09/29/92
 SAMPLE WT: 0.3204 g
 FREE SPACE: 98.1027 cc
 EQUIL INTRVL: 5 sec

SUMMARY REPORT

AREA

BET SURFACE AREA:	242.0156	sq. m/g
LANGMUIR SURFACE AREA:	328.7775	sq. m/g
SINGLE POINT SURFACE AREA AT P/Po 0.2188:	248.0158	sq. m/g
BJH CUMULATIVE ADSORPTION SURFACE AREA OF PORES BETWEEN 17.0000 AND 3000.0000 A DIAMETER:	34.8916	sq. m/g
BJH CUMULATIVE DESORPTION SURFACE AREA OF PORES BETWEEN 17.0000 AND 3000.0000 A DIAMETER:	32.8111	sq. m/g
MICROPORE AREA:	189.3903	sq. m/g

VOLUME

SINGLE POINT TOTAL PORE VOLUME OF PORES LESS THAN 1527.5946 A DIAMETER AT P/Po 0.9873:	0.131958	cc/g
BJH CUMULATIVE ADSORPTION PORE VOLUME OF PORES BETWEEN 17.0000 AND 3000.0000 A DIAMETER:	0.041890	cc/g
BJH CUMULATIVE DESORPTION PORE VOLUME OF PORES BETWEEN 17.0000 AND 3000.0000 A DIAMETER:	0.024635	cc/g
MICROPORE VOLUME:	0.080523	cc/g

PORE SIZE

AVERAGE PORE DIAMETER (4V/A BY LANGMUIR):	16.0543	A
BJH ADSORPTION AVERAGE PORE DIAMETER (4V/A):	48.0233	A
BJH DESORPTION AVERAGE PORE DIAMETER (4V/A):	30.0930	A

SAMPLE DIRECTORY/NUMBER: DATA1 /236
 SAMPLE ID: R202
 SUBMITTER: Ozlem E.KARTAL
 OPERATOR: Isa DEMIRICIOGLU
 UNIT NUMBER: 1
 ANALYSIS GAS: Nitrogen

START 10:18:34 09/28/92
 COMPL 13:19:51 09/28/92
 REPR 06:23:36 09/29/92
 SAMPLE WT: 0.4814 g
 FREE SPACE: 94.1566 cc
 EQUIL INTRVL: 5 sec

SUMMARY REPORT

AREA

BET SURFACE AREA:	264.0293	sq. m/g
LANGMUIR SURFACE AREA:	358.1261	sq. m/g
SINGLE POINT SURFACE AREA AT P/Po 0.2164:	269.4986	sq. m/g
BJH CUMULATIVE ADSORPTION SURFACE AREA OF PORES BETWEEN 17.0000 AND 3000.0000 A DIAMETER:	47.0773	sq. m/g
BJH CUMULATIVE DESORPTION SURFACE AREA OF PORES BETWEEN 17.0000 AND 3000.0000 A DIAMETER:	48.7203	sq. m/g
MICROPORE AREA:	172.1235	sq. m/g

VOLUME

SINGLE POINT TOTAL PORE VOLUME OF PORES LESS THAN 2109.5000 A DIAMETER AT P/Po 0.9908:	0.153062	cc/g
BJH CUMULATIVE ADSORPTION PORE VOLUME OF PORES BETWEEN 17.0000 AND 3000.0000 A DIAMETER:	0.052920	cc/g
BJH CUMULATIVE DESORPTION PORE VOLUME OF PORES BETWEEN 17.0000 AND 3000.0000 A DIAMETER:	0.046376	cc/g
MICROPORE VOLUME:	0.081434	cc/g

PORE SIZE

AVERAGE PORE DIAMETER (4V/A BY LANGMUIR):	17.0958	A
BJH ADSORPTION AVERAGE PORE DIAMETER (4V/A):	44.9643	A
BJH DESORPTION AVERAGE PORE DIAMETER (4V/A):	38.4856	A

SAMPLE DIRECTORY/NUMBER: DATA1 /235
 SAMPLE ID: R 201
 SUBMITTER: Ozlem E.KARTAL
 OPERATOR: I.DEMIRCIOGLU
 UNIT NUMBER: 1
 ANALYSIS GAS: Nitrogen

START 06:19:38 09/28/92
 COMPL 09:13:35 09/28/92
 REPR 05:47:48 09/29/92
 SAMPLE WT: 0.4564 g
 FREE SPACE: 34.9117 cc
 EQUIL INTRVL: 5 sec

SUMMARY REPORT

AREA

BET SURFACE AREA:	291.5049	sq. m/g
LANGMUIR SURFACE AREA:	396.1919	sq. m/g
SINGLE POINT SURFACE AREA AT P/Po 0.2157:	295.8456	sq. m/g
BJH CUMULATIVE ADSORPTION SURFACE AREA OF PORES BETWEEN 17.0000 AND 3000.0000 A DIAMETER:	55.0850	sq. m/g
BJH CUMULATIVE DESORPTION SURFACE AREA OF PORES BETWEEN 17.0000 AND 3000.0000 A DIAMETER:	42.3948	sq. m/g
MICROPORE AREA:	171.8298	sq. m/g

VOLUME

SINGLE POINT TOTAL PORE VOLUME OF PORES LESS THAN 2032.7506 A DIAMETER AT P/Po 0.9905:	0.187116	cc/g
BJH CUMULATIVE ADSORPTION PORE VOLUME OF PORES BETWEEN 17.0000 AND 3000.0000 A DIAMETER:	0.059035	cc/g
BJH CUMULATIVE DESORPTION PORE VOLUME OF PORES BETWEEN 17.0000 AND 3000.0000 A DIAMETER:	0.041901	cc/g
MICROPORE VOLUME:	0.081027	cc/g

PORE SIZE

AVERAGE PORE DIAMETER (4V/A BY LANGMUIR):	18.8722	A
BJH ADSORPTION AVERAGE PORE DIAMETER (4V/A):	42.8682	A
BJH DESORPTION AVERAGE PORE DIAMETER (4V/A):	39.5342	A